Contract NAS8-32390
DRD-MA-04

SYSTEMS DEFINITION STUDY FOR SHUTTLE DEMONSTRATION FLIGHTS OF LARGE SPACE STRUCTURES

volume 3
thermal analyses

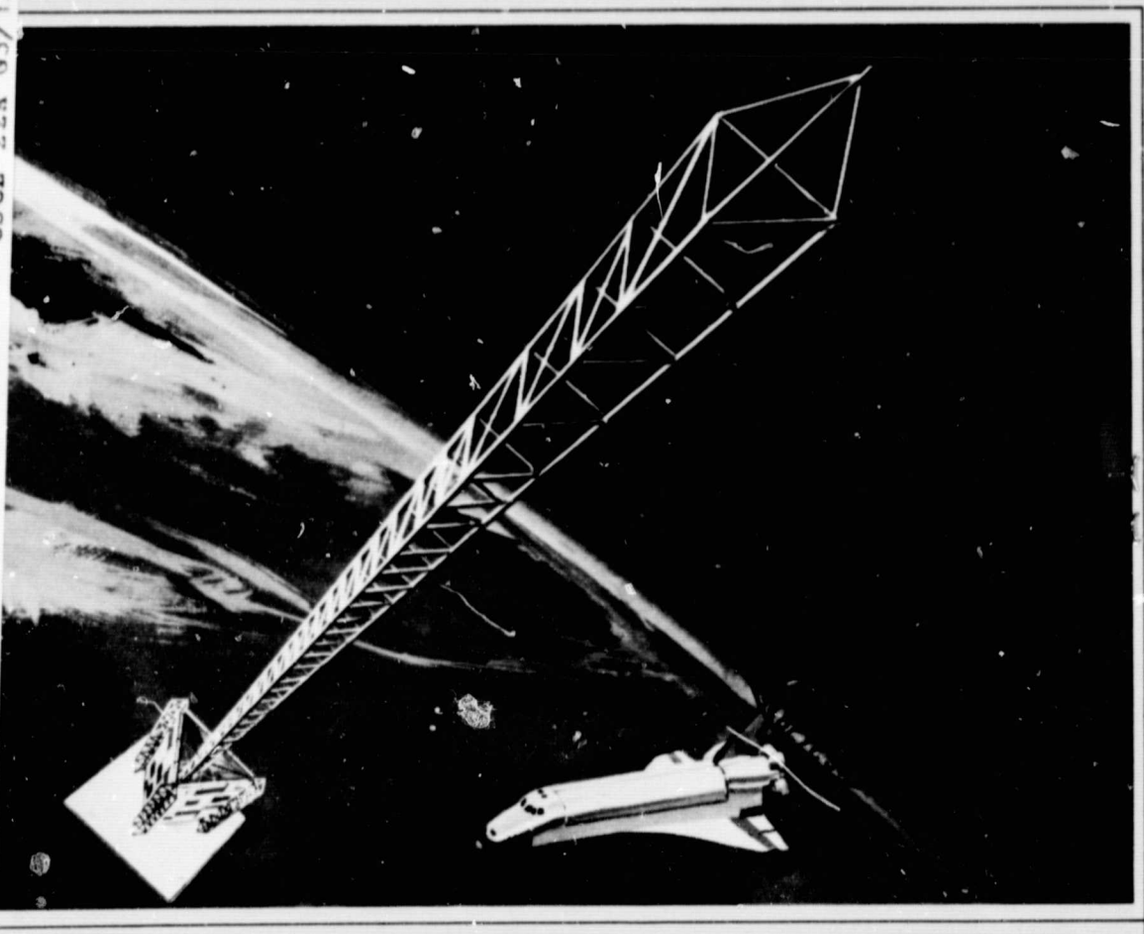

GRUMMAN AEROSPACE CORPORATION

contract NAS8-32390
DRD-MA-04

SYSTEMS DEFINITION STUDY FOR SHUTTLE DEMONSTRATION FLIGHTS OF LARGE SPACE STRUCTURES

volume 3
thermal analyses

prepared for
National Aeronautics and Space Administration
George C. Marshall Space Flight Center
Marshall Space Flight Center, Alabama 35812

by
Grumman Aerospace Corporation
Bethpage, N.Y. 11714

July 1979

FOREWORD

This study was conducted for the Marshall Space Flight Center (MSFC) and directed by the Contracting Officer's Representative (COR), Mr. J. Harrison. The Grumman Aerospace Corporation's study manager was John Mockovciak, Jr.

This final report is presented in three volumes:

- Volume 1 - Executive Summary
- Volume 2 - Technical Report
- Volume 3 - Thermal Analyses
- Volume 3A - Thermal Analyses Appendix .

3

CONTENTS

3

CONTENTS (contd)

ILLUSTRATIONS

3

ILLUSTRATIONS (contd)

ILLUSTRATIONS (contd)

3

ILLUSTRATIONS (contd)

TABLES

1 - INTRODUCTION

The development of technology for constructing large-area, low density space structures must, of necessity, include the development of appropriate, accurate analytical models for predicting the in-orbit response of Large Space Structures (LSS). Among areas of major concern in LSS are the thermal characteristics and response of a structure under orbital conditions.

Space fabricated structures, which are automatically manufactured in space from sheet-strip materials, allow the application of "building block" structural elements for a wide spectrum of future large space structures. The "building block" structure is fabricated by an Automated Beam Builder (ABB) which could allow for production of continuous beam elements in excess of kilometer dimensions. A ground demonstration version of the ABB has been constructed for MSFC by Grumman (NASA Contract NAS8-32472) and is presently undergoing operational evaluation (Fig. 1-1). The machine has been designed to fabricate a 1-meter deep truss beam from 0.016 in. (0.4 mm) 2219 aluminum. Cap members are formed from strip stock, and automatically spotwelded to preformed vertical/diagonal members stored in appropriate magazines.

The LSS flight demonstration mission plans to utilize the ABB and its space fabricated 1-meter beam to establish that on-orbit manufacturing and assembly of large structures is feasible and practical from the Orbiter. Accurate thermal models of a 1-meter beam are thus required to evaluate alternate thermal coatings and to predict deflections, stresses, and stiffness variations resulting from the effects of varying flight orientations and solar conditions during both beam fabrication and construction of a large space structure. Just as analytical techniques must be developed to understand the thermal effects associated with a 1-meter beam, so must similar techniques be developed for combinations of 1-meter beams in Tribeam configurations or other spatial geometries.

To initiate this process, a detailed transient thermal analysis was performed of a 1-meter beam, and its structural response analyzed in terms of linear motions and distortion. The transient thermal analysis was also extended to a representative Tribeam

structure to determine thermal characteristics both in the vicinity of the Orbiter payload bay and as a free-flying LSS.

This report presents the results and conclusions developed during this thermal analysis phase of the study.

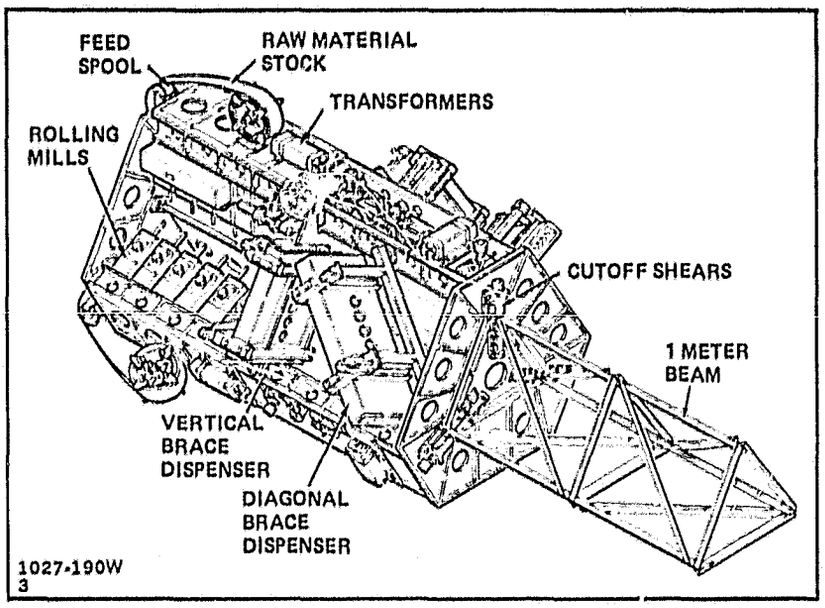

Fig. 1-1 Automated Beam Builder – Ground Demo Flight Version

2 - STUDY APPROACH

The overall approach for performing the thermal analysis is shown in Fig. 2-1. A detailed transient thermal analysis of the 1-meter beam was performed assuming a circular earth orbital altitude of 300 n mi, and inclination of 28 1/2 deg. This included consideration of caps, verticals and diagonals of the beam, the effects of shadowing of elements of the structure by other elements, the thermal effects of the cavities in the structure, and radiant interchange between the elements. Four surface thermal coatings, covering a range of absorptivity and emissivity, were considered.

The outputs of the 1-meter beam transient thermal analysis were analyzed to determine the structural response of the beam. Information has been generated to reflect the linear motions of the beam and its distortion during an orbit transit.

The thermal model developed for the 1-meter beam was used as the basis for further analysis of a single bay of a Tribeam structure. Beam/structural element temperatures and gradients have been identified for both Free-Flyer and Orbiter-attached modes.

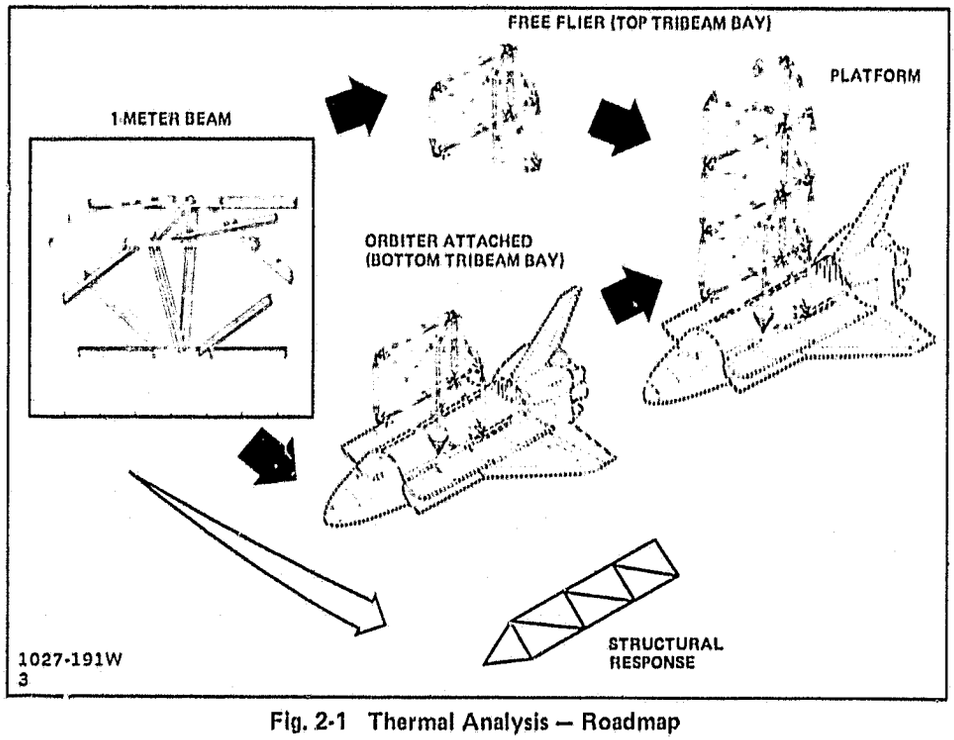

Fig. 2-1 Thermal Analysis – Roadmap

3

3 - ONE-METER BEAM THERMAL ANALYSIS

3.1 ORBIT ORIENTATION

The earth orbit considered for this analysis is circular with an altitude of 300 n mi and an inclination of 28½ deg. As shown in Fig. 3-1 and 3-2, an orientation has been assumed, wherein one face of the 1-meter beam (surface 2-3) is in a plane aligned with the local vertical for an entire orbit. This orbital attitude was selected because it will cause one of the more severe conditions of thermal gradients in the 1-meter beam structure.

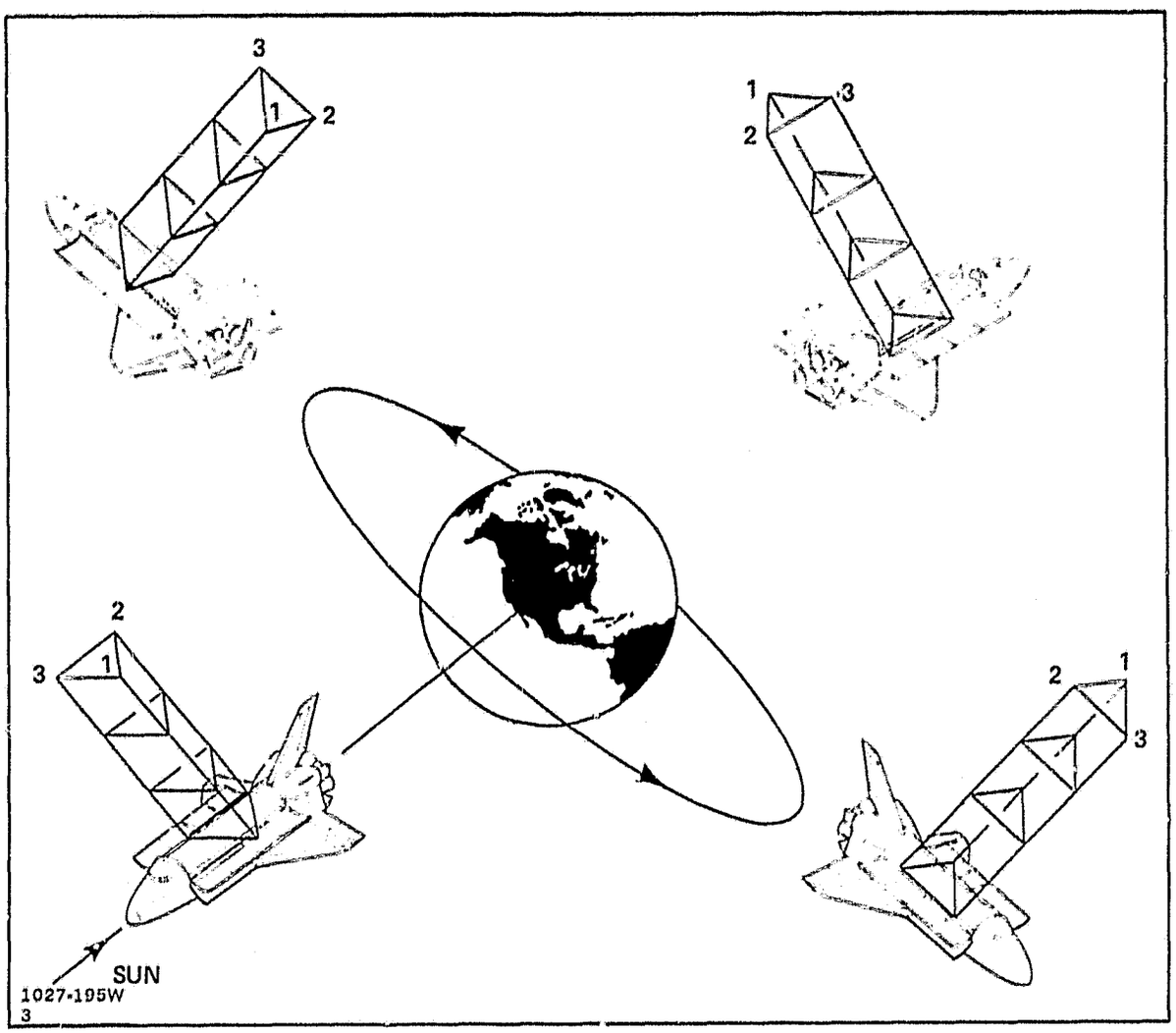

Fig. 3-1 Orientation Assumed for Transient Thermal Analysis

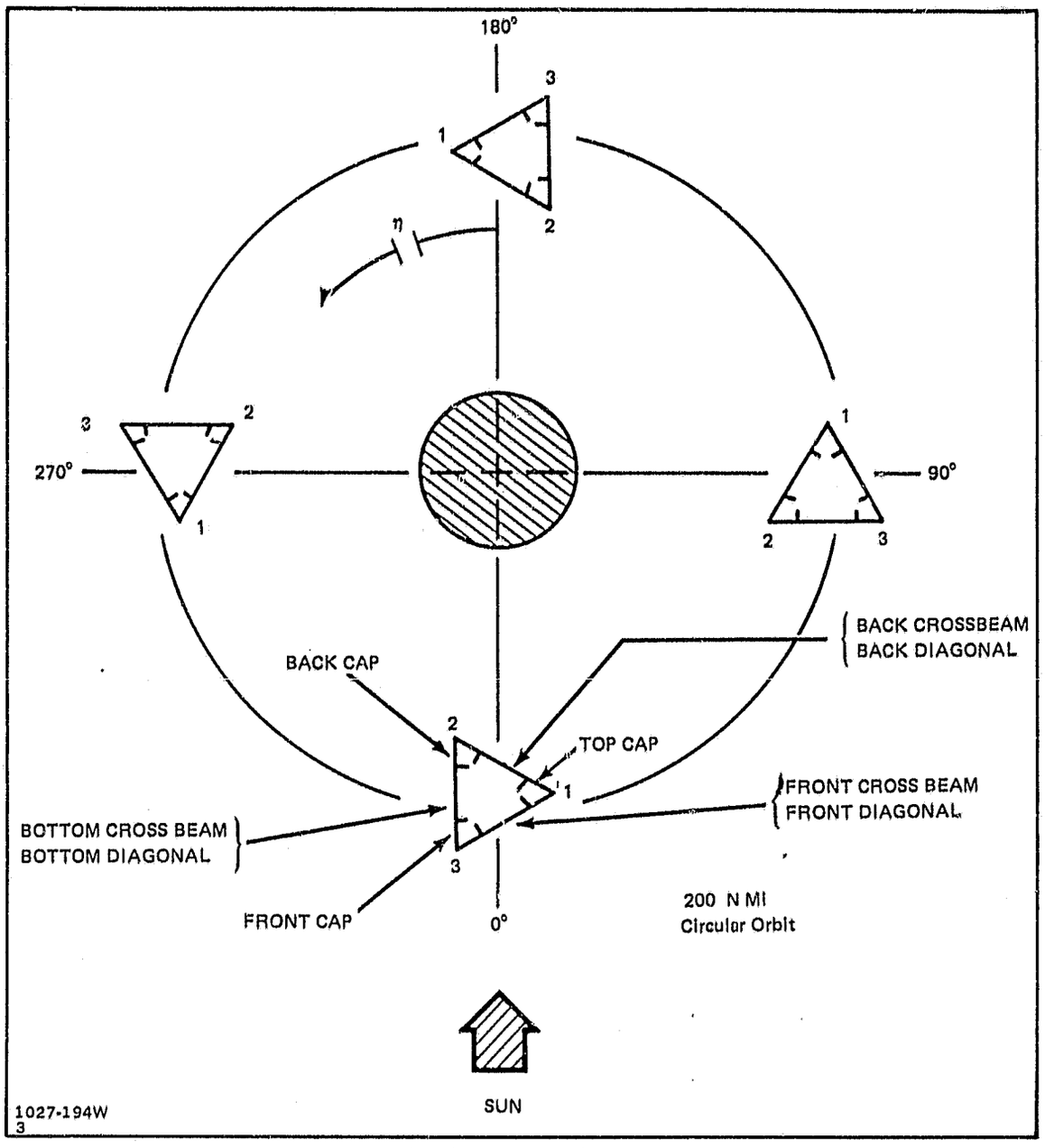

Fig. 3-2 Orientation Diagram

3.2 THERMAL MODEL

A thermal model of the 1-meter beam has been constructed, and a computer graphics display of the model is shown in Fig. 3-3. To obtain proper thermal symmetry the model was cut in mid-bay, thus, the center of symmetry is formed by the verticals. As shown in Fig. 3-3 the structural elements of the model are identified by letters A through S. They are designated as follows:

Element	Letter Identification
Caps	A through F
Diagonals	G, H, J, N, P, Q
Verticals	K, L, M
Joints	R, S, T

Further element identification is made by using the designation, FRONT, BACK, LEFT and RIGHT. For example, in Fig. 3-3, element B is cap back left, element N is diagonal front right, and element M is vertical bottom.

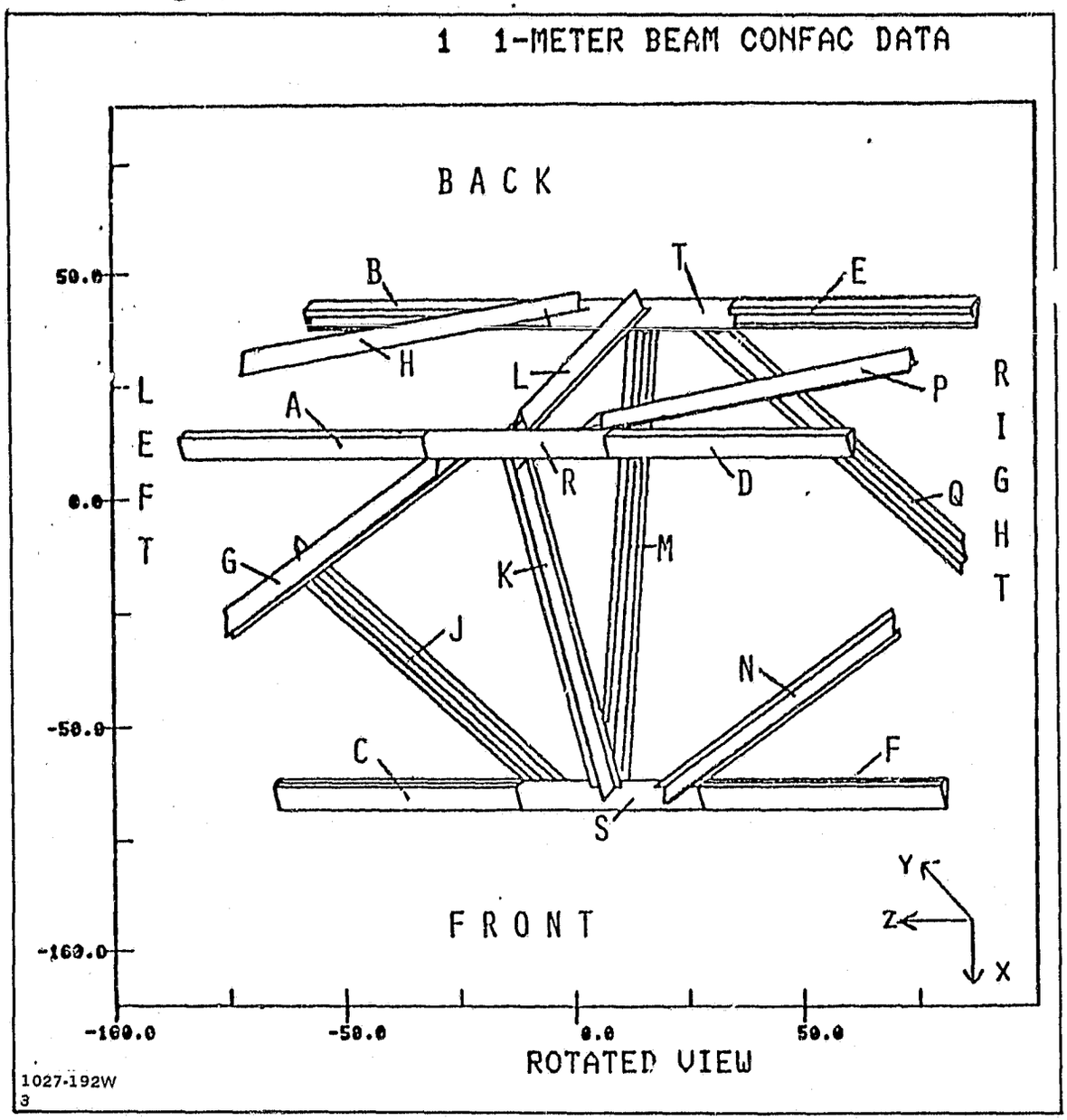

Fig. 3-3 One-Meter Beam Thermal Model-Element Designation

The caps, verticals, and diagonals are each composed of four thermal nodes as shown in Fig. 3-2. In the radiation modeling, both surfaces of each nodes are considered. Specific identification of the total of 63 nodes used within the thermal model are provided in Appendix A.

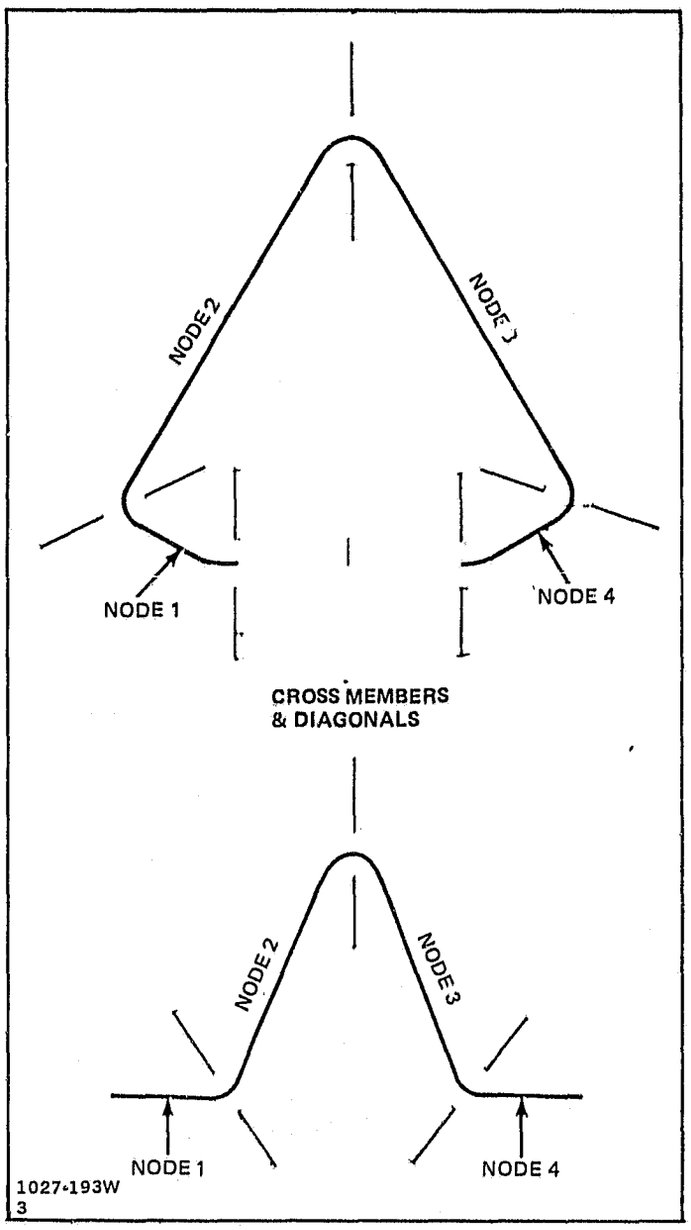

Fig. 3-4 Nodal Modeling of One-Meter Beam Elements

3.3 STRUCTURAL ELEMENT BLOCKAGE

Blockage of each element by the others was calculated by the use of computer graphics. The model can be rotated on the three axes to the proper position for the start of an orbit, then rotated to simulate orbital travel. Three computer graphics

views are shown in Fig. 3-5, corresponding to 0°, 5°, and 270° orbital positions. It is seen that at the 0° position, the front cap completely shadows the back cap and even after 5° of travel, a diagonal is still partially blocking the back cap.

A total of 20 computer graphics views were taken, and are documented in Appendix B. These cover orbital positions ranging from 0° to 135°. The remainder are simply repeats of these previous views.

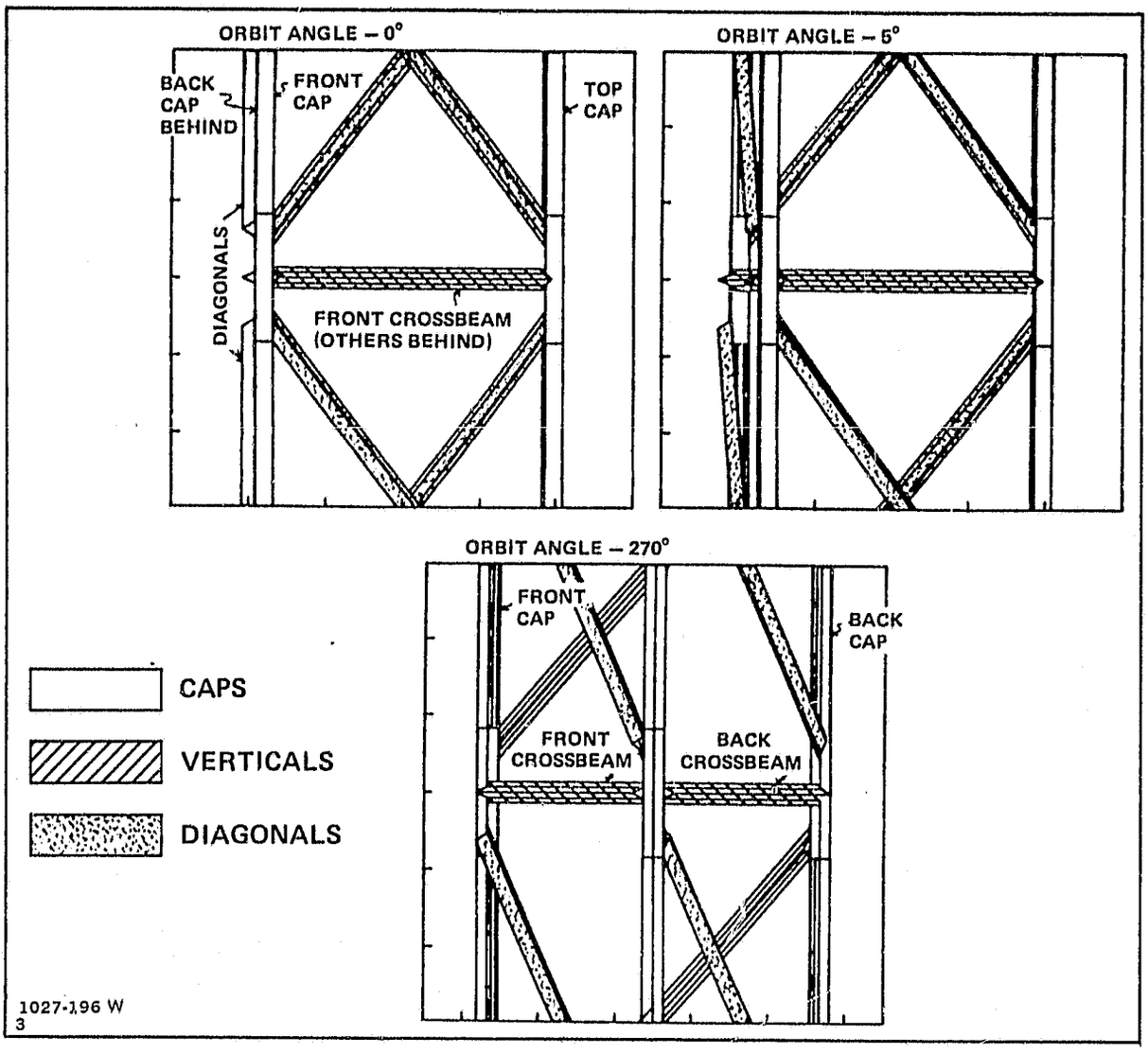

Fig. 3-5 Computer Graphics

3.4 THERMAL COATINGS

The analysis was performed for four coatings covering the applicable range of emissivity and solar absorptivity. Their thermo-optical properties are:

Coating	α_s	ϵ	α_s/ϵ
Black Anodize	0.86	0.83	1.04
Alzak	0.17	0.72	0.24
Z-93 White Paint	0.17	0.90	0.19
Sicon 3 x 245	0.23	0.23	1.00

3.5 COMPUTER PROGRAM

The basic computer program used for this analysis was the Grumman T-15 Thermal Analyzer. This program requires a data file and a fortran file.

3.5.1 Data File

This file provides the basic heat transfer data for the thermal model. Included within it are the mass specific heat of each node, the conductance between nodes, the radiant interchange between the nodes, and the conductance and radiation exchange with fixed boundary nodes, such as the temperature of space.

This file also contains the tables that describe the solar flux, the albedo, and the earth IR incident (per unit area) on each of the 63 nodes. These heat loads, along with the radiant interchange factors, were generated from the thermal model data using two Grumman computer programs, FLUX and CONFAC 68.

Blockage of the solar flux is also expressed as tables in this file.

3.5.2 Fortran File

This file is necessary to take the flux data (in table form in the Data File) and combine them, along with the blockage factors to determine the total heat flux on each node. These are expressed within the file in the form of equations. As an example, the equation for the total heat load on Node 1 is described in the Equation Diagram (Fig. 3-6).

3.6 DISCUSSION OF RESULTS

The output of the computer program is a temperature-time history for each node during one orbit (total orbit time is 95.8 min). A typical example is shown in Fig. 3-7 where the temperature of the four nodes of the cap (element A of Fig. 3-3) are plotted over an orbit. The temperature spikes caused by the shadow from a diagonal and from another cap are readily identifiable. Similarly, Fig. 3-8 shows the four nodal temperatures of a diagonal (element G in Fig. 3-3) where the thermal spike is caused by blockage from a cap.

3

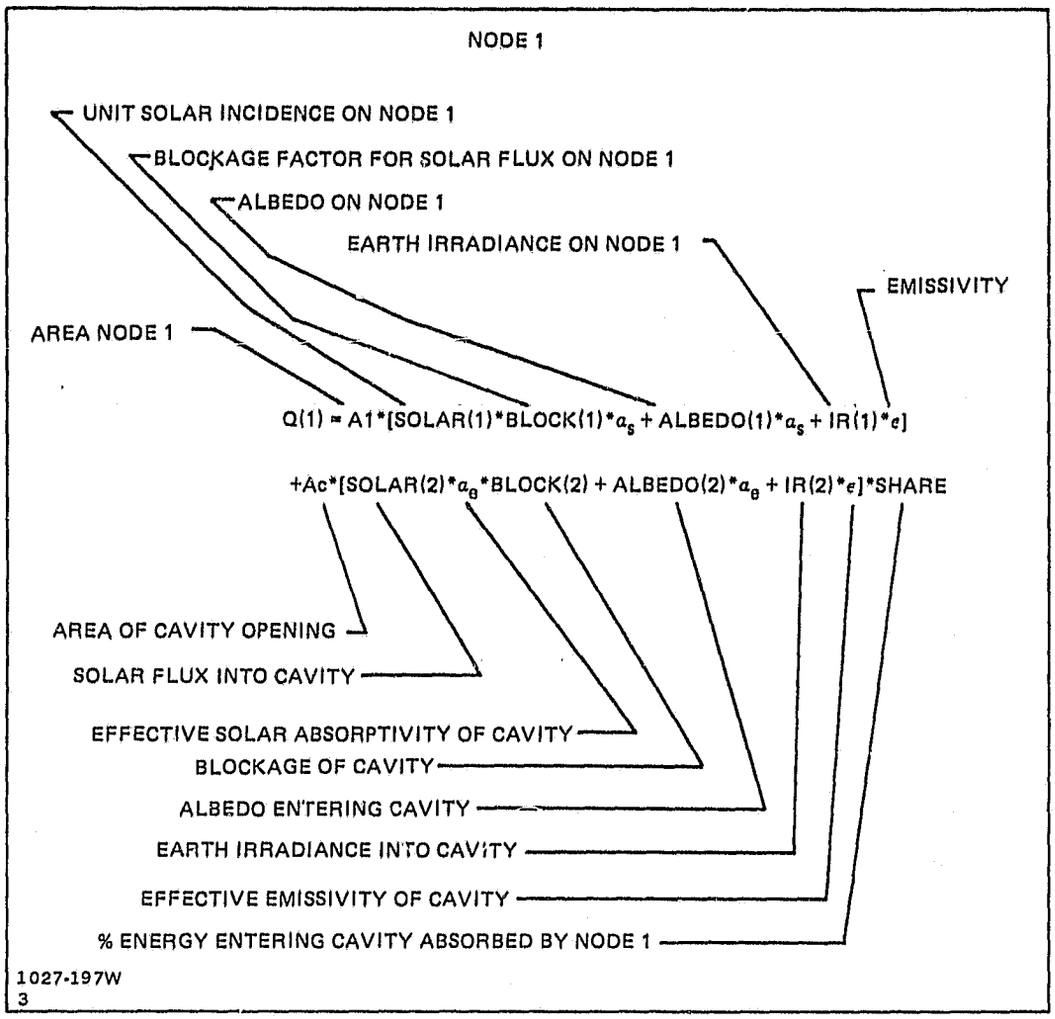

Fig. 3-6 Equation Diagram

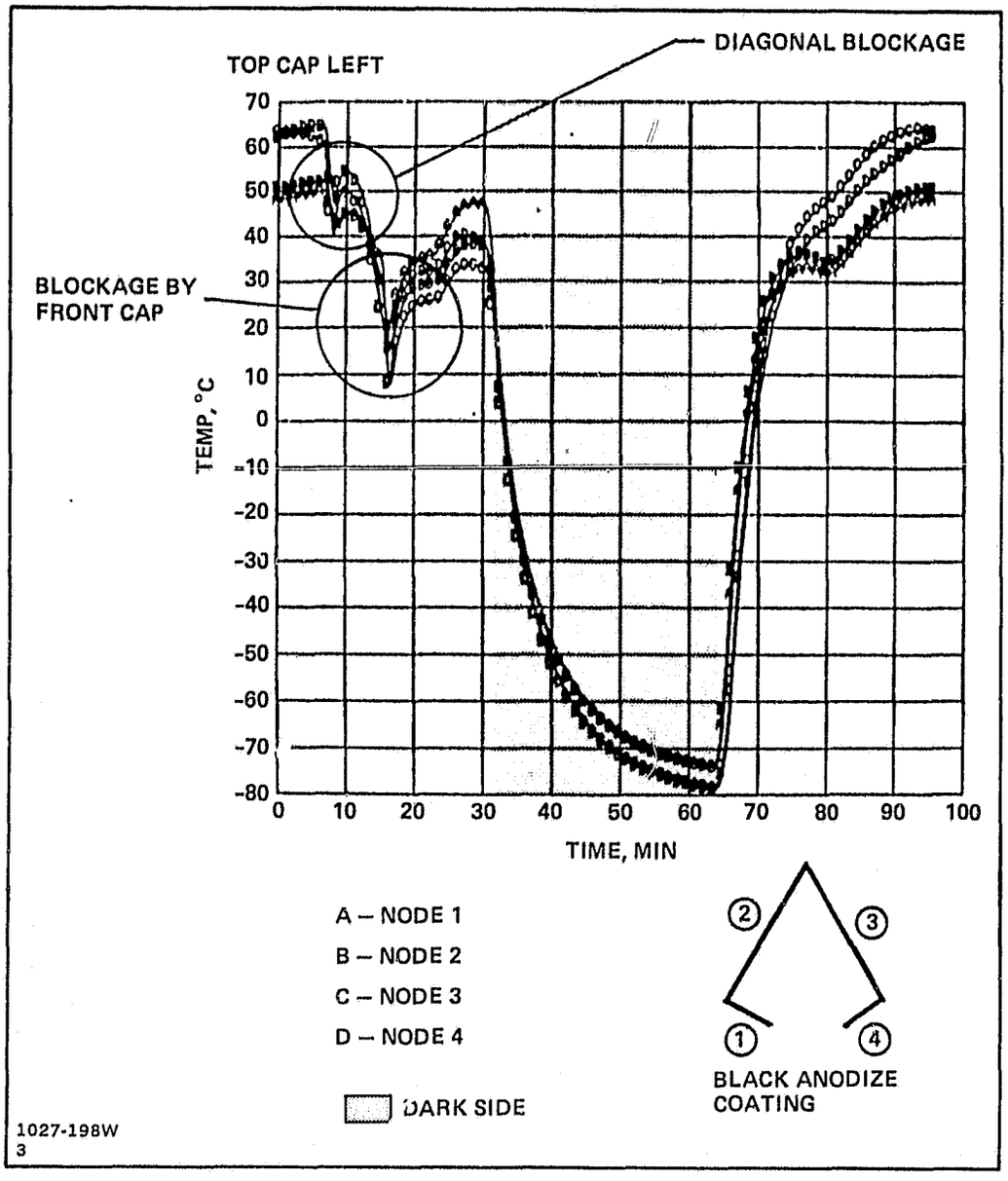

Fig. 3-7 Computer Printout-One-Meter Beam Cap

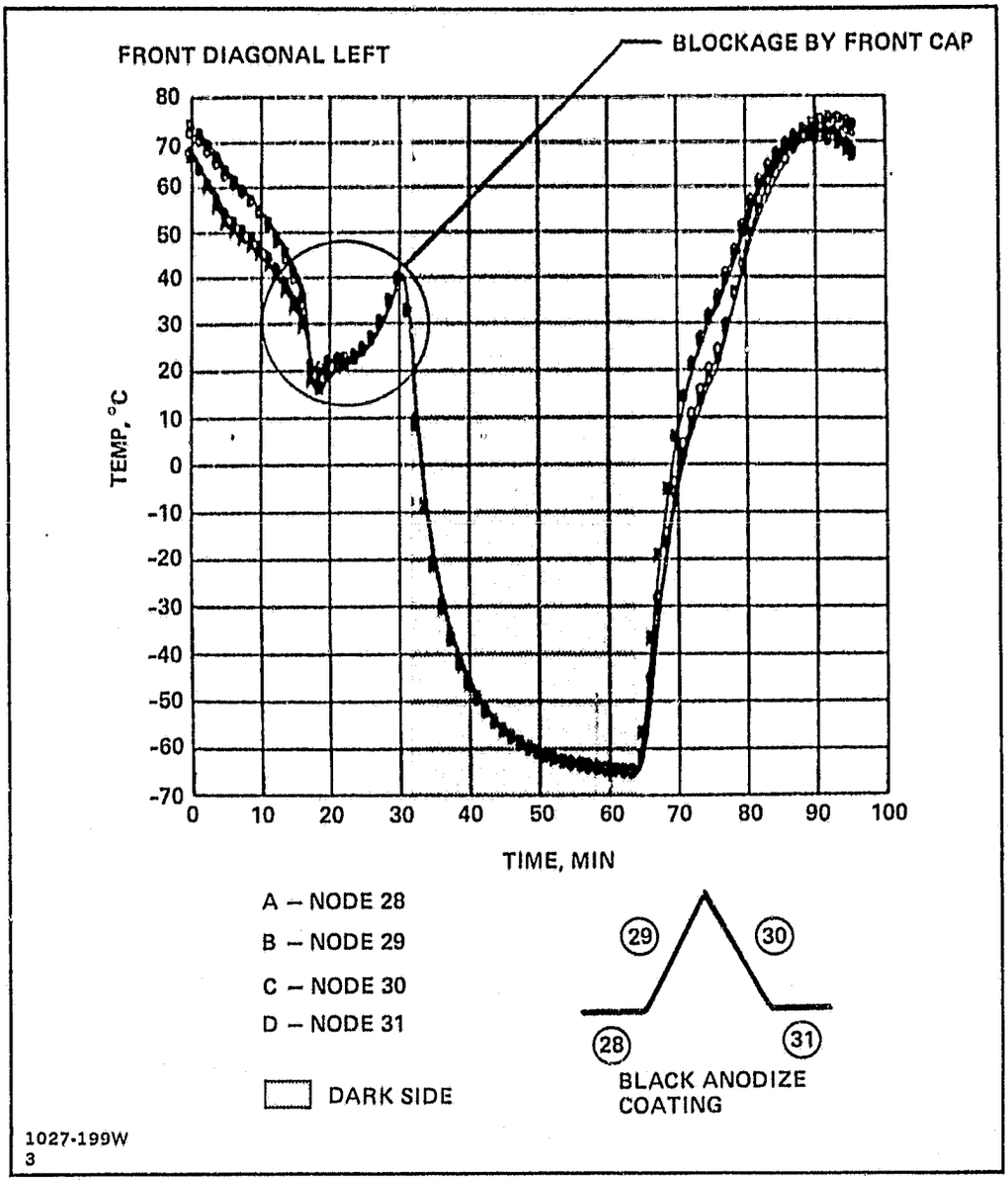

Fig. 3-8 Computer Printout-Diagonal

3

Transient temperature profiles during an orbit were developed for each of the 18 structural elements (caps, verticals diagonals) in the thermal model. The nodal temperature-time histories have been developed for four surface finishes and are provided in the following appendixes of this report:

Appendix C - Black anodize
Appendix D - Alzak
Appendix E - Z-93 White Paint
Appendix F - Sicon 3 x 245

Appendixes C through F present the temperatures of each node, and thus gradients within each structural element can be determined. The maximum termperatures and maximum gradients found within the elements are identified in Table 3-1 and illustrated in Fig. 3-9. It can be seen that the structure with black anodize and or Sicon operate at significantly higher temperatures, relative to Alzak or Z-93 white paint. Maximum temperature gradients within the 1-meter beam elements (e.g., through a cross-section) are similar for either Alzak, white paint or sicon coatings, with the maximum gradients occurring for the black anodize case. Note that in all cases the local gradients are higher within the caps than the verticals and diagonals.

Table 3-1 shows that the gradients within the elements are 2 to 3 times higher with the black anodize than with the other three coatings. This is due to the fact that the black anodize has both a higher absorptivity and a high emissivity (i.e., the nodes facing the sun have a high rate of heat input while the nodes facing away have a high rate of output).

Table 3-1 Gradient Comparison for Four Different Coatings

	BLACK ANODIZE	ALZAK	Z-93 WHITE PAINT	SICON 3 x 245 PAINT
MAX. TEMPERATURE (°C/°F)				
CAPS	66/151	8/46	0/32	75/167
DIAGONALS	81/178	1/34	-9/16	92/198
VERTICALS	72/162	-3/27	-11/12	93/199
JOINTS	64/147	-17/1.5	-26/-15	60/140
MAX. GRADIENTS IN ELEMENTS (°C/°F)				
CAPS	25/45	11/20	9/16	8/14
DIAGONALS	12/22	3/5.5	3/5.5	4/7
VERTICALS	3/5.5	1/2	1/2	1/2

1027-201W
3

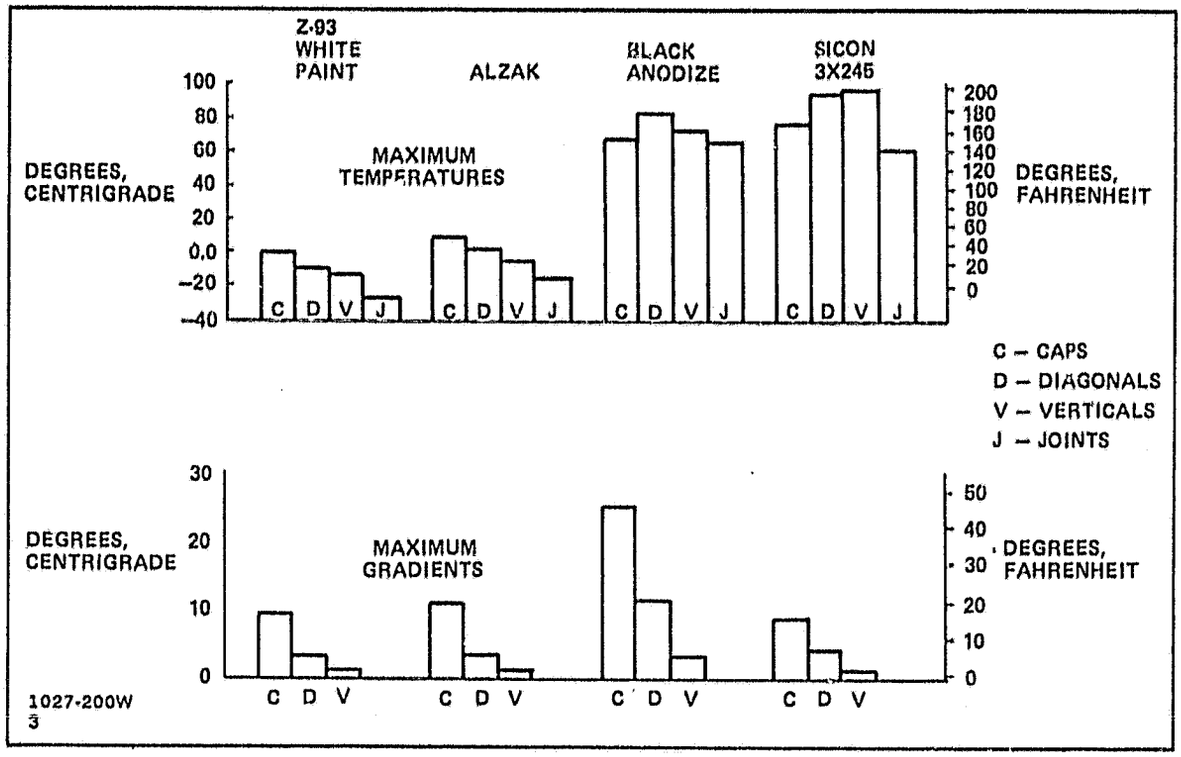

Fig. 3-9 One-Meter Beam Element Temperatures — Coatings Comparison

Earlier analyses dealing with selection of coatings considered the case where the sun's rays entered the cavity of one cap while impinging on the outer surfaces of the others. Since the cavity will absorb most of the entering energy, it will appear to have a high absorptivity regardless of the surface properties. It is reasonable, therefore, from this consideration, to coat the outer surfaces for a high absorptivity so that all caps would respond similarly to the solar incidence. Since solar blockage of one element by another was not considered in the original investigation, the black anodize appeared to be the favorable coating.

In the present transient thermal analysis, the effects of solar blockage of the structural elements by other elements is fully considered. Here the element in the shadow drops in temperature, during the shadow period, and this drop is proportional to the emissivity and to the fourth power of the temperature level. Again, since the black anodize has a high emissivity and operates at a high temperature, the thermal spikes are most pronounced and become the dominant gradient in that case. A comparison of black anodize (Fig. 3-10) and Alzak (Fig. 3-11) cap elements, readily illustrates that the spikes caused by blockage extend the gradients much more in the case of black anodize. As regards Alzak and the Z-93, the reduced effect of the shadowing is due to their lower operating temperature levels; in the case of the Sicon, it is the low emissivity.

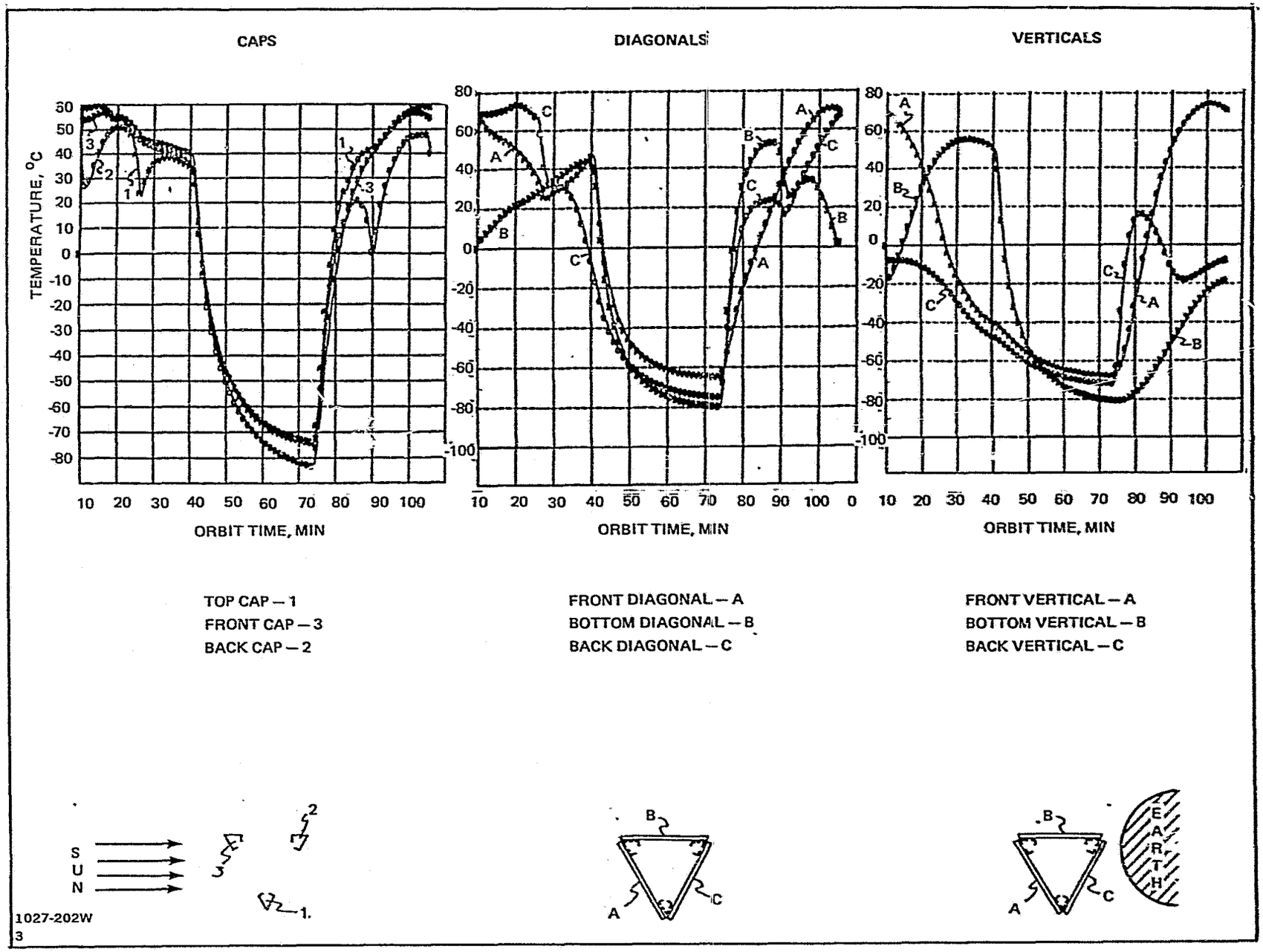

Fig. 3-10 One-Meter Beam Temperatures — Black Anodize — $\epsilon = 0.83, \alpha = 0.86$

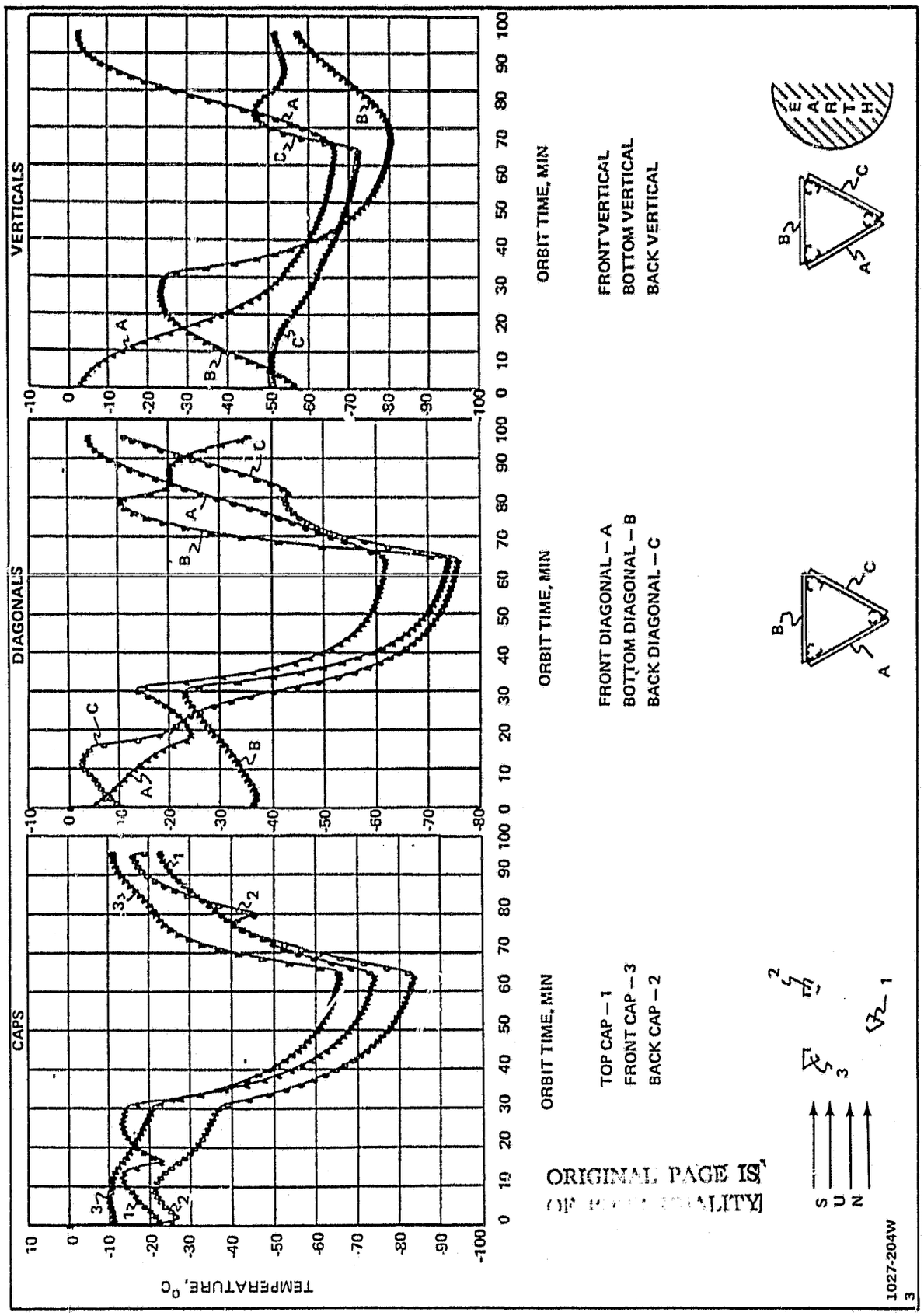

Fig. 3-11 One-Meter Beam Temperatures – Alzak – $\epsilon = 0.73, \alpha = 0.17$

Weighted average temperature characteristics have been developed to facilitate structural analyses related to stress and deformation of a 1-meter beam. These were calculated by the computer program and are presented in Fig. 3-10 through 3-13 for the four coatings analyzed. The plots are the results of weight-averaging the nodes that comprise the structural elements. Figure 3-14 shows a comparison between the weighted average temperatures of the three 1-meter beam caps for black anodize and Z-93 white paint coatings. Note that the effects of blockage (the spikes in the curves) are considerably less for white paint than black anodize (e.g., the temperature spikes are about 10°C in white paint and over 20°C in black anodize).

The maximum differential temperatures between caps, diagonals, and verticals during a full orbit are shown in Fig. 3-15. Clearly, Alzak and Z-93 white paint appear most favorable.

Maximum temperature differences experienced between caps, verticals and diagonals are identified in Table 3-2 and illustrated in Fig. 3-16. Again, the Alzak and the Z-93 white paint coatings are clearly more advantageous in regard to thermal gradients. Because of its potential beam-machine suitability and simpler handling problems, the Z-93 white paint coating has been baselined for subsequent analyses of a Tribeam. For prolonged orbital operations, however, Alzak's improved coating decay characteristics should be considered, although considerable handling problems may be encountered.

Temperature excursions experienced by the structure, during an orbit, affect the structure's response during the assembly process. The maximum temperature excursions of the 1-meter beam's structural elements, as reflected by the data in Appendixes C through F, are identified in Table 3-3 and illustrated in Fig. 3-17. The overall maximum temperature excursions for black anodize and Sicon are about double those for Alzak and Z-93 white paint.

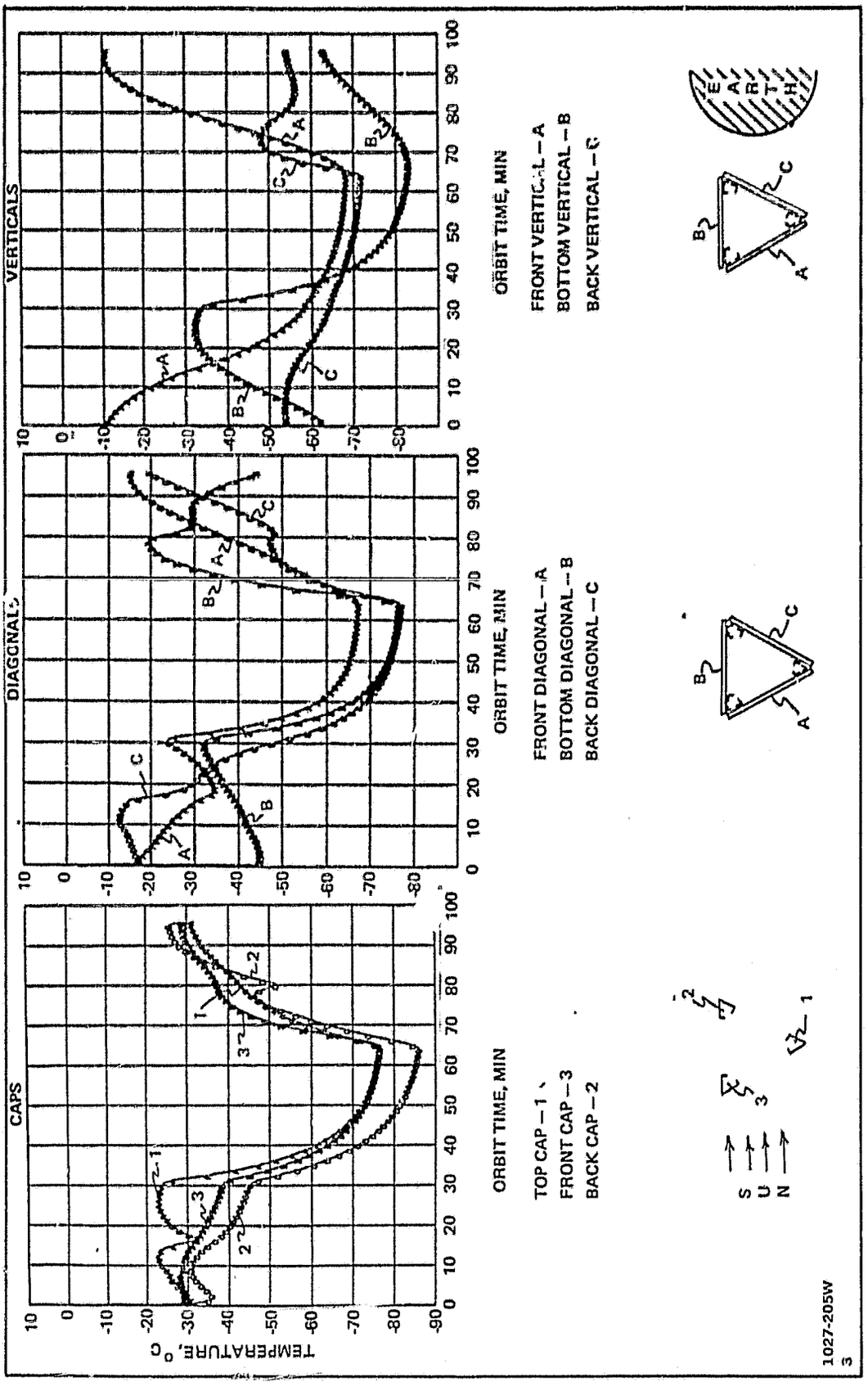

Fig. 3-12 One-Meter Beam Temperatures — Z-93 White Paint — $\epsilon = 0.90$, $\alpha = 0.17$

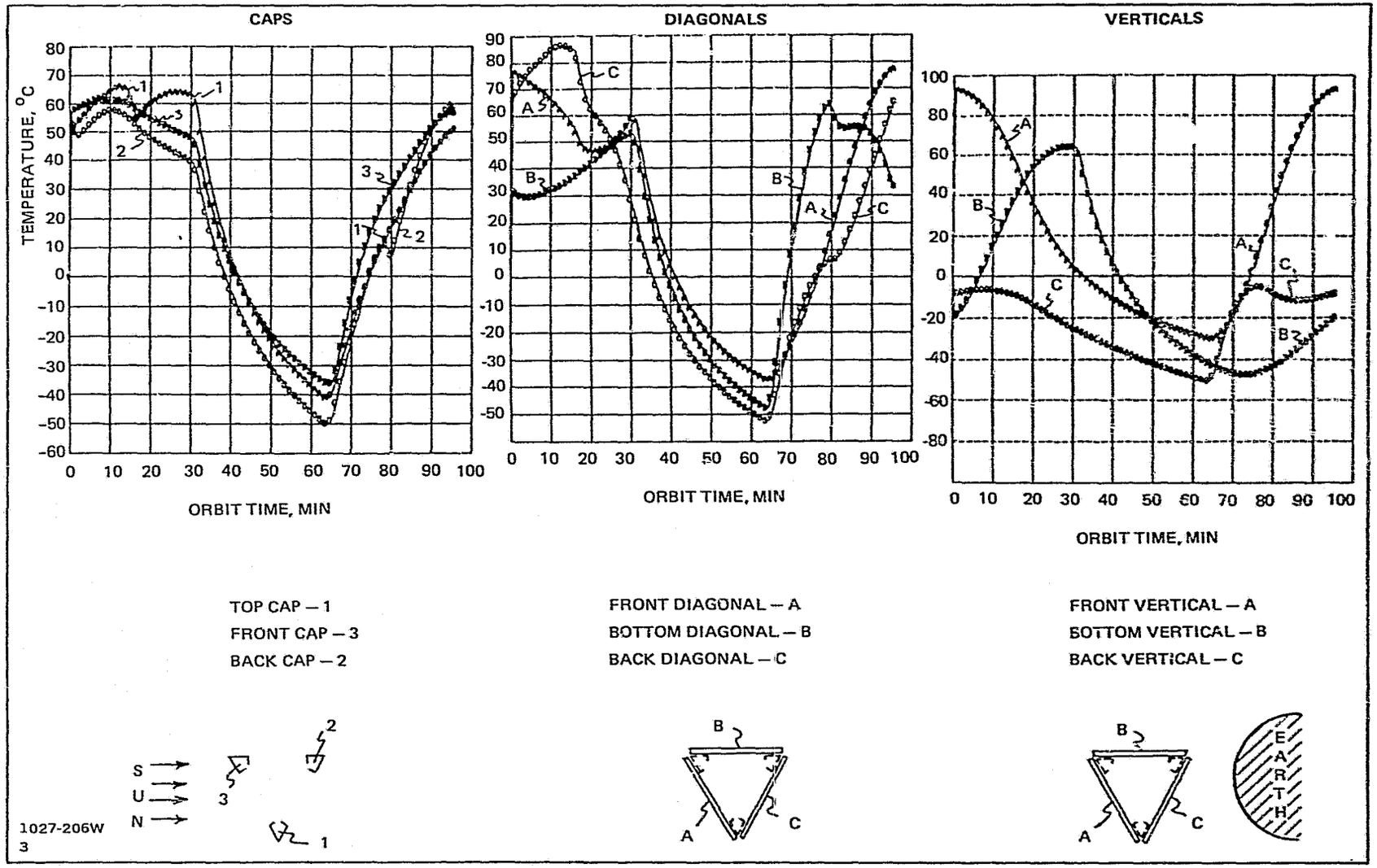

Fig. 3-13 One-Master Beam Temperatures — Sicon 3 x 245, $\epsilon = 0.23$, $\alpha = 0.23$

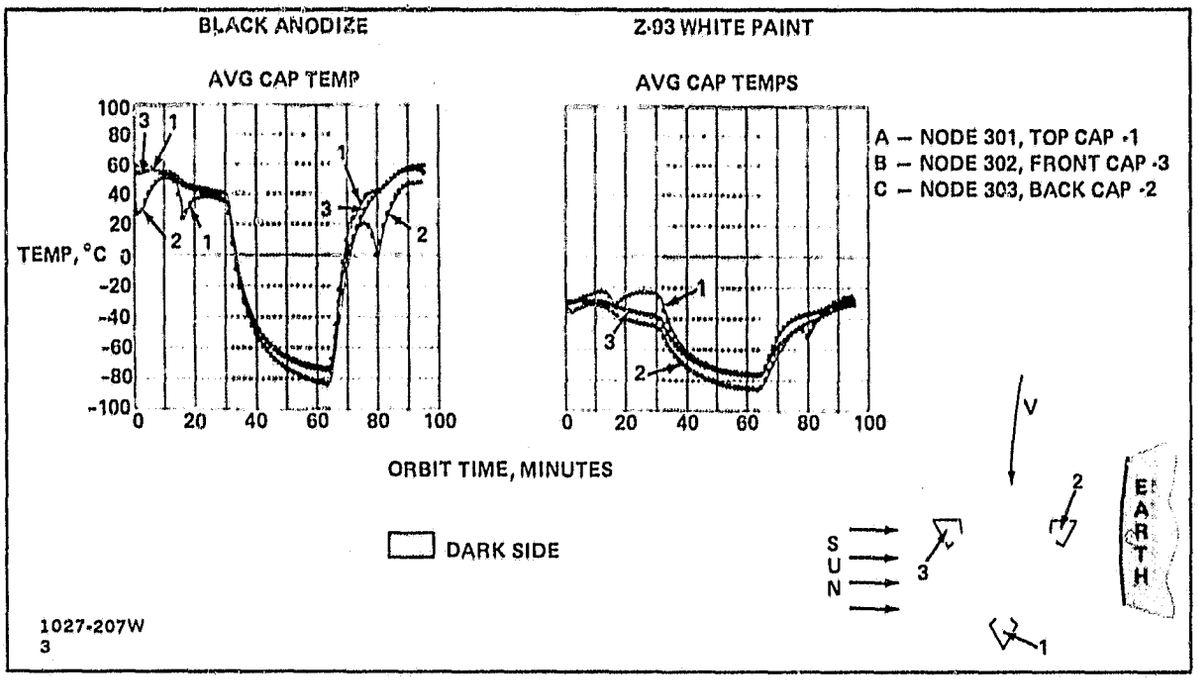

Fig. 3-14 One-Meter Beam Caps — Weighted Average Temperatures

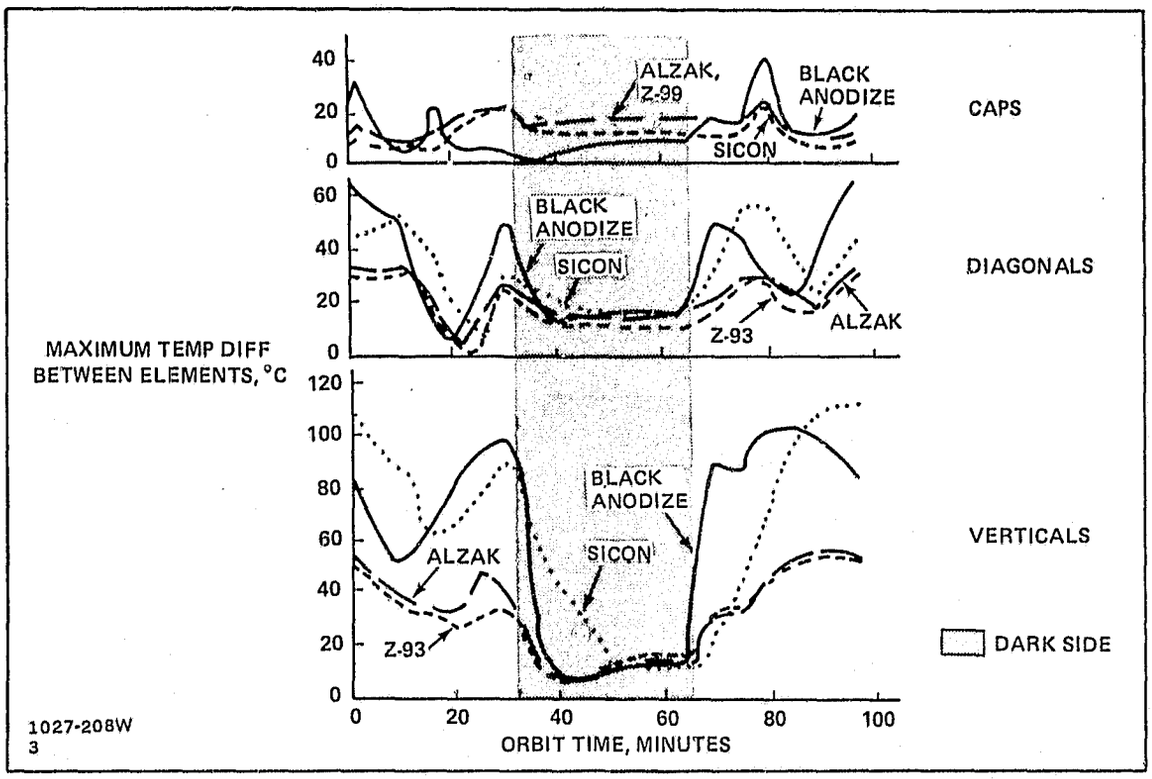

Fig. 3-15 Variation in One-Meter Beam Structural Element Maximum Temperature Differences During an Orbit

3

Table 3-2 Maximum Gradients Between Elements (°C/°F)

	BLACK ANODIZE	ALZAK	Z-93 WHITE PAINT	SICON 3 x 245 PAINT
CAPS	42/76	24/43	23/41	23/41
DIAGONALS	64/115	33/59	31/56	58/104
VERTICALS	103/185	57/103	54/97	111/200

1027-209W
3

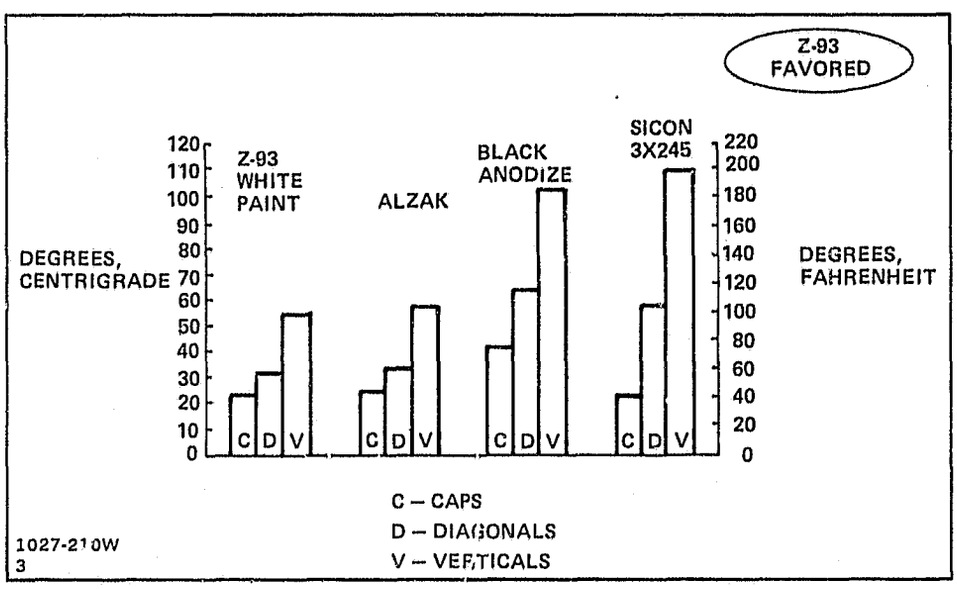

Fig. 3-16 Peak Temperature Differences Between Structural Elements

Table 3-3 Maximum Temperature Excursions (°C/°F)

	BLACK ANODIZE	ALZAK	Z-93 WHITE PAINT	SICON 3 x 245 PAINT
CAPS	144/269	77/139	69/124	123/24
DIAGONALS	148/266	76/137	67/121	144/259
VERTICALS	144/269	66/119	58/104	123/221

1027-211W
3

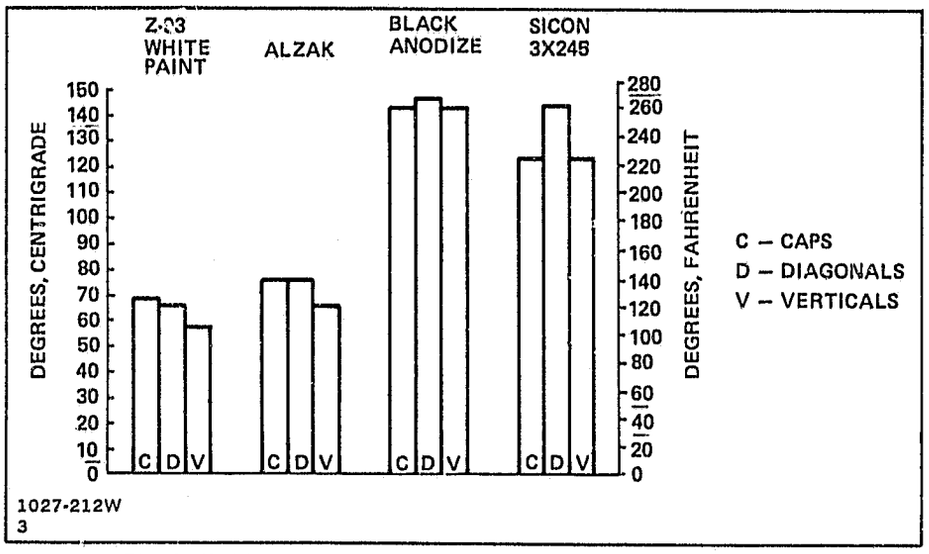

Fig. 3-17 Maximum Temperature Excursions During an Orbit

3.7 SIMPLIFIED THERMAL MODEL

As part of the thermal analysis program, the thermal model was simplified to determine if computer time could be reduced without affecting accuracy. The nodal system was combined as shown in Fig. 3-18, indicating that the number of nodes has been reduced in half. The revised nodal identification is provided in Appendix G.

As discussed previously, the Z-93 white paint has been baselined as the thermal coating for the 1-meter beam. Figure 3-19 shows the weighted-average element temperatures, during an orbit, for the caps, diagonals, and verticals of a 1-meter beam. No readable difference was found in comparing either caps, diagonals or verticals. From the tabular printouts, the maximum temperature difference noted between the original and simplified models was 0.4°C (0.7°F). . . . clearly a negligible quantity. This simplified model, therefore, has been used for the Tribeam thermal analysis.

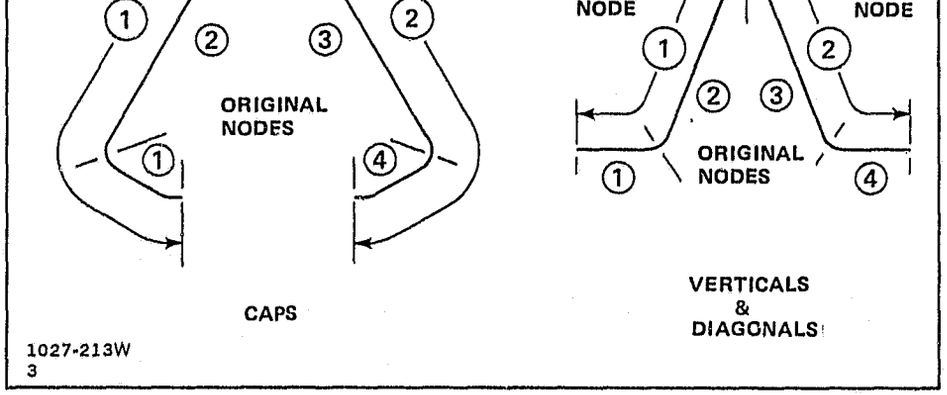

Fig. 3-18 Simplifying the Thermal Model

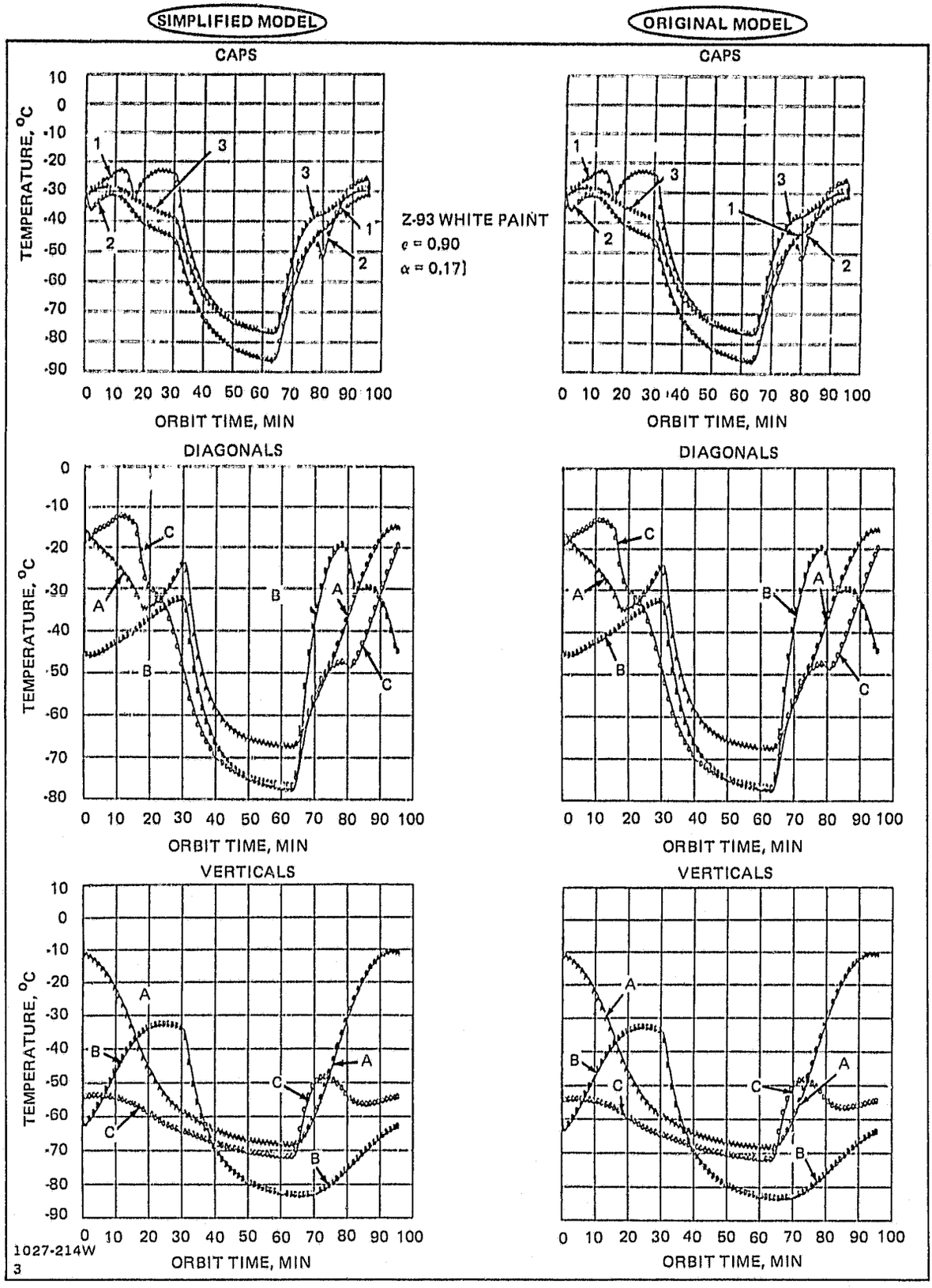

Fig. 3-19 Comparison of Original & Simplified Thermal Models

4 - ONE-METER BEAM STRUCTURAL RESPONSE

The outputs of the 1-meter beam transient thermal analysis have been analyzed, in Grumman's IRAD effort, to determine the structural response of the beam (Fig. 4-1). Information has been generated to reflect the linear motions of the beam and its distortion during an orbit. Fixed-free beam response (e.g., representing an ABB-attached condition) and free-free beam response (e.g., the condition of a beam during a construction/assembly process) have been analyzed.

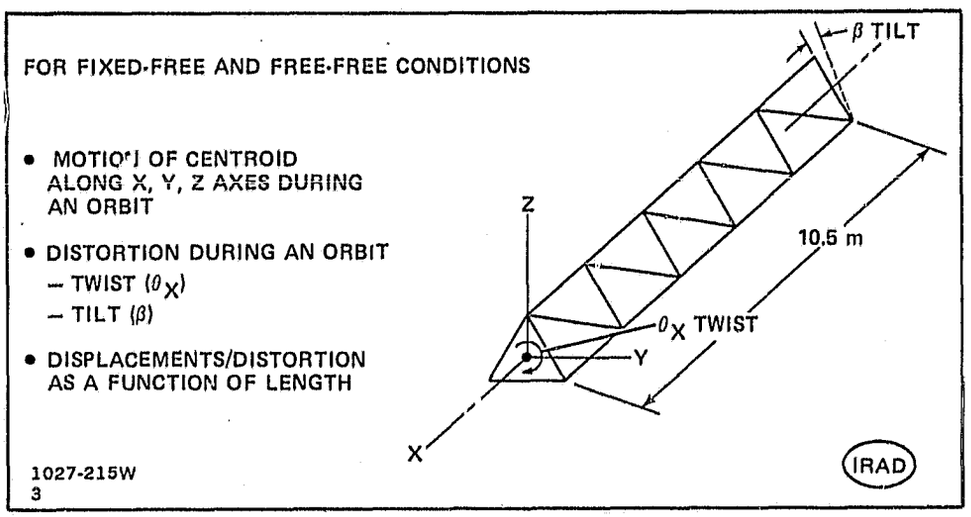

Fig. 4-1 One-Meter Beam Structural Response

4.1 STRUCTURAL MODEL

A finite element model of the 1-meter beam was developed, with appropriate restraints applied to simulate support of the ABB. Fabrication of the beam was assumed to occur in a thermally controlled environment at a temperature of 70°F (21°C). The element, node and reaction point designation applied to the finite element model of a 10.5 meter length of the one-meter beam is illustrated in Fig. 4-2. Elements of the model were assumed as frictionless pin-connected bars with a common end node for the caps, verticals, and intersecting diagonal elements.

For the fixed-free case, the upper end of the beam was allowed to twist (θ), tilt (β), and deflect (ΔX, ΔY, and ΔZ) without restraint during an orbit transit. Free-free restraint conditions were also analyzed. Two thermal coatings were also included in the analysis; black anodize and Z-93 white paint.

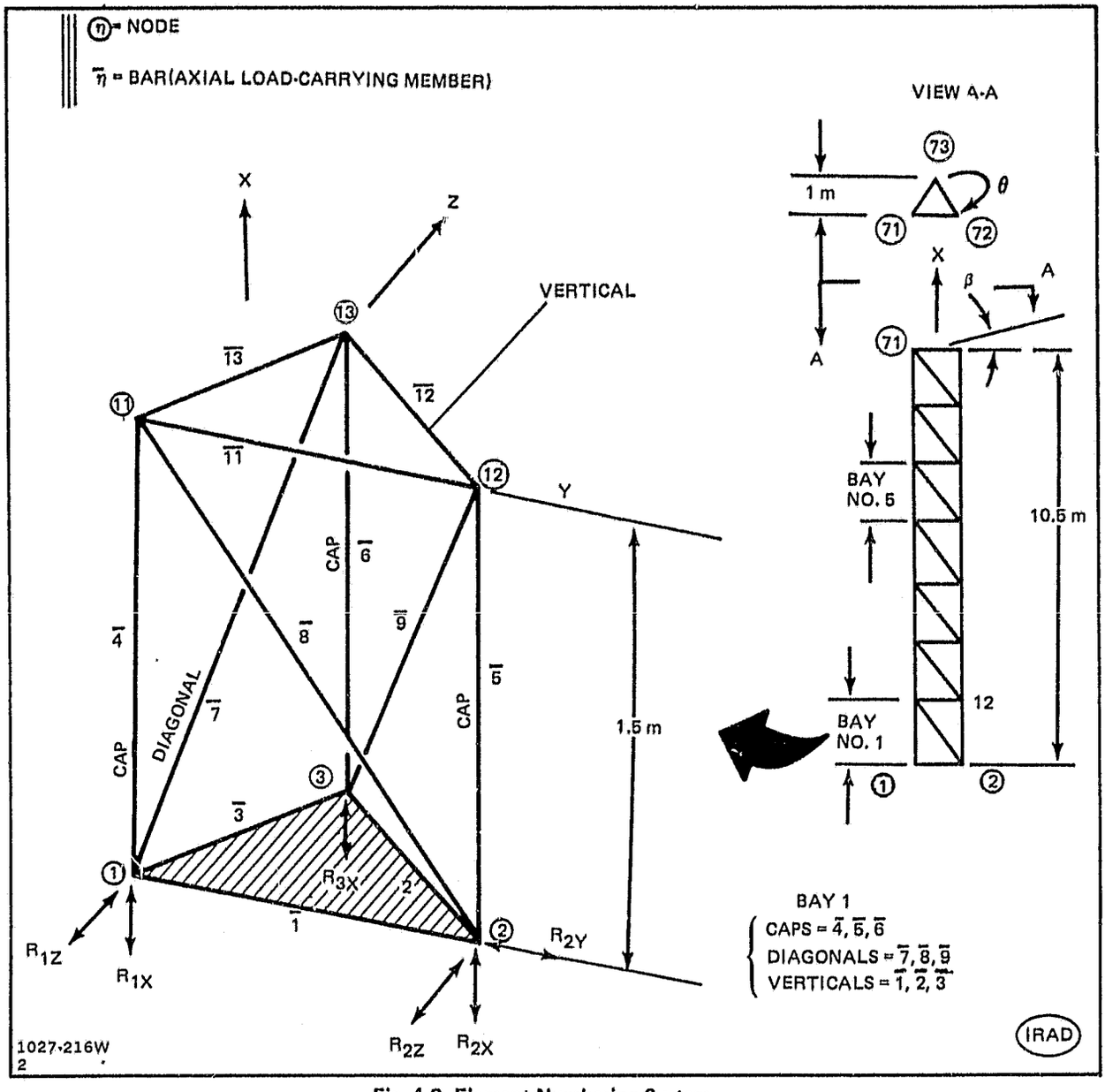

Fig. 4-2 Element Numbering System

Both aluminum and composite materials were considered in analyzing the beam's twist characteristics. The all-aluminum, all-composite, and "hybrid" combinations of these materials that were considered are shown in Fig. 4-3.

Fourteen discrete "time slices," during an orbit, were selected for the analysis. The cap, vertical, and diagonal temperatures corresponding to these "time slices," and for which member strains were developed, are shown in Fig. 4-4 for both the white paint and black anodize coatings.

3

CAPS	DIAGONALS	VERTICALS	
ALUM	ALUM	ALUM	
ALUM	ALUM	COMPOSITE	
ALUM	COMPOSITE	COMPOSITE	
COMPOSITE	COMPOSITE	COMPOSITE	
0.102	0.0689	0.0689	X-SECTIONAL AREA (SQ IN.)

ALUMINUM: $\alpha = 12.5 \times 10^{-6}$ IN./IN./°F; $E = 10.5 \times 10^{6}$ psi

COMPOSITE: $\alpha = 2.0 \times 10^{-6}$ IN./IN./°F; $E = 10.5 \times 10^{6}$ psi

1027-217W
3

IRAD

Fig. 4-3 Material Combinations

		VERTICALS			CAPS			DIAGONALS		
		1	2	3	4	5	6	7	8	9
Z-93 WHITE PAINT	ORBIT TIME, MIN									
	W 0	-11	-54	-62	-20	-30	-28	-44	-17	-17
	10	-22	-54	-47	-20	-24	-31	-42	-24	-13
	16	-36	-56	-36	-23	-33	-36	-38	-34	-20
	20	-45	-59	-34	-25	-25	-40	-37	-34	-30
	30	-58	-64	-33	-29	-24	-45	-32	-24	-48
	40	-63	-67	-69	-56	-61	-71	-66	-58	-69
	50	-67	-70	-79	-65	-72	-81	-74	-66	-74
	W 60	-68	-72	-82	-68	-76	-85	-76	-67	-75
	65	-68	-72	-83	-69	-77	-86	-77	-67	-77
	70	-60	-50	-82	-45	-59	-64	-40	-55	-56
	76	-40	-50	-77	-31	-47	-47	-20	-46	-48
	80	-30	-53	-75	-29	-42	-52	-21	-38	-48
	90	-12	-55	-66	-22	-34	-28	-31	-18	-31
	W 95	-11	-54	-63	-20	-31	-25	-45	-15	-19
BLACK ANODIZE	ORBIT TIME, MIN									
	B 0	70	-8	-18	55	59	28	0	67	68
	10	40	-10	30	56	55	50	21	50	75
	16	0	-20	50	46	23	45	30	26	60
	20	-17	-30	55	45	36	43	33	26	32
	30	-40	-47	52	40	35	36	43	42	-5
	40	-55	-60	-53	-45	-45	-50	-58	-45	-59
	50	-64	-66	-72	-66	-66	-73	-73	-60	-70
	B 60	-66	-71	-80	-72	-72	-81	-79	-64	-75
	65	-66	-72	-81	-73	-73	-83	-80	-64	-76
	70	-30	15	-77	-10	10	0	30	-20	10
	76	12	12	-60	30	38	20	53	12	22
	80	50	-10	-50	40	41	0	52	30	18
	90	74	-12	-23	57	58	47	30	68	50
5183-218W 3	B 95	72	-8	-19	55	60	48	2	70	68

Fig. 4-4 One-Meter Beam: Induced Temperatures During an Orbit (Degrees Centigrade) IRAD

3

4.2 CENTROIDAL MOTION

The centroidal motion of the X-axis (along the length of the beam) of a 10.5 meter length of one-meter beam is shown in Fig. 4-5 for both black anodize and Z-93 white paint coatings. The motion during an orbit is the same for both fix-free and free-free end conditions. The black anodize beam expands and contracts during an orbit transit, with the contraction occurring on the dark side. The white paint-coated beam, operating significantly cooler with this coating, exhibits a negative X-axis centroidal motion during an orbit transit. Namely, the beam has "shrunk" relative to its originally fabricated length. The overall range of linear motion of the white paint coated beam is about 0.5 in.

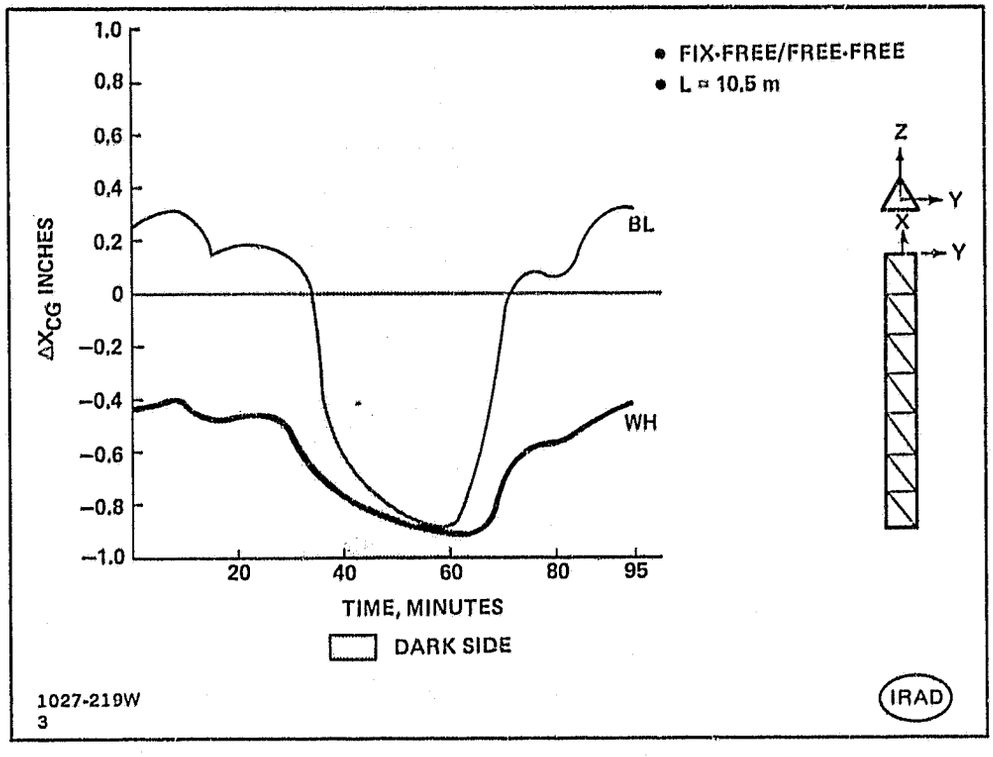

Fig. 4-5 One-Meter Beam X-Axis Motion During an Orbit

The centroidal motion of the Y-axis (lateral motion) of a 10.5 meter length of a one-meter beam is shown in Fig. 4-6. The lateral motions during an orbit range from positive to negative, with similar dimensional excursions applying to both coating conditions. The overall range of lateral motion of the white paint-coated beam is about 1.4 in.

The centroidal motion of the Z-axis (toward an apex) of a 10.5 meter length of a one-meter beam is shown in Fig. 4-7. Motions during an orbit range from positive to negative, with the lesser dimensional excursions of about 1.5 in. applying to the white paint coated beam.

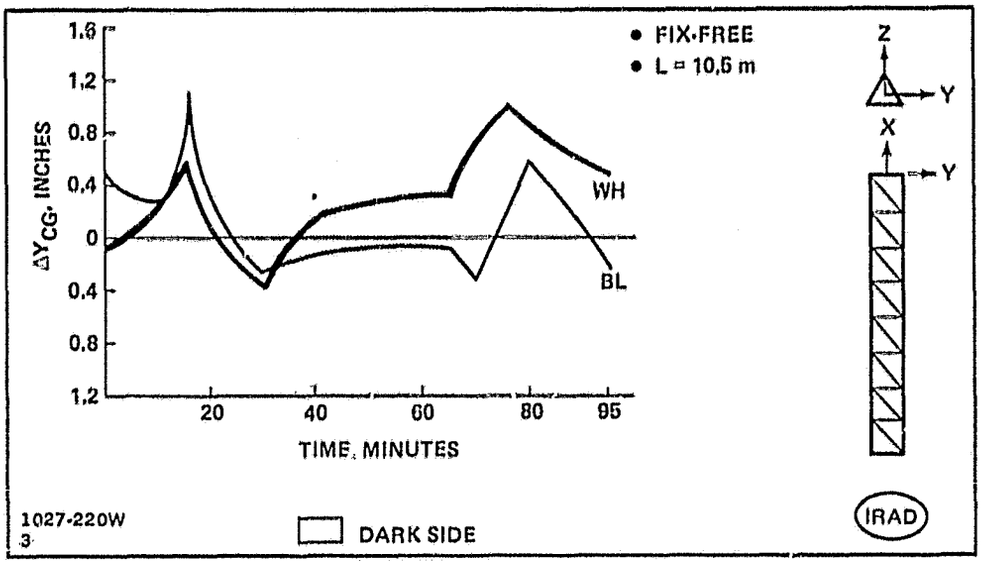

Fig. 4-6 One-Meter Beam Y-Axis Motion During an Orbit

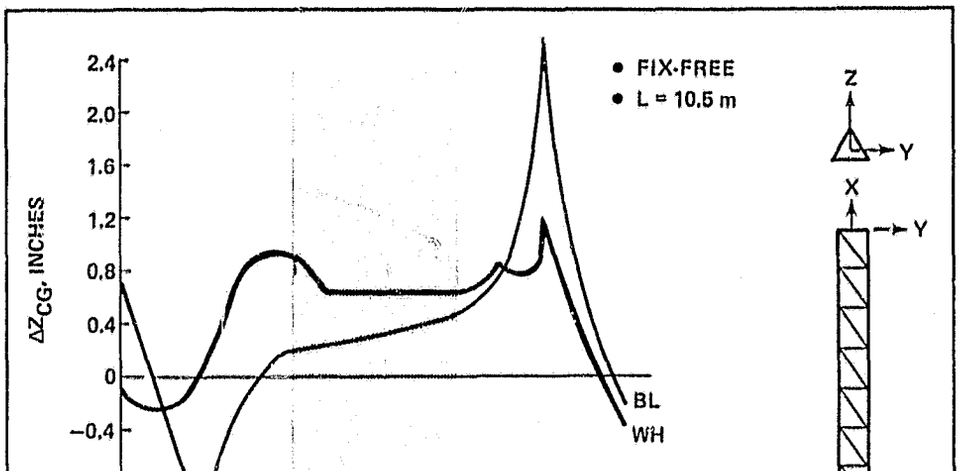

Fig. 4-7 One-Meter Beam Z-Axis Motion During an Orbit

3

4.3 DISTORTION DURING AN ORBIT

4.3.1 One-Meter Beam Tilt

The variation of tilt angle (β), during an orbit, that occurs at the tip of a one-meter beam is shown in Fig. 4-8 for both black anodize and Z-93 white paint coatings. These characteristics apply to both fixed-free and free-free beam conditions, with the β angle defined as the plane connecting the three beam caps. Considerable tilt angle motions occur during an orbit for the black anodize beam, ranging from positive to negative. In contrast, the white paint coated beam maintains a positive tilt angle condition during a complete orbit, with moderate overall excursions of about 0.2°.

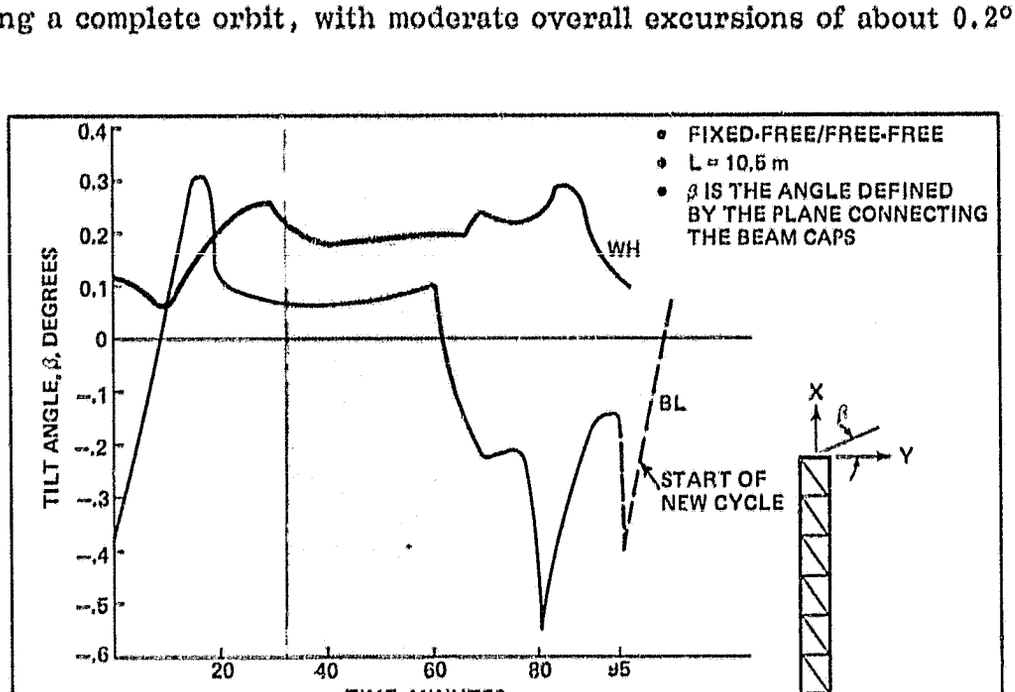

Fig. 4-8 One-Meter Beam Tilt During an Orbit

4.3.2 One-Meter Beam Twist

The twist of a 10.5-m length of a one-meter all-aluminum beam, during an orbit, is shown in Fig. 4-9 for both black anodize and Z-93 white paint coatings. The twist characteristics exhibited by a white paint-coated beam are about half those of a black anodized beam. The white paint beam generally maintains a positive twist condition, with overall excursions of about 0.8°.

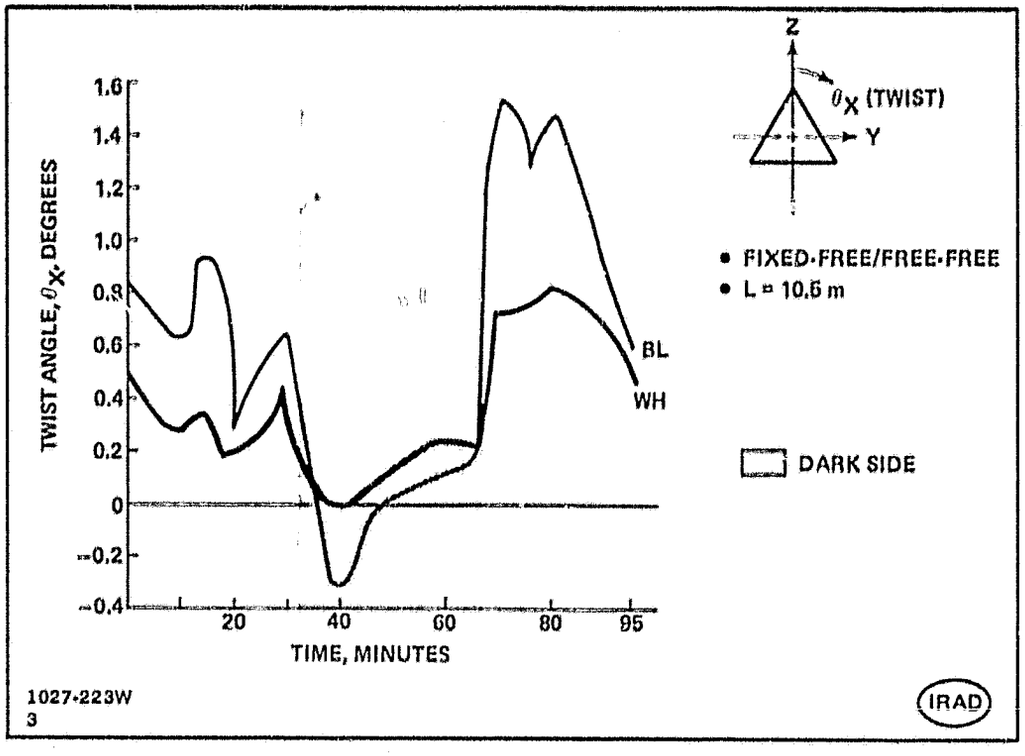

Fig. 4-9 One-Meter Beam Twist During an Orbit — Aluminum Structure

Figure 4-10 illustrates the twist of a 10.5-m length of a one-meter beam made of aluminum caps and composite diagonals/verticals, also for both black anodize and Z-93 white paint coating characteristics. During an orbit transit, the maximum twist angle of this hybrid beam combination is over four times greater than the white paint-coated, all-aluminum beam (4.5° max vs 0.8° max). This hybrid beam with a white paint coating maintains a positive twist condition, with overall excursions of about 2.5°.

The twist of a 10.5-m length of a 1-meter beam made of aluminum caps/diagonals and composite verticals, is illustrated in Fig. 4-11 for the black anodize and Z-93 white paint coating. During an orbit transit, the maximum twist angle of this hybrid beam combination is more than double the white paint-coated, all-aluminum beam (2.3° max vs 0.8° max). In contrast to the composite diagonals/verticals hybrid combination, this hybrid beam with white paint coating maintains a negative twist condition, with overall excursions of about 1.2°.

The twist characteristics, during an orbit, of a 10.5-m length of a one-meter, all-composite beam is shown in Fig. 4-12, also for the black anodize and Z-93 white paint coatings. The twist characteristics of the white paint-coated beam are about half those of the black coated beam (similar to the all-aluminum beam). Both types of coatings

3

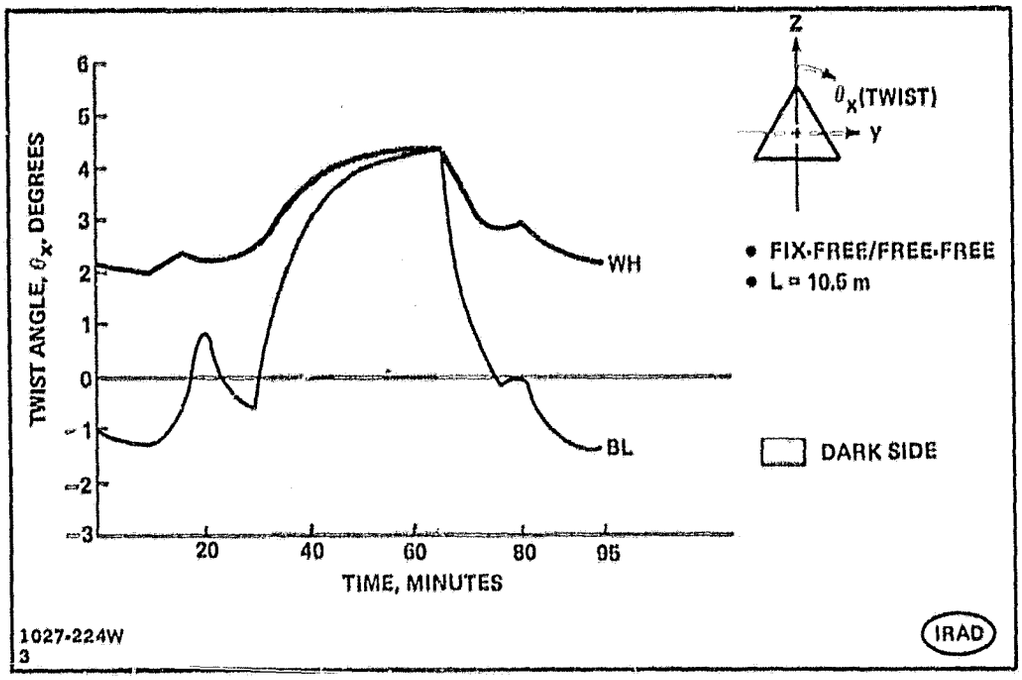

Fig. 4-10 One-Meter Beam Twist During an Orbit — Aluminum Caps, Composite Diagonals/Verticals

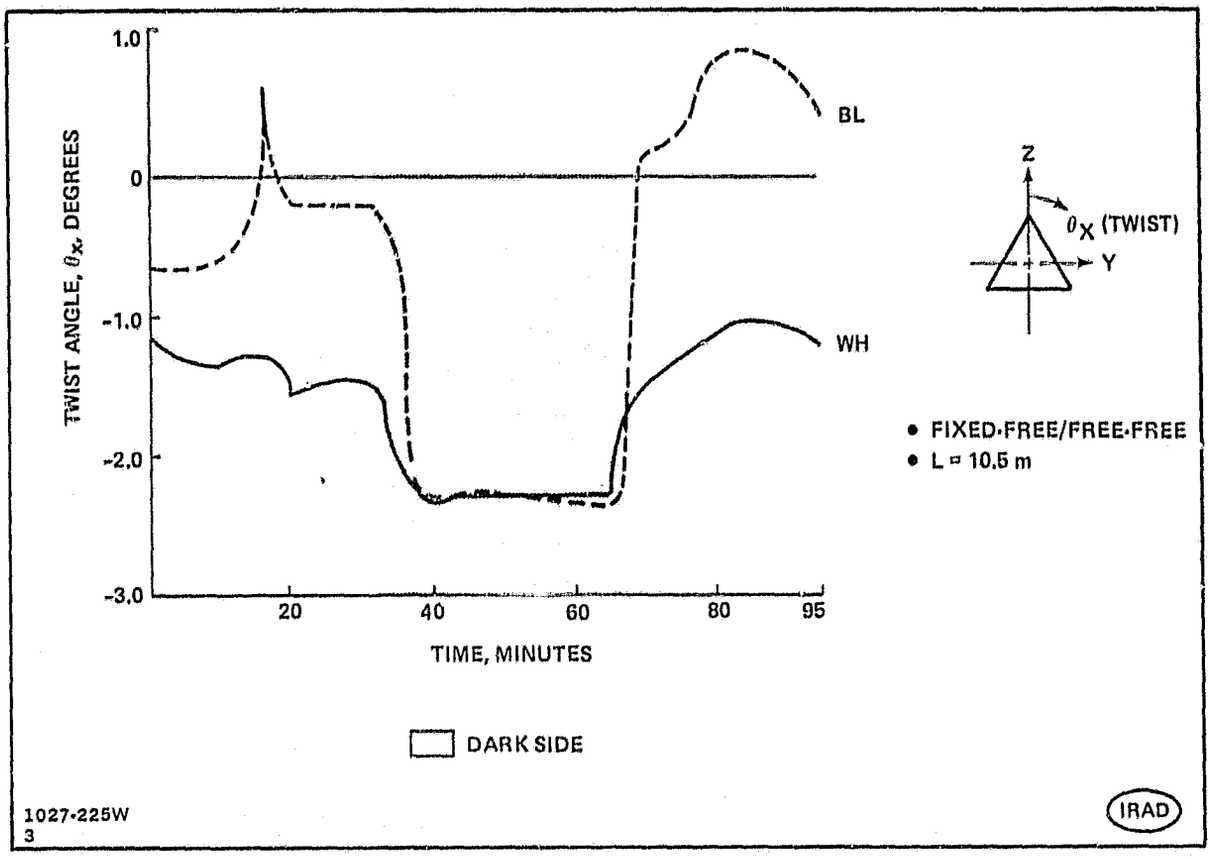

Fig. 4-11 One-Meter Beam Twist During an Orbit — Aluminum Caps/Diagonals, Composite Verticals

indicate a positive twist condition of the 1-meter beam, with the white paint conditions showing a peak twist of about 0.1°, and also an excursion of about 0.1°. The twist of an all-composite structure, therefore, in terms of overall excursion of a 1-meter beam, is about 1/6 that of an all-aluminum structure.

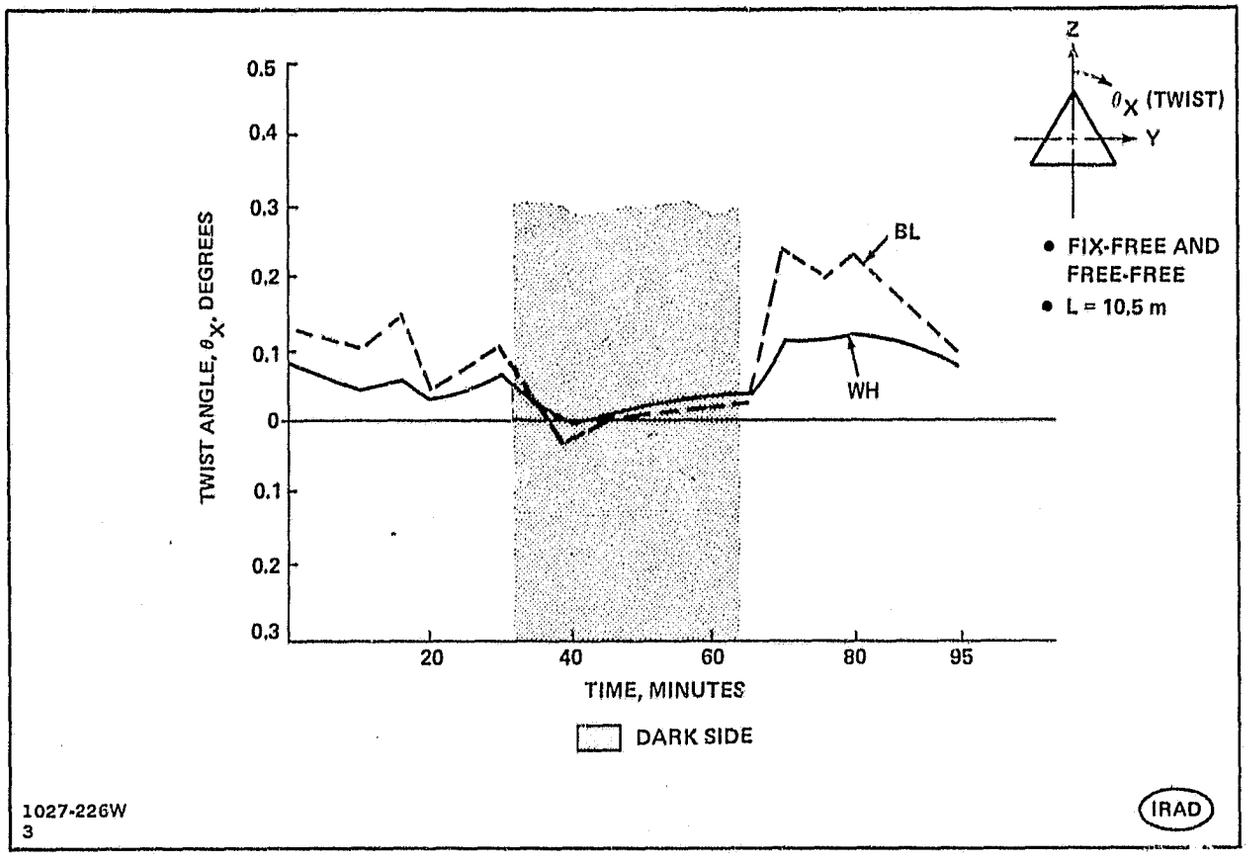

Fig. 4-12 One-Meter Beam Twist During an Orbit — Composite Structure

Figure 4-13 summarizes the twist characteristics during an orbit, of the various white paint-coated, one-meter beam material combinations investigated in this study. Clearly, the all-aluminum or all-composite beam is favored over the hybrid beam variations. Although the all-composite beam reduces twist by 1/6, the specific structural application would dictate its usage over an all-aluminum beam.

4.4 DISPLACEMENTS/DISTORTION AS A FUNCTION OF BEAM LENGTH

The maximum linear displacements in X, Y, and Z axis directions for fixed-free and free-free white paint-coated one-meter aluminum beams, are shown in Fig. 4-14 and 4-15, as a function of beam length. The fixed-free situation represents the condition of the one-meter beam during fabrication by the ABB, whereas the free-free situation represents the condition of the beam as would be available for construction/assembly of a LSS.

3

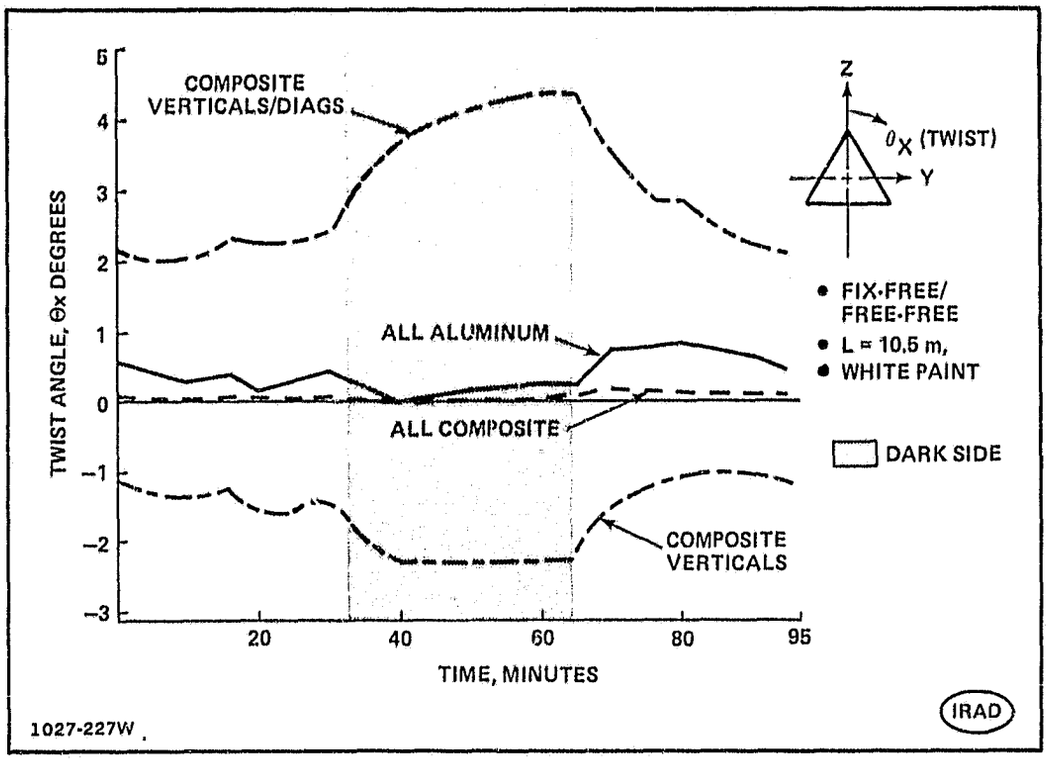

Fig. 4-13 One-Meter Beam Twist During an Orbit

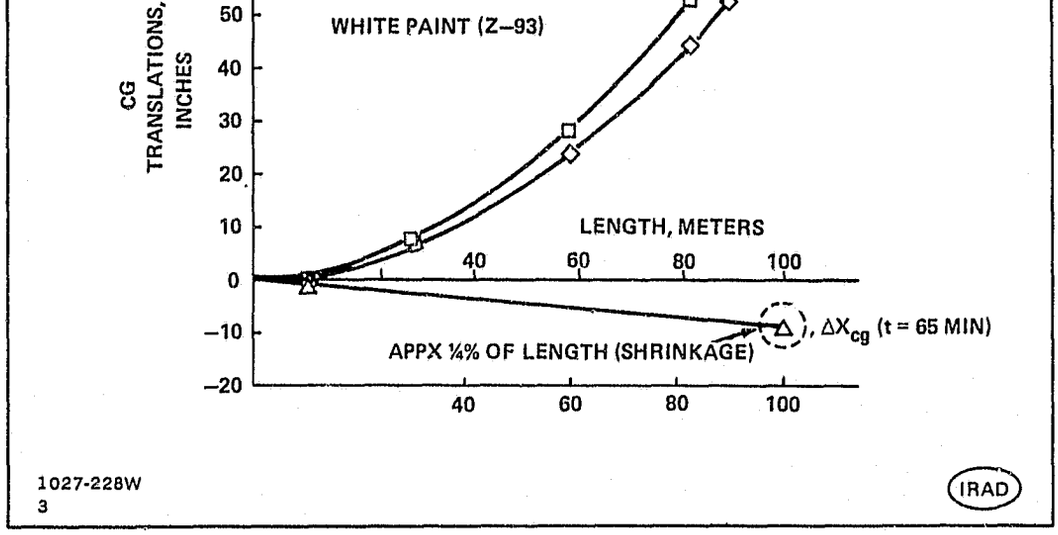

Fig. 4-14 Centroid Motions vs Length (Aluminum)-Fix-Free

3

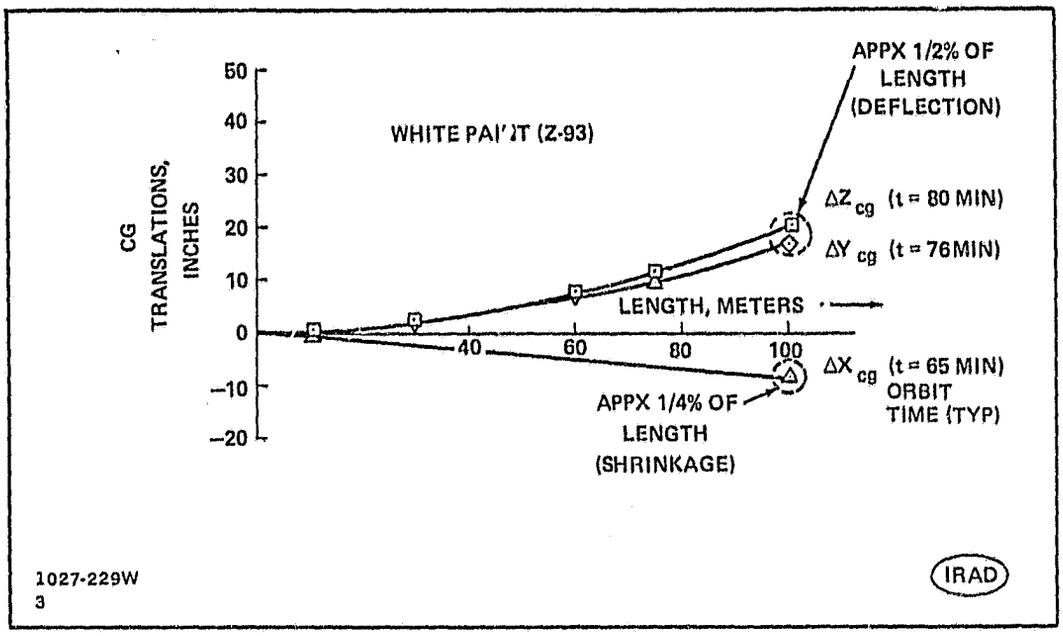

Fig. 4-15 Centroid Motions vs Length (Aluminum)-Free-Free

The maximum X, Y, and Z displacements generally correspond to terminator entry or exit positions in the orbit. As shown in Fig. 4-14, for the fixed-free condition, at the 100-m beam length, the Y and Z-axis centroidal deflection is less than 2% of the beam's length, with the X-axis motion indicating a "shrinkage" of about 1/4% length. For the free-free condition (Fig. 4-15), at a 100 meter beam length, the Y and Z-axis centroidal deflection is about 1/2% of beam length, with the X-axis motion also indicating a "shrinkage" of about 1/4% length.

The maximum twist and tilt angles observed for the white paint-coated, one-meter aluminum beam are shown in Fig. 4-16 as a function of beam length. The data applies to both fixed-free and free-free beam conditions, and represent the time intervals in the orbit during which the peak distortions occur. The maximum distortions, which occur at discrete positions in the orbit, generally correspond to entry or exit from the terminator. At these orbital positions, a 100-m beam length would exhibit a 2-1/2 degree tilt (before entry into the terminator) and a twist of about 8° (following exit from the dark side).

It should be noted, however, that the maximum twist and tilt angles are in reference to the as-built condition of the beam (e.g., 70°F ABB construction temperature). A new reference will be established when the beam is physically joined as part of a completed structural assembly. The on-orbit condition of the beam (corresponding to an orbit time) at which the joining/restraint is accomplished, will establish the new reference about which the beam's twist and tilt excursions will occur.

3

It is also of interest to compare the beam's linear motion and distortion (in orbit) with potential manufacturing tolerances associated with ABB fabrication. The fabrication tolerances associated with 1-m beam production (Fig. 4-17) indicate that the "bow" of a beam is expected to be limited to 0.5% of length, while the overall length is to be controlled to ±0.5 mm/ m (0.05% of length). Twist characteristics of the beam produced by the ABB will be determined from ground tests, although no visible twist has been discerned in tests conducted to date.

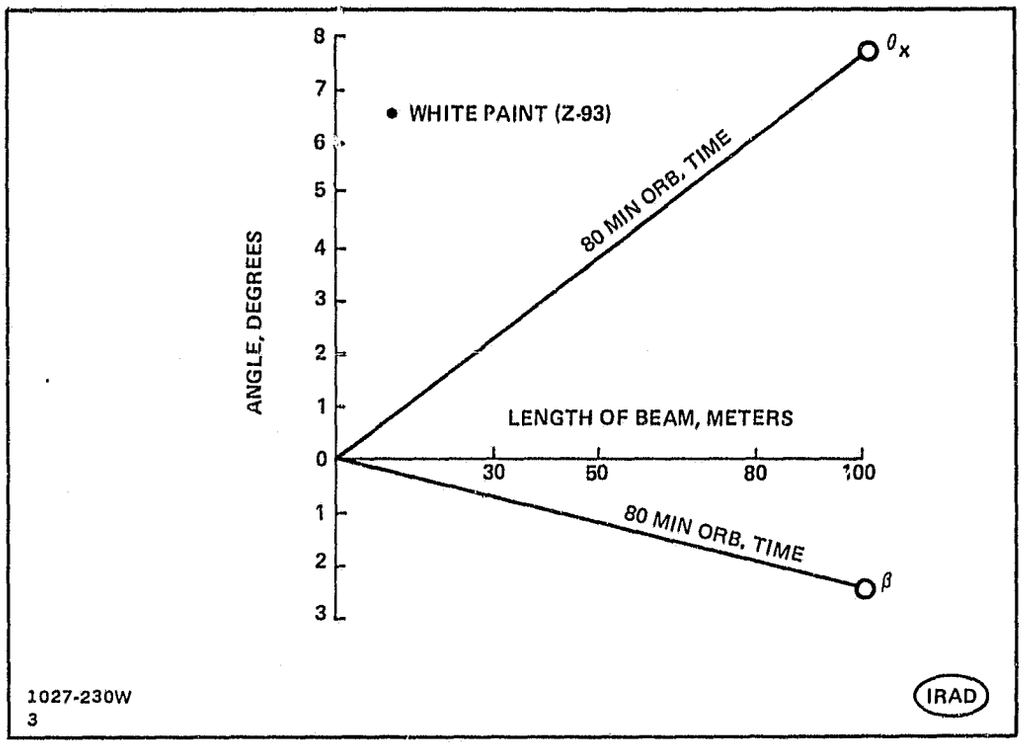

Fig. 4-16 Twist (θ_x) and Tilt (β) vs Length (Aluminum) Fix-Free/Free-Free

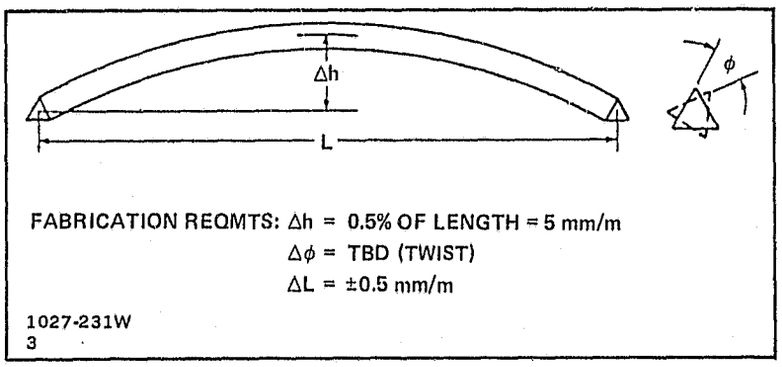

Fig. 4-17 Manufacturing Tolerances — 40-Meter Beam Length

The fabrication tolerances, in terms of "bow," are suggestive of Y and Z axis motions of the beam. As indicated in Fig. 4-15, these motions are comparable to the beam's response in orbit. It would also appear that the 1-meter beam's twist, when exposed to the orbital environment, is of the same order as likely manufacturing tolerances that would be associated with continuous-length structures of comparable lengths.

4.5 RESTORING LOADS

4.5.1 Restoring Tilt Loads

Thermally-induced deflections cause the three beam caps to have different elongations in the X-direction. External restoring moments can be applied to make all three caps have equal elongations in the X-direction. The moments are applied as pure moments so as to not inhibit the overall axial expansion/contraction (X) or lateral motions (Y and Z) of the beam. These moments, applied in two directions (My and Mz, as illustrated in Fig. 4-18) can be combined into a resultant moment vector, Mr, oriented in a direction identified by the angle $\gamma = \tan Mz/My$. The tilt moment would be applied by an end attachment, for example, as to force all X-deflections to be the same amount at the tip (see Fig. 4-18).

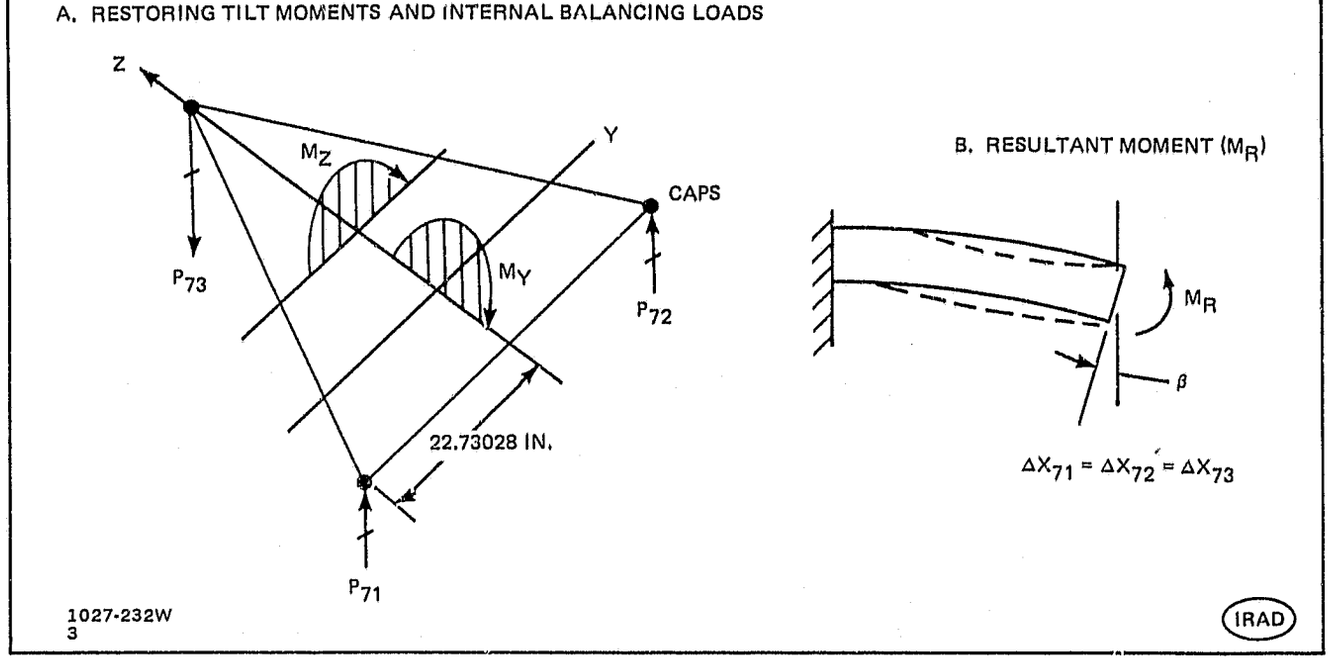

Fig. 4-18 Restoring Tilt Moment

3

The induced compression loads in the caps caused by a maximum limit restoring tilt moment (Mr) are shown in Fig. 4-19. The orbit time intervals approximately correspond to the maximum tilt (β) experienced during an orbit. The loads induced within the 1-meter beam by the restoring tilt moment appear as cap loads only; diagonal and vertical element loads are zero. As shown in Fig. 4-19, the Z-93 white paint, all-aluminum beam exhibits a maximum compressive cap load of about 80% of allowable, versus the black anodize beam with a cap load of about 95% of allowable. Loads in the other caps may or may not be tension under this restoring moment (Mr) condition.

THERMAL COATING	BEAM MATERIAL	ORBIT TIME, MIN	TILT MOMENT, M_R		INDUCED COMPRESSION LOADS (LIMIT)		
					CAP	DIAGONAL	VERTICAL
			(LIMIT)	IN.-LB	LB	LB	LB
WHITE	ALL ALUMINUM	80	MAX	12650	-290	0	0
	COMPOSITE VERTICALS	80	MAX	12650	-290	0	0
	COMPOSITE VERTICALS/ DIAGONALS	80	MAX	12650	-290	0	0
	ALL COMPOSITE	80	MAX	2025	-46	0	0
BLACK	ALL ALUMINUM	80	MAX	25620	-337	0	0
	COMPOSITE VERTICALS	80	MAX	25620	-337	0	0
	COMPOSITE VERTICALS/ DIAGONALS	80	MAX	25620	-337	0	0
	ALL COMPOSITE	80	MAX	4099	-54	0	0
	ALLOWABLE COMPRESSION*				-358	-100	-200
1027-233W 3	*ALUMINUM AND COMPOSITE ALLOWABLES ASSUMED IDENTICAL						IRAD

Fig. 4-19 Induced Loads Due to Restoring Tilt Moment; Beam Length = 10.5 m

4.5.2 Restoring Rotational Loads

The beam caps also deflect in the Y and Z directions, due to thermal effects, resulting in an overall rotation in a plane normal to the beam's X-axis (see Fig. 4-20). This rotation is expressed in terms of an angle, θ_x. When the rotation angle is forced back to zero by an external restoring moment (M_x), loads are induced in the diagonals,

caps, and verticals. The average deflections of the three tip nodes (nodes 71, 72, and 73) in all directions (X, Y, Z) remain the same before and after the tip rotational angle is restored to zero.

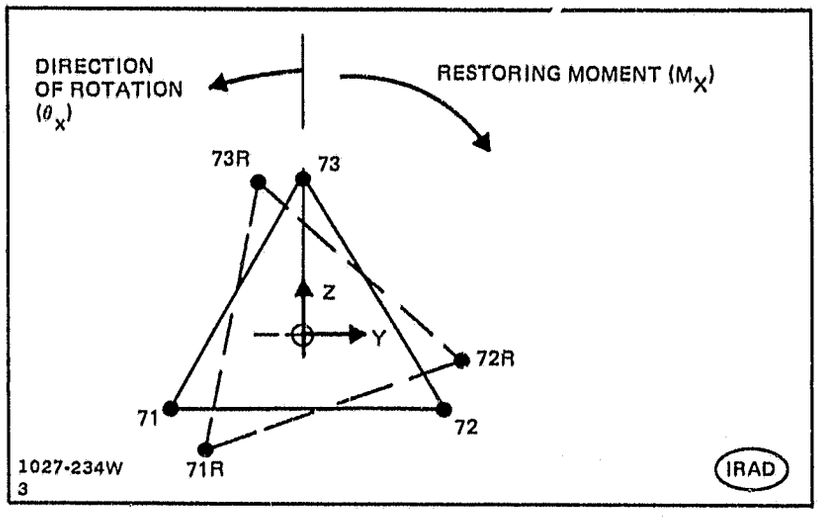

Fig. 4-20 Restoring Rotational Moment

The induced loads in the caps, verticals and diagonals caused by a maximum limit restoring rotational moment (M_x) are shown in Fig. 4-21. The loading conditions shown reflect the orbit time interval during which extreme twist conditions (Θ_x) occur. As shown in Fig. 4-21, allowable compression loads are exceeded within the diagonals of the hybrid (aluminum/composite) beams and all-aluminum beams. The Z-93 white paint coated diagonal is only slightly over the limit load condition, however, suggesting that the addition of stabilizing "lips" along the unsupported edges of the member would be in order to increase its load-carrying capability.

4.5.3 Combined Rotation and Tilt Restoring Loads

Restoring the thermally-deflected nodes at the beam tip back to zero rotation and tilt conditions simultaneously, results in induced loads in caps, verticals and diagonals. The maximum compression loads induced into the caps, however, do not necessarily occur at the same orbit time interval as the maximum compression loads in the verticals and diagonals. This "happens" to be the case for the Z-93 white paint coated all-aluminum and all-composite beams, but not for the other hybrid combinations or black anodize variations considered.

The overall ranges of cap, vertical, and diagonal loads induced by applying the combined restoring rotational and tilt moments are shown in Fig. 4-22 and 4-23. The high (e.g., tensile) and low (e.g., compressive) loading conditions are shown corre-

sponding with the orbit time interval of occurrence. The diagonal and vertical loads shown in Fig. 4-22 are those coexistent with the cap loads indicated. In like manner, Fig. 4-23 shows the cap loads coexistent with the diagonal and vertical loads.

Figures 4-22 and 4-23 show, that for the "preferred" Z-93 white paint-coated, all-aluminum beam the overall load ranges are:

Cap	Diagonal	Vertical
+339 lb to -209 lb	+3 lb to -102 lb	+62 lb to -2 lb

Under these conditions the only allowable load exceeded is the compressive diagonal load of 102 lb vs 100 lb allowable. As indicated previously, the addition of stabilizing "lips" to the unsupported edges of the diagonal cross-section should readily provide sufficient load-carrying capability.

Figure 4-24 summarizes the loading conditions in all of the structural elements of the 10.5 meter length of 1-meter beam. Both the black anodize and Z-93 white paint conditions are shown for the orbit time interval of 80 minutes.

THERMAL COATING	BEAM MATERIAL	ORBIT TIME, MIN	ROTATIONAL MOMENT, M_X (LIMIT)	INDUCED LOADS (LIMIT)		
				CAP	DIAGONAL	VERTICAL
			IN.-LB	LB	LB	LB
WHITE	ALL	40	79.2	-2	3	-2
	ALUMINUM	80	-2450	81	(-102)	62
	COMPOSITE	50	7018	-232	292	-178
	VERTICALS	90	3302	-109	137	-84
	COMPOSITE VERTICALS/ DIAGONALS	10	-6128	202	(-255)	156
		65	-13252	437	(-551)	337
	ALL	40	12.7	0	0	0
	COMPOSITE	80	-392	13	-16	10
BLACK	ALL	40	978	-32	41	-25
	ALUMINUM	70	-4583	151	(-191)	116
	COMPOSITE	40	7085	-234	295	-180
	VERTICALS	80	-2530	83	(-105)	64
	COMPOSITE VERTICALS/ DIAGONALS	95	4166	-137	173	-106
		65	-13101	432	(-545)	333
	ALL	40	156	-5	7	-4
	COMPOSITE	70	-733	24	-31	19
	ALLOWABLE COMPRESSION*			-358	-100	-200
1027-235W 3/	*ALUMINUM AND COMPOSITE ALLOWABLES ASSUMED IDENTICAL					(IRAD)

Fig. 4-21 Induced Loads Due to Restoring Rotational Moment; Beam Length = 10.5 m

3

THERMAL COATING	BEAM MATERIAL	ORBIT TIME, MIN	M_R TILT MOMENT	M_X ROTATIONAL MOMENT	INDUCED LOADS (LIMIT)		
					CAP	DIAGONAL	VERTICAL
			IN.-LB	IN.-LB	LB	LB	LB
WHITE	ALL	30	12008	-1283	339	-53	33
	ALUMINUM	80	12650	-2450	-209	(-102)	62
	COMPOSITE VERTICALS	80	12650	3390	153	141	-86
		65	9330	6913	(-429)	288	-176
	COMPOSITE VERTICALS/ DIAGONALS	65	9330	-13252	646	(-551)	337
		80	12650	-8694	-3	(-362)	221
	ALL	30	1493	-205	54	-8	5
	COMPOSITE	80	2025	-392	-33	-16	10
BLACK	ALL	80	25620	-4468	798	(-186)	113
	ALUMINUM	80	25620	-4468	-190	(-186)	113
	COMPOSITE VERTICALS	95	6604	-1283	26	-64	33
		65	6353	70[illegible]	-312	292	178
	COMPOSITE VERTICALS/ DIAGONALS	80	25620	72	649	3	-2
		0	18472	3109	(-383)	129	-79
	ALL	80	4100	-715	128	-30	18
	COMPOSITE	80	4100	-715	-30	-30	18
	ALLOWABLE COMPRESSION*				-358	-100	-200
1027-236W 3	*ALUMINUM AND COMPOSITE ALLOWABLES ASSUMED IDENTICAL						(IRAD)

Fig. 4-22 Range of Induced Cap Loads Due to Combined Restoring Rotational and Tilt Moments; Beam Length = 10.5 m

3

THERMAL COATING	BEAM MATERIAL	ORBIT TIME, MIN	M_R TILT MOMENT	M_X ROTATIONAL MOMENT	INDUCED LOADS (LIMIT)		
					CAP	DIAGONAL	VERTICAL
			IN.-LB	IN.-LB	LB	LB	LB
WHITE	ALL	40	8356	79.2	-162	3	-2
	ALUMINUM	80	12650	-2450	-209	(-102)	62
	COMPOSITE	50	8786	7018	(-417)	292	-178
	VERTICALS	90	6573	3302	-254	137	-84
	COMPOSITE VERTICALS/ DIAGONALS	10	2530	-6128	234	(-255)	156
		65	9329	-13252	646	(-551)	337
	ALL	40	1337	12.7	-26	0	0
	COMPOSITE	80	2025	-392	-33	-16	10
BLACK	ALL	40	3176	978	-73	41	-25
	ALUMINUM	70	10955	-4583	-90	(-191)	116
	COMPOSITE	40	3176	7085	-275	295	-180
	VERTICALS	80	25620	-2530	-254	(-105)	64
	COMPOSITE VERTICALS/ DIAGONALS	95	6604	4166	-274	173	-106
		65	6353	-13101	593	(-545)	333
	ALL	40	508	156	-11	7	-4
	COMPOSITE	70	1753	-733	-15	-31	19
	ALLOWABLE COMPRESSION*				-358	-100	-200
1027-237W 3	*ALUMINUM AND COMPOSITE ALLOWABLES ASSUMED IDENTICAL						(IRAD)

Fig. 4-23 Range of Induced Vertical and Diagonal Loads Due to Combined Restoring Rotational and Tilt Moments; Beam Length = 10.5 m

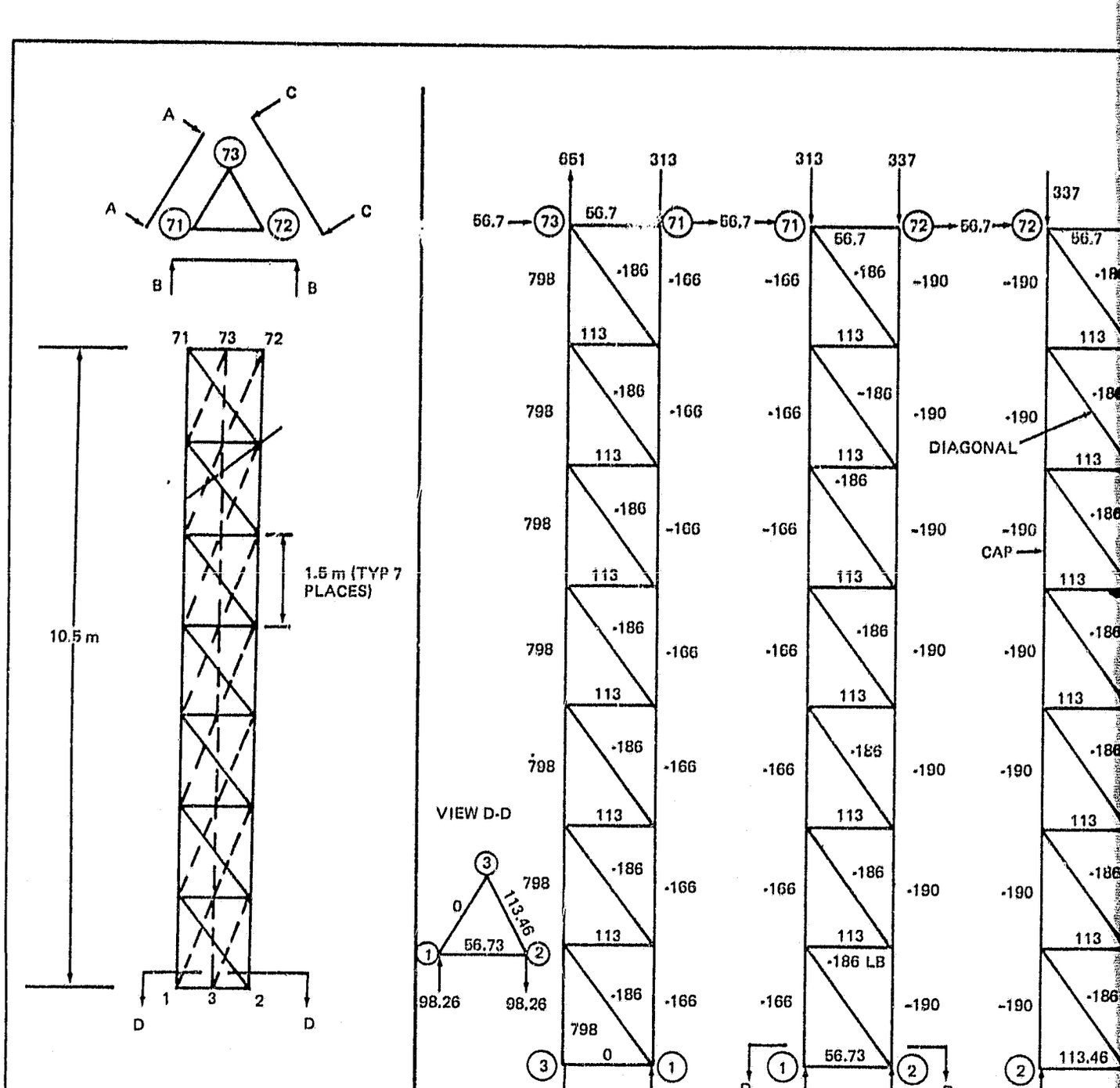

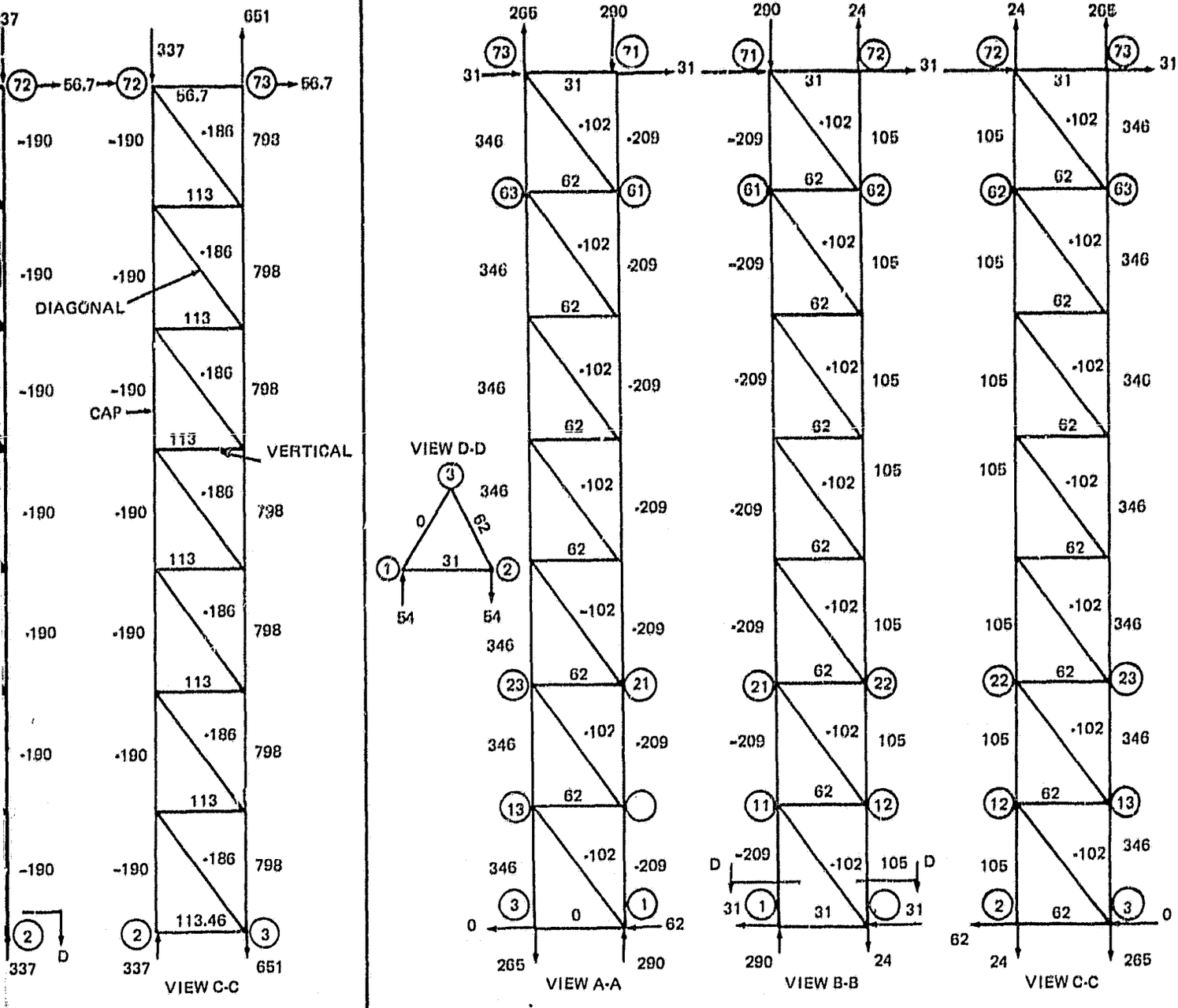

Fig. 4-24 Combined Member Loads (Lb) Due to Restoring Rotational and Tilt Moments: All-Aluminum Beam; Orbit Time Interval — 80 Minutes

FOLDOUT FRAME 2

5 - TRIBEAM THERMAL ANALYSIS

The 1-meter beam thermal analysis was extended to analyze a Tribeam structure as a free-flier, and as attached to the Orbiter. Figure 5-1 shows the flight orientation assumed for the analysis of a representative LSS Tribeam structure composed of 1-meter beam elements. The Tribeam was analyzed at the six locations shown, and the one-meter beams have been designated as follows:

- POP Beam - The beam perpendicular to the orbit plane.
- LV Beam - The beam aligned with the local vertical
- AVV Beam- The beam approximating the direction of the velocity vector.

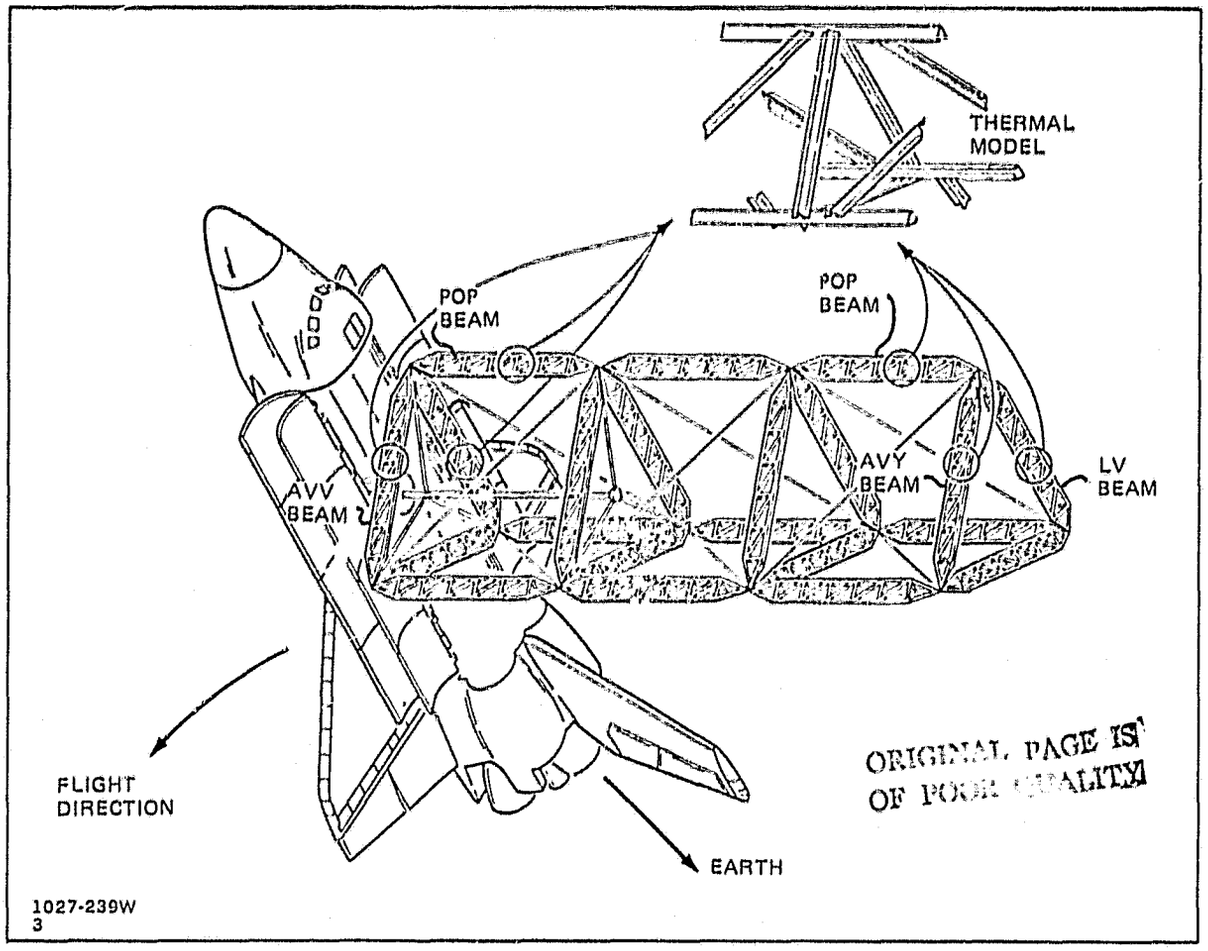

Fig. 5-1 Orientation Assumed for Tribeam Thermal Analysis

A separate analysis showed that the effect of the Orbiter on the temperatures of the upper bay, through radiant interchange and by blockage of earth emission and reflection, is negligible. Therefore, the analysis of the upper bay of the Orbiter-attached Tribeam assembly is applicable to a free-flier structure in the assumed orientation.

All Tribeam analyses are based upon the use of Z-93 white paint coating and the simplified 1-meter beam thermal model, as previously discussed in Section 3 of this report.

5.1 SOLAR BLOCKAGE

Two types of solar blockage occur in the case of the Tribeam analysis: the blockage of a 1-meter beam by another beam, and, as previously discussed, blockage of a structural element within the 1-meter beam by another element. Because of the distances between the 1-meter beams, in general, the beam-to-beam blockages are not complete due to the solar viewing angle; these were calculated by simple geometry. The more complex blockage of element by element was done by computer graphics.

Since the POP beam is in the same orientation as the original 1-meter beam analysis, its blockage is identical to that presented in Section 3 and Appendix B. For the LV beam, the graphics model (Thermal Model) was rotated to the position corresponding to the location of the LV beam, and then rotated about the Tribeam axis to represent the views as presented to the sun. Three of these solar views, from which the blockage can be calculated, are shown in Fig. 5-2. Additional views used to determine the blockage characteristics for the LV beam are presented in Appendix H. Since the AVV beam has the same orientations as the LV beam, except offset by 120° in orbit angle, the LV beam, corrected by that angle, can be used in calculating AVV beam solar blockages.

5.2 FREE-FLIER

The free-flier thermal analysis program, consisted of the 1-meter beam analysis modified for the proper solar, earth-emitted, and earth-reflected energy with the appropriate blockage factors. The resulting temperatures of the POP, LV, and AVV beams are shown in Fig. 5-3, 5-4, and 5-5 respectively, where the average temperatures of the caps, diagonals, and verticals are shown over the period of an orbit. These temperatures can subsequently be used in a structural analysis program for calculating the stresses and deformations of the Tribeam. All of the individual nodal temperatures that form these structural element average temperatures are documented in Appendices J, K, and L.

3

ORIGINAL PAGE IS
OF POOR QUALITY

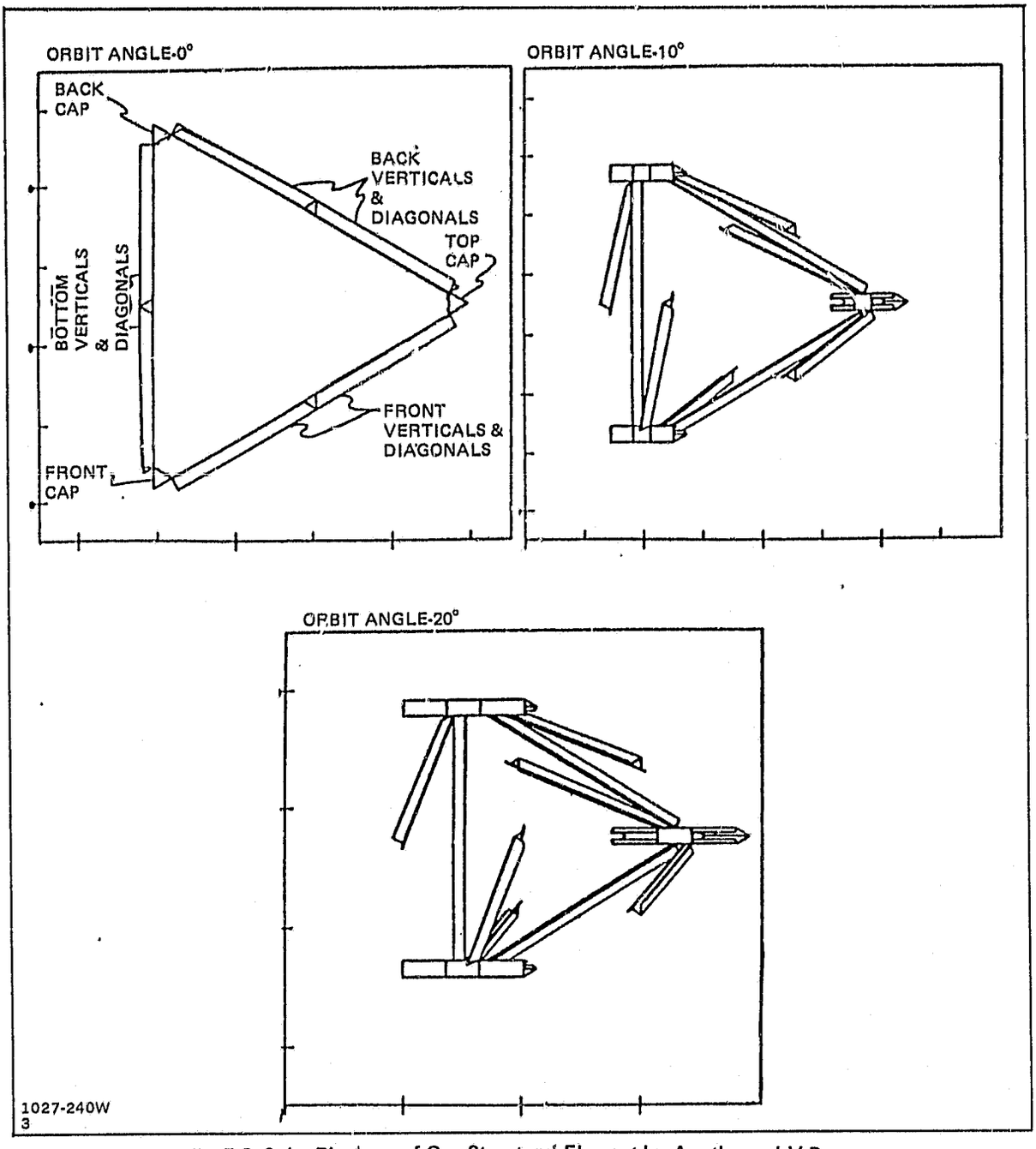

Fig. 5-2 Solar Blockage of One Structural Element by Another — LV Beam

3

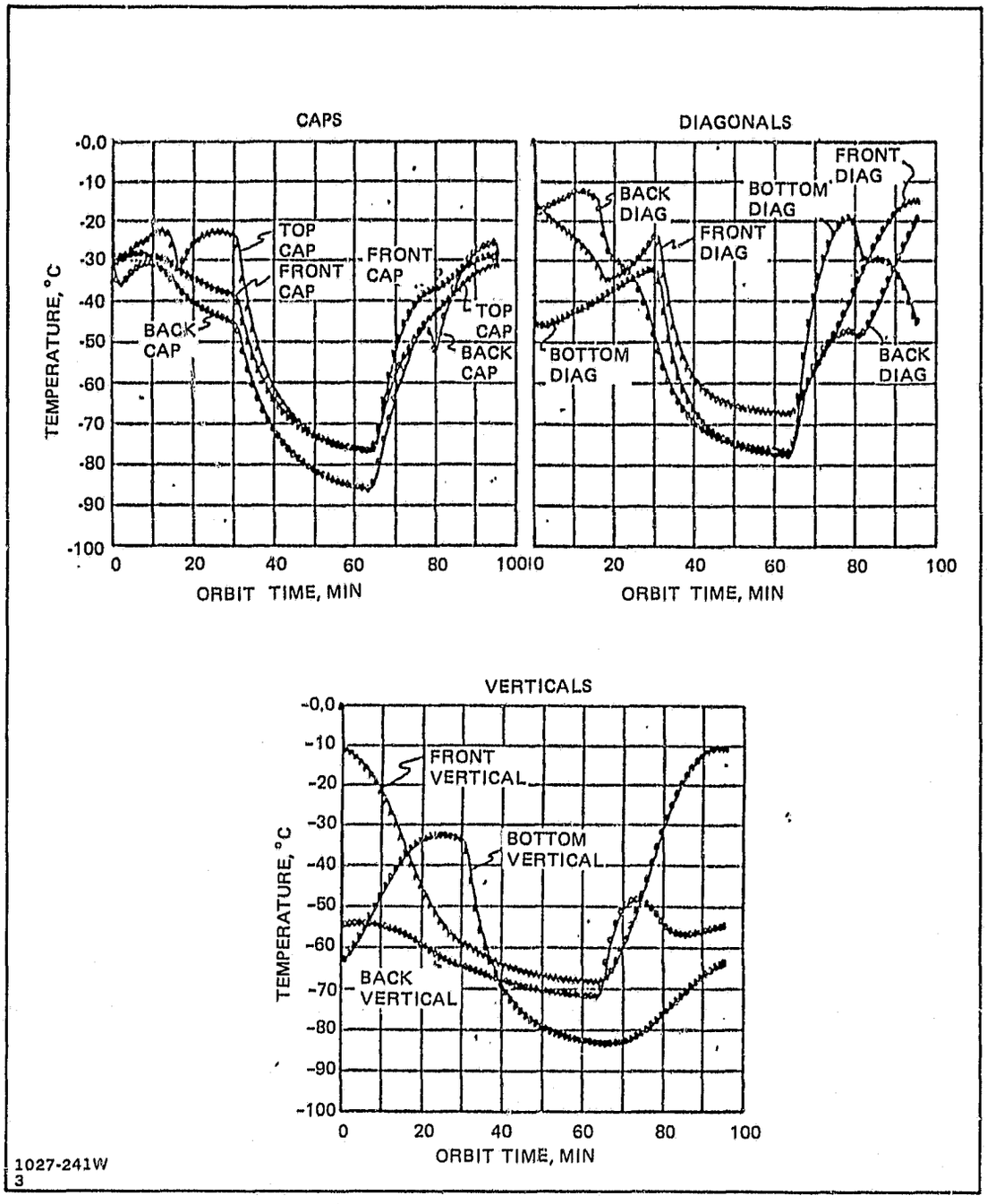

Fig. 5-3 Free-Flier — POP Beam Temperatures

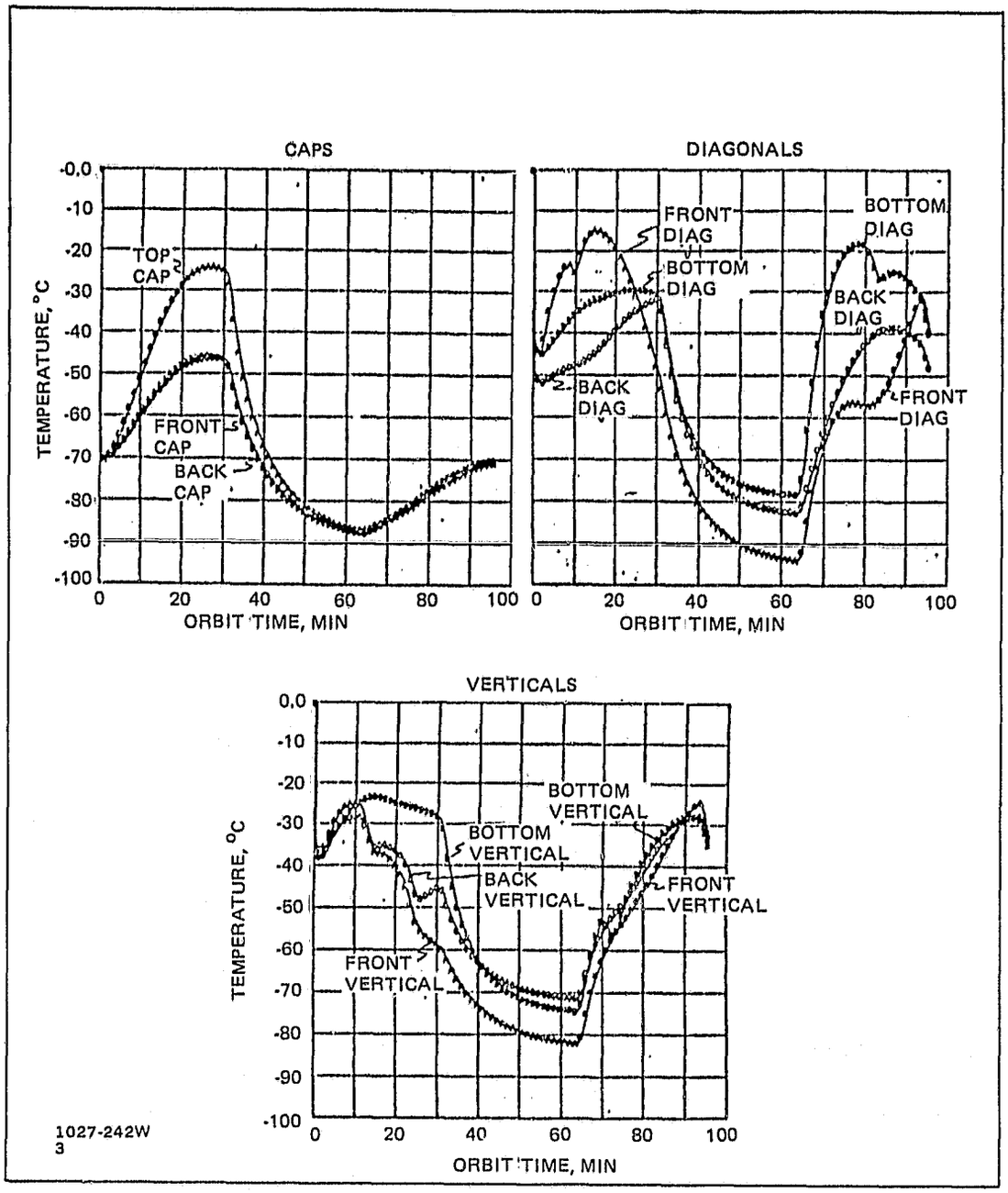

Fig. 5-4 Free-Flier – LV Beam Temperatures

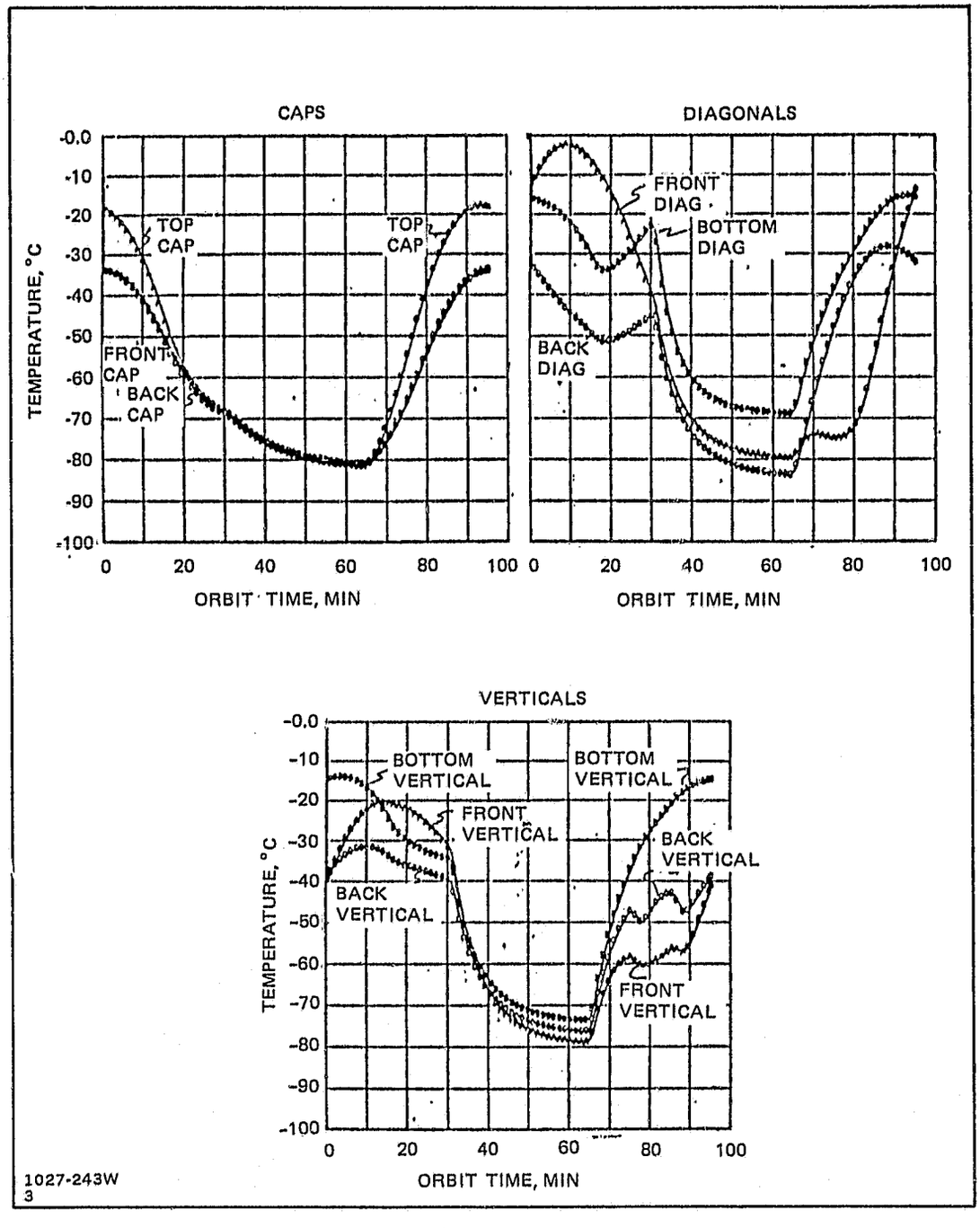

Fig. 5-5 Free-Flier -- AVV Beam Temperatures

The maximum gradients between elements of the three beams of the free-flier are shown in the following table:

Maximum Gradients Between Elements-(°C/°F)

	POP Beam	LV Beam	AVV Beam
• Caps	23/41	23/41	16/29
• Diagonals	31/56	39/70	42/76
• Verticals	54/97	30/54	26/47

Figures 5-6, 5-7, and 5-8 compare the respective cap, diagonal, and vertical temperature characteristics of the three 1-meter beams forming the free-flying Tribeam. As shown in Fig. 5-6, the cap temperatures of the POP and AVV beams are quite similar; the LV beam caps, however, are about 40°C (72°F) lower than the others at the beginning (or end) of an orbit transit. The curves also indicate that the temperatures and overall temperature excursions of the LV and AVV beams are generally within the range of the POP beam. It would appear, therefore, that an individual 1-meter beam in the POP attitude could be used to generally describe the thermal characteristics of Tribeam structures built from 1-meter beams. However, the transient temperature characteristics of the beams and their respective structural elements are necessary to determine the distortion of the structure during an orbit transit.

5.3 ORBITER ATTACHED

The basic 1-meter beam program, modified to suit the three beams of the free-flier, was modified again to account for the proximity of the Orbiter. To the free-flier thermal analysis program was added the radiative interchange with the radiator and cold surfaces of the Orbiter, and the blockage of the earth's emitted and reflected solar energy. Figure 5-9 shows the orientation of the lower Tribeam bay and the Orbiter radiators. The Orbiter radiator temperatures * used for panels 1 through 4 were 35°, 43°, 74° and 95° respectively (2°, 6°, 23°, 35°C). The Orbiter cold surfaces (using surface properties from JSC 07700, Vol. XIV, Rev. F, "Space Shuttle Systems Payload Accommodations") were calculated to be -57°C (-71°F) for this orbit.

---

*Ref: Telecon with Jim Jax of Marshall Space Flight Center

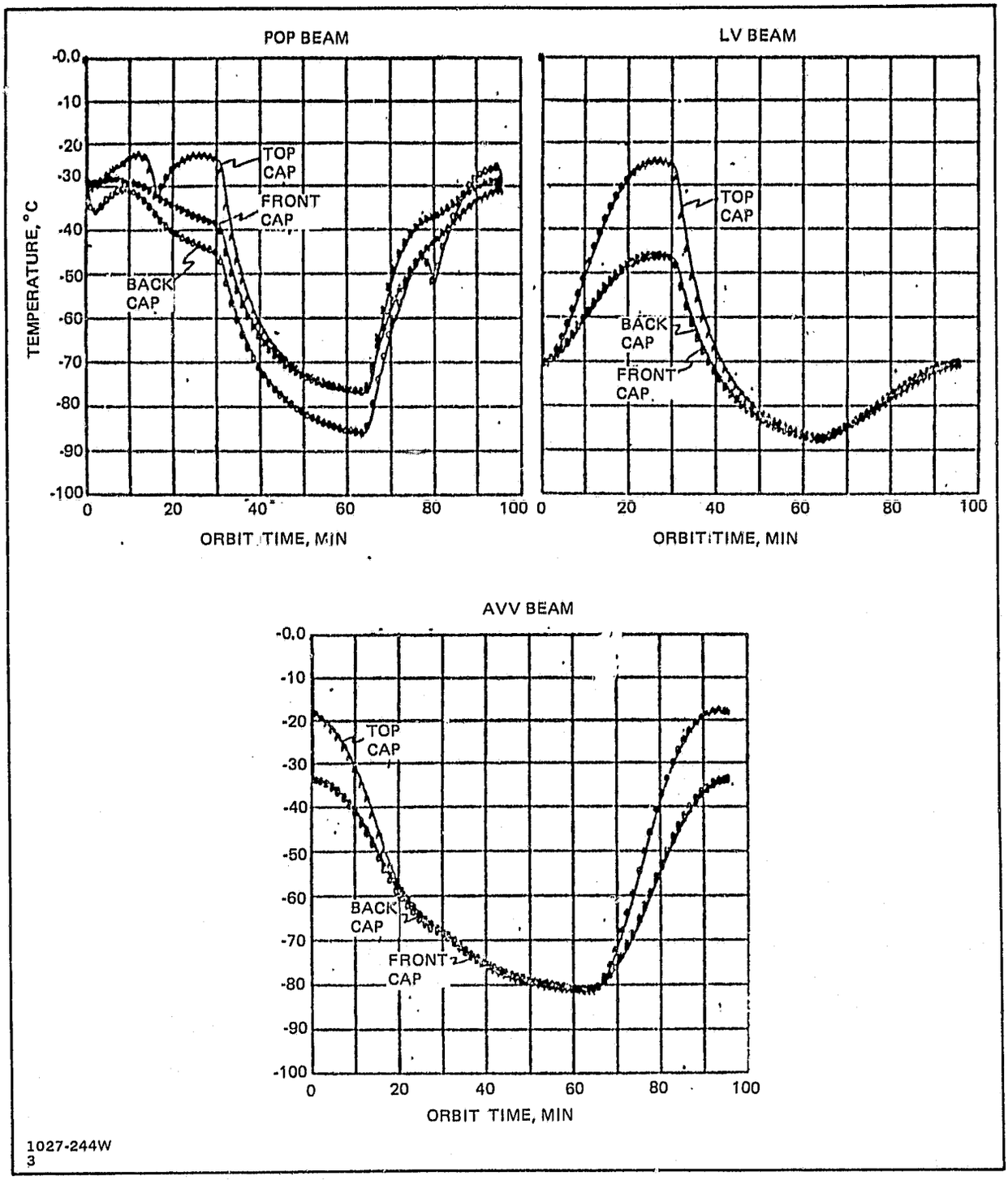

Fig. 5-6 Free-Flier — Cap Temperatures

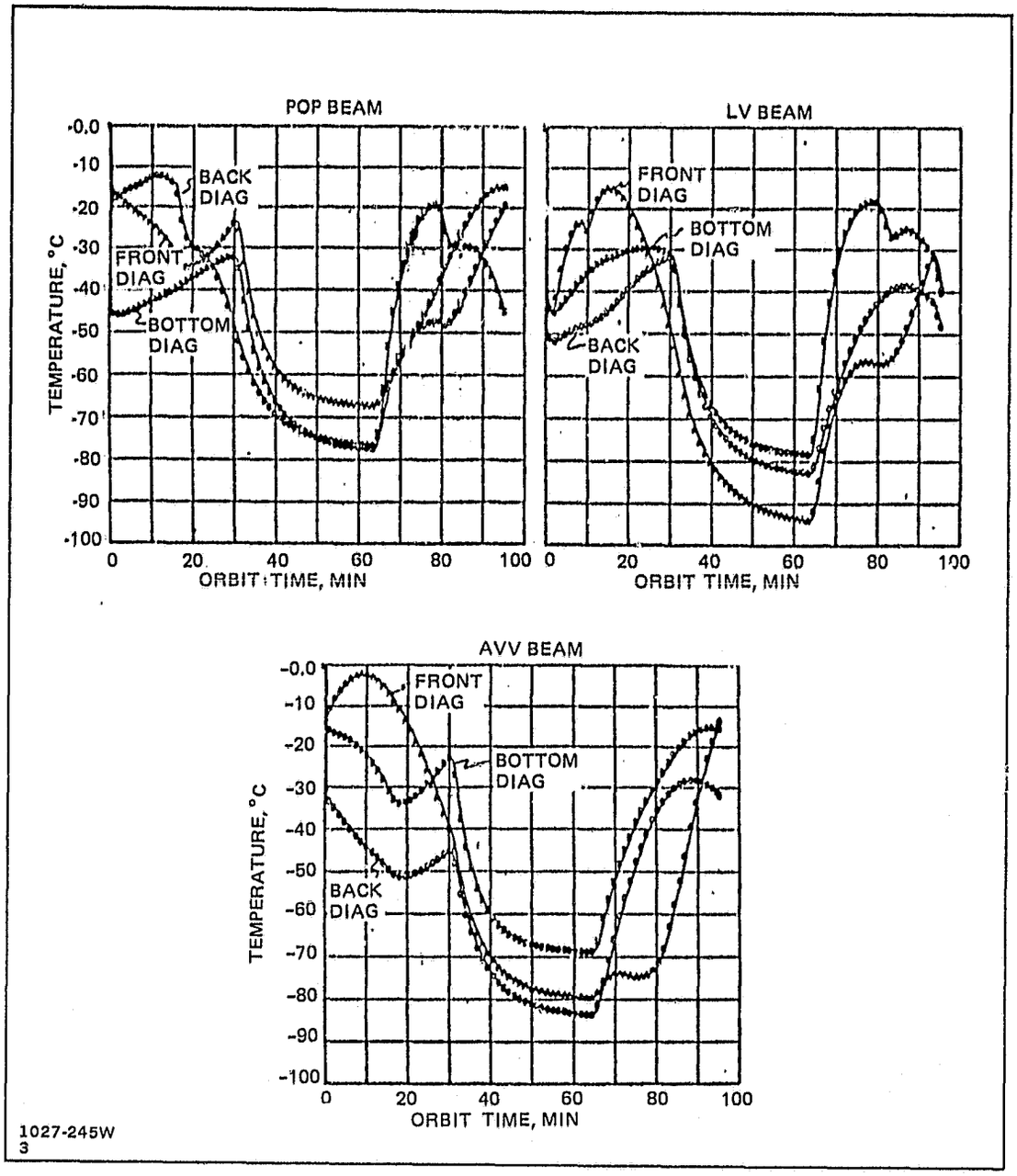

Fig. 5-7 Free-Flier — Diagonal Temperatures

3

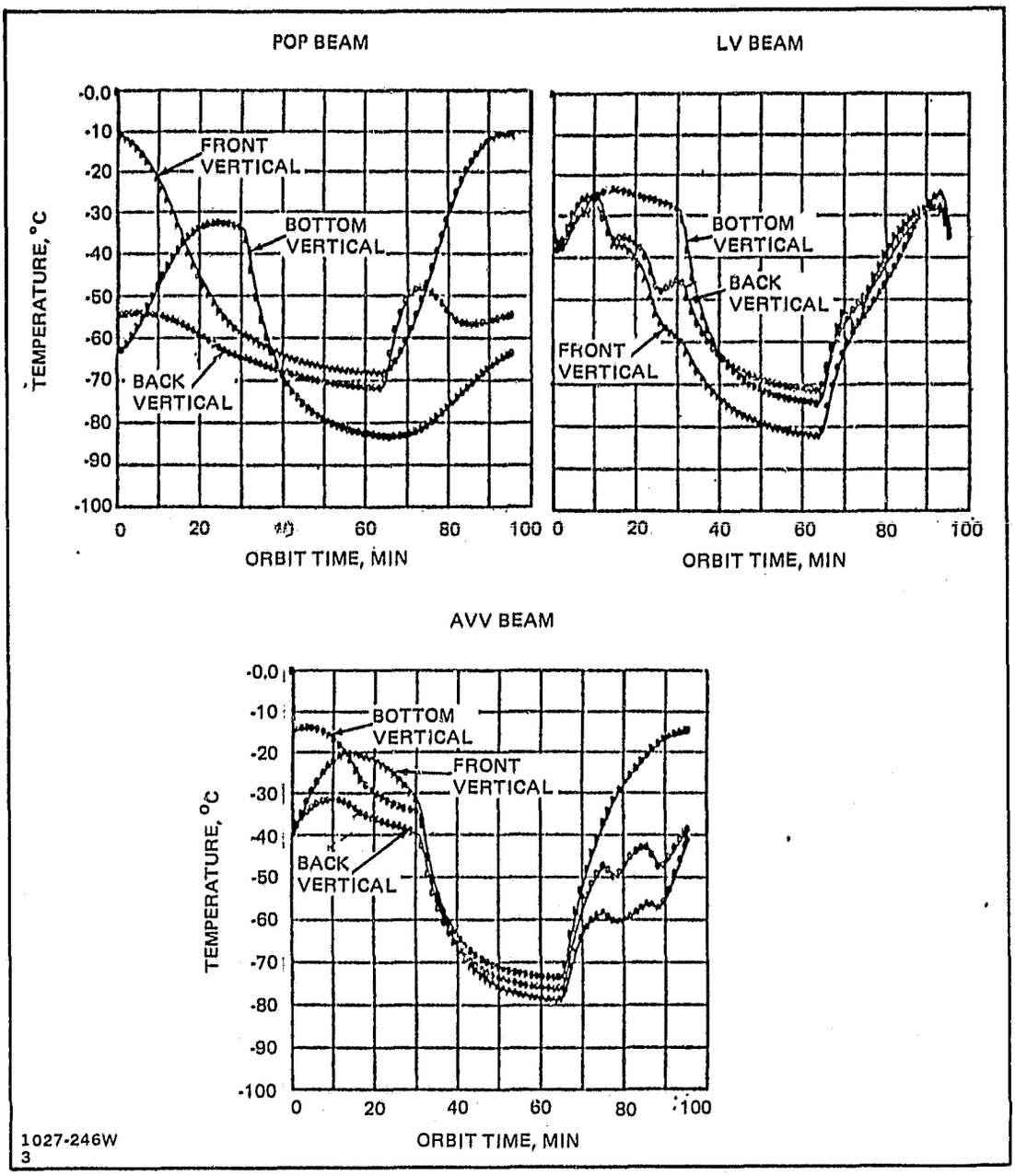

Fig. 5-8 Free-Flier — Vertical Temperatures

3

ORIGINAL PAGE IS
OF POOR QUALITY

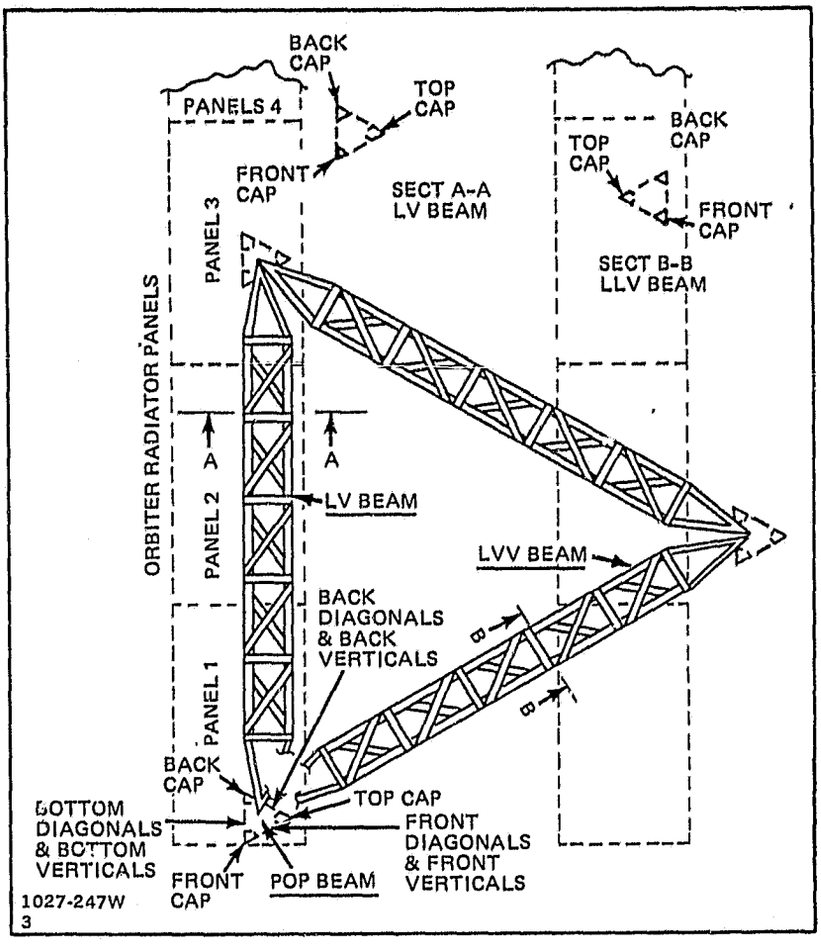

Fig. 5-9 Tribeam in Relation to Orbiter Radiator Panels

The three beam temperatures calculated herein correspond to the three lower areas designated in Fig. 5-1. The temperatures of the structural elements of these POP, LV, and AVV beams are shown in Figs. 5-10, 5-11 and 5-12, respectively. The individual nodal temperatures that composed these element averages are documented in Appendices M, N, and P.

The maximum gradients between elements of the three beams of the Orbiter-attached Tribeam are shown in the following table:

Maximum Gradients Between Elements-(°C/°F)

	POP Beam	LV Beam	AVV Beam
• Caps	20/36	27/49	16/29
• Diagonals	28/50	29/52	48/86
• Verticals	45/81	27/49	30/54

A comparison of the cap, diagonal, and vertical element temperatures among the three 1-meter beams of the attached Tribeam is shown in Figs. 5-13, 5-14, and 5-15.

5.4 COMPARISON OF FREE-FLIER AND ORBITER-ATTACHED TRIBEAMS

The cap temperatures of the free-flier and Orbiter-attached 1-meter beams are compared in Figs. 5-16, 5-17, and 5-18 for the POP, LV, and AVV beams. Figure 5-19 compares the differential cap temperatures for the three beams. The POP and AVV beam cap temperature characteristics are very similar; the LV beam, because of its proximity to the Orbiter radiator is somewhat affected, with the caps operating about 20°C higher.

Similar comparisons of the diagonal and vertical element temperatures, between the free-flier and Orbiter-attached 1-meter beams are provided in Figs. 5-20 through 5-25.

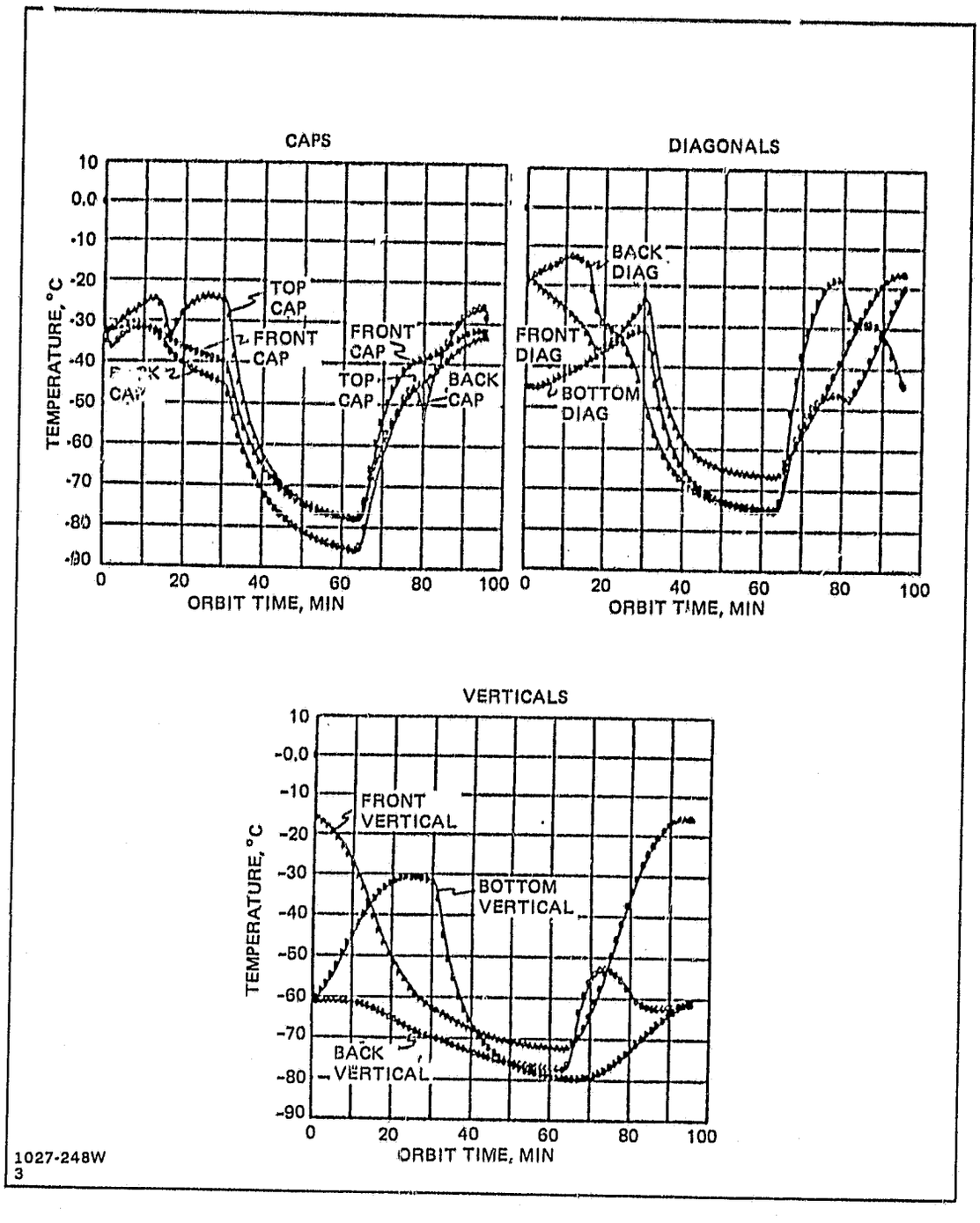

Fig. 5-10 Orbiter Attached – POP Beam Temperatures

3

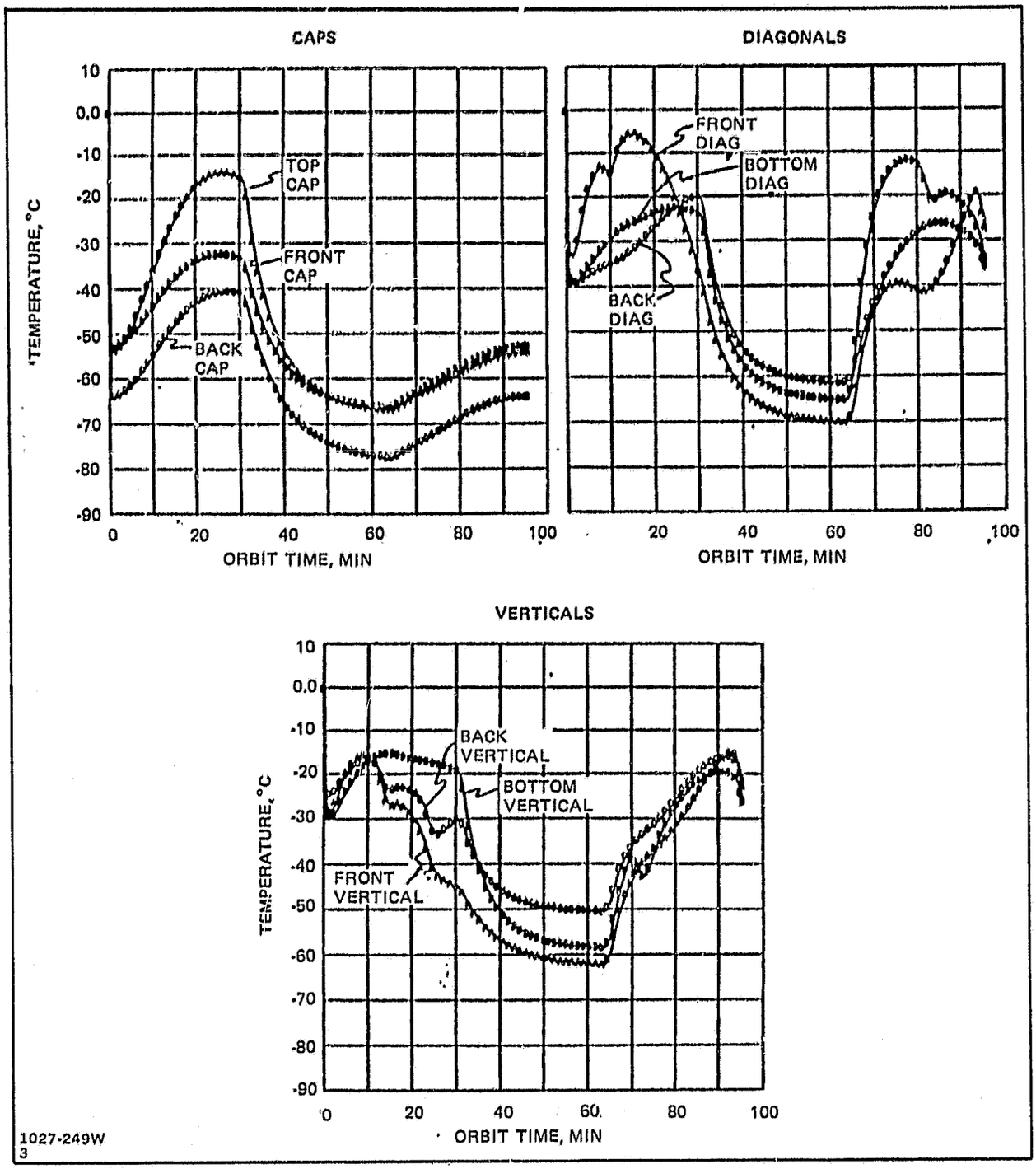

Fig. 5-11 Orbiter Attached — LV Beam

3

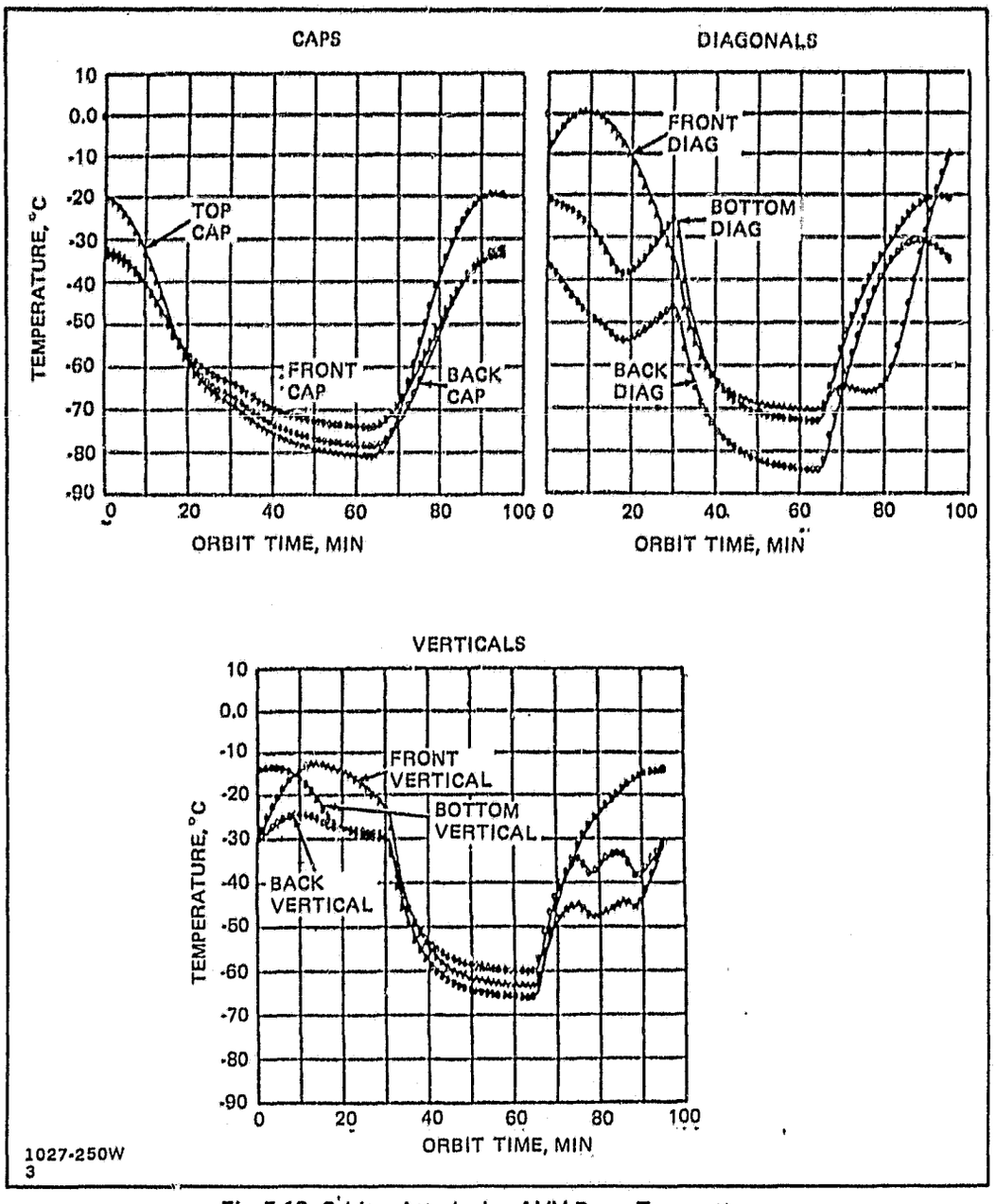

Fig. 5-12 Orbiter Attached – AVV Beam Temperatures

3

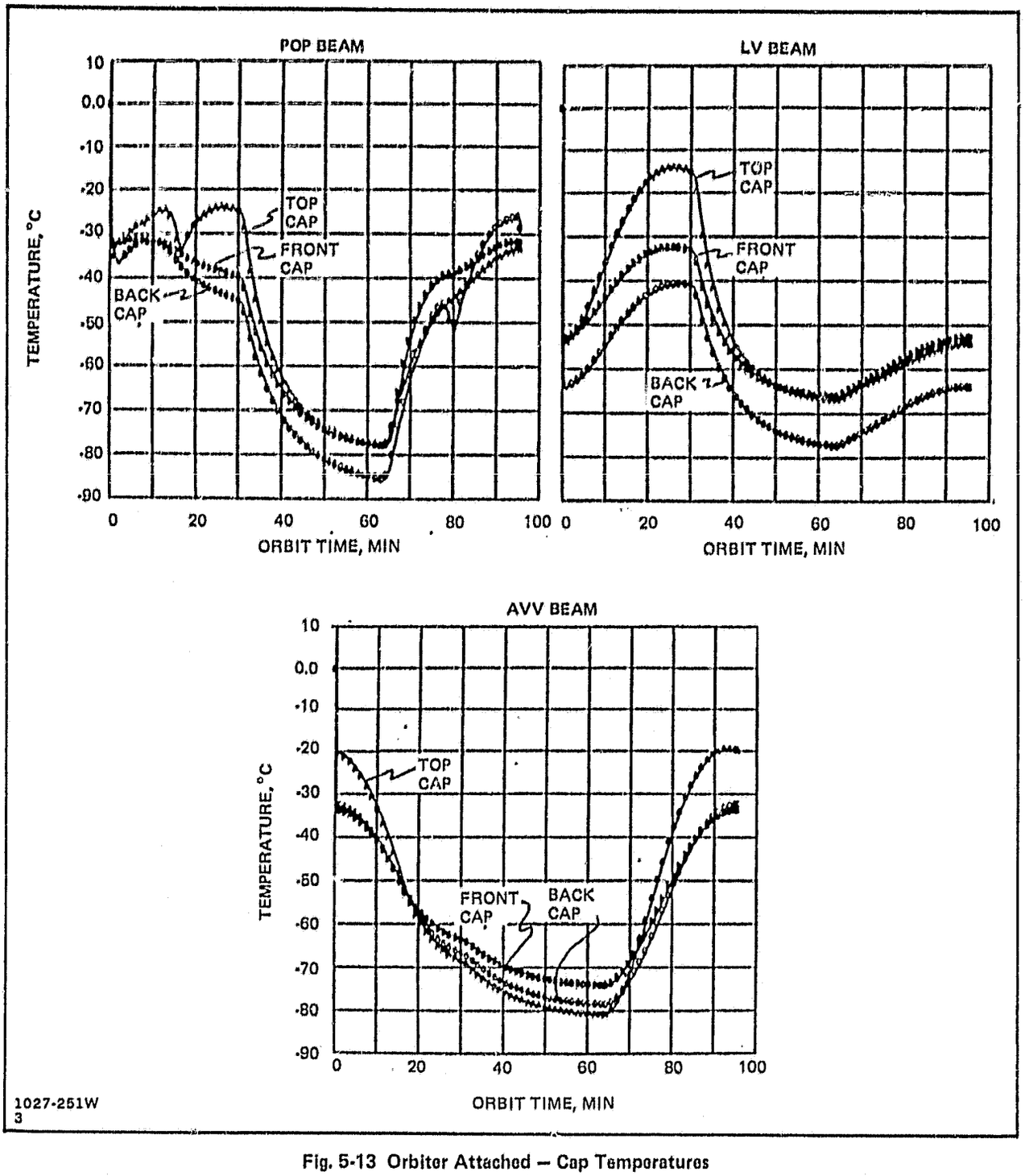

Fig. 5-13 Orbiter Attached — Cap Temperatures

3

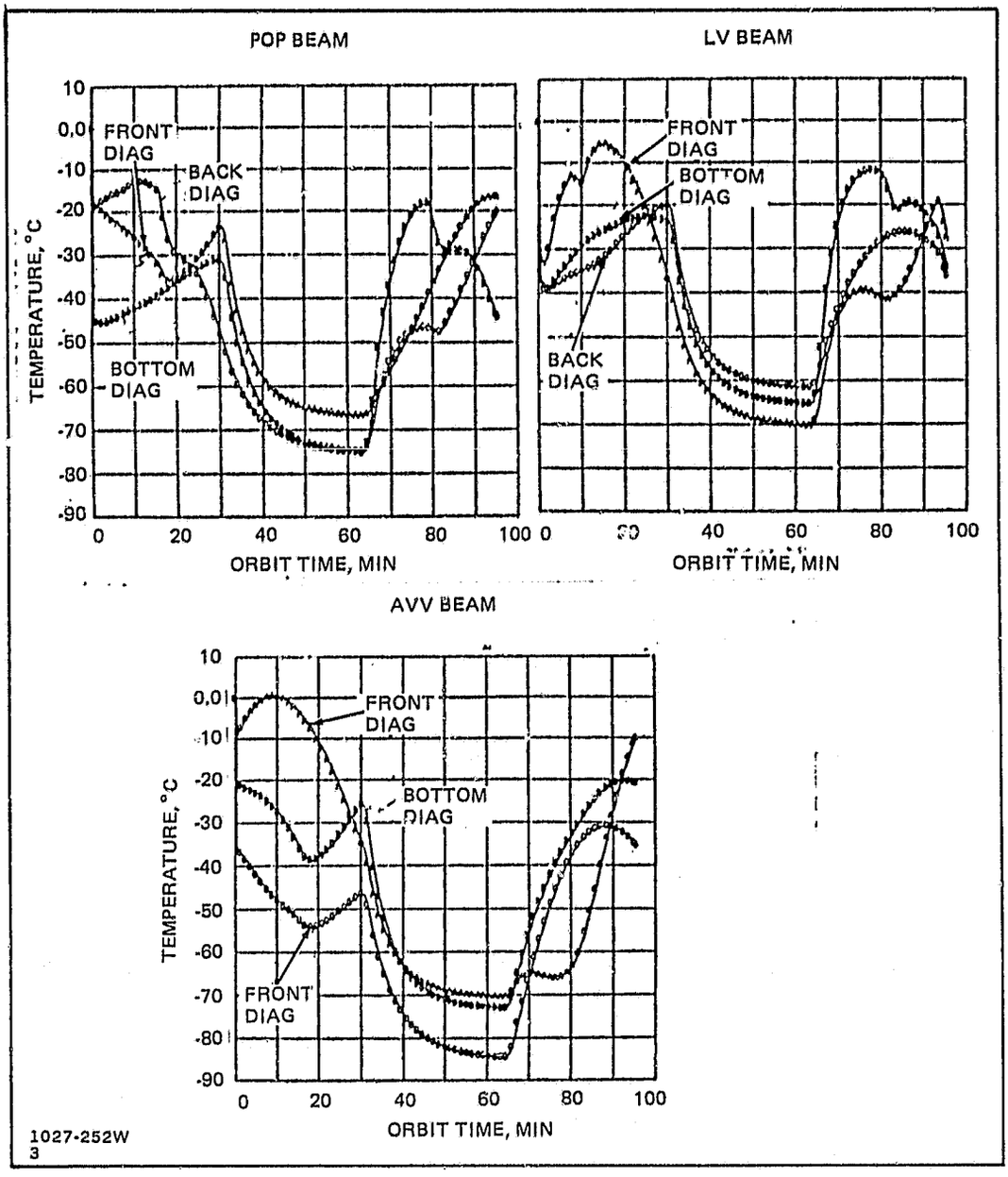

Fig. 5-14 Orbiter Attached — Diagonal Temperatures

3

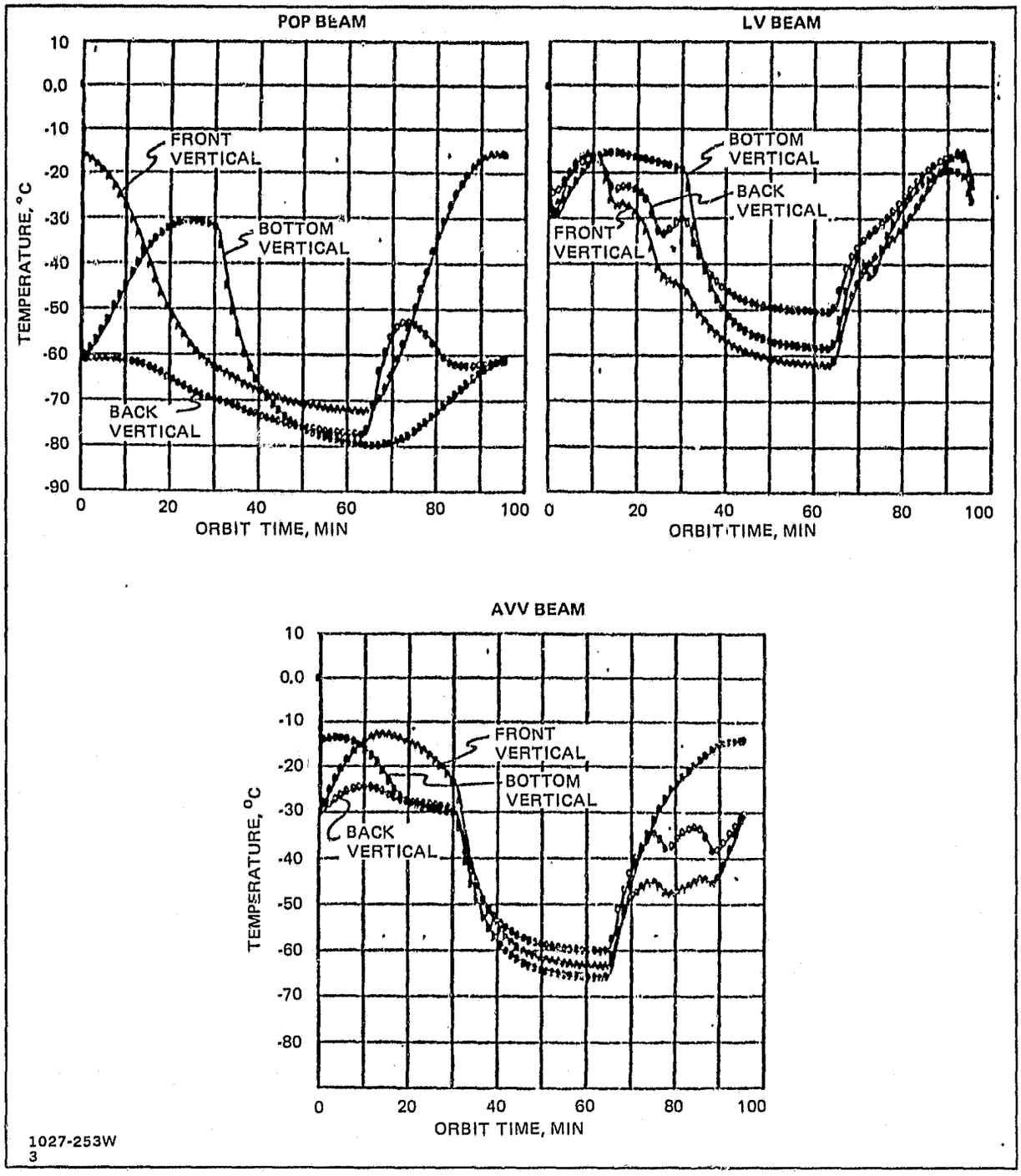

Fig. 5-15 Orbiter Attached — Vertical Temperatures

3

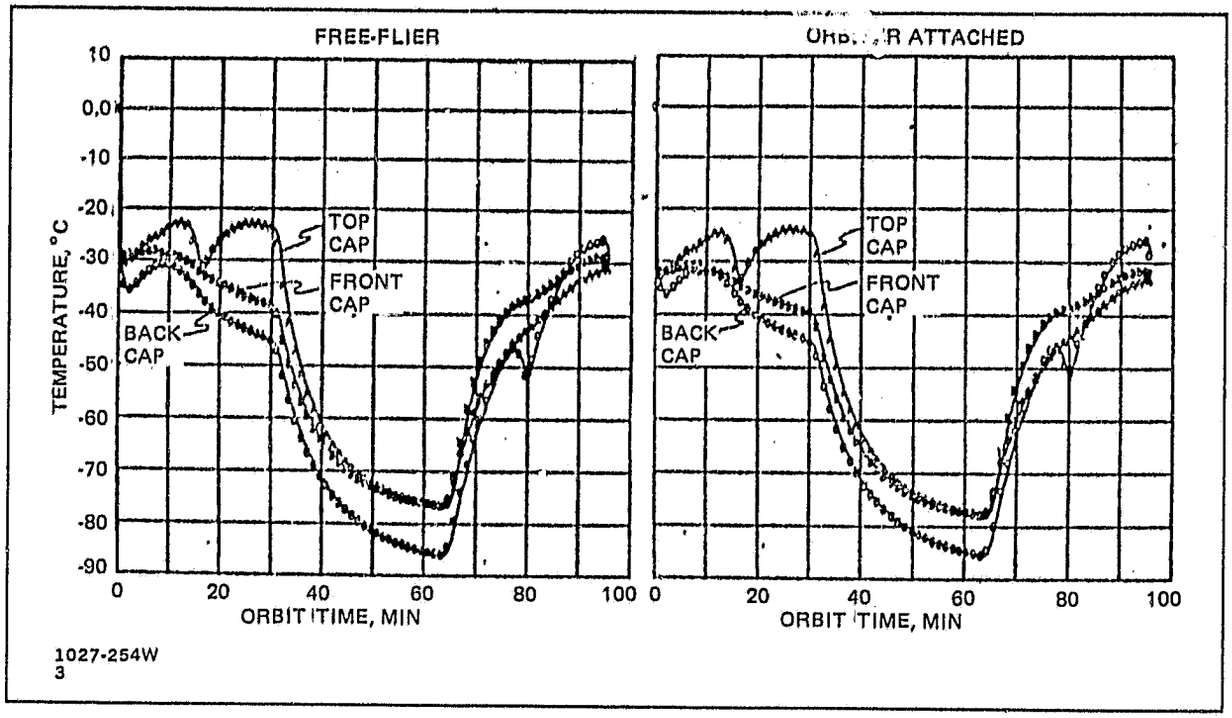

Fig. 5-16 Comparison of Free-Flier and Orbiter Attached Temperatures: POP Beam Caps

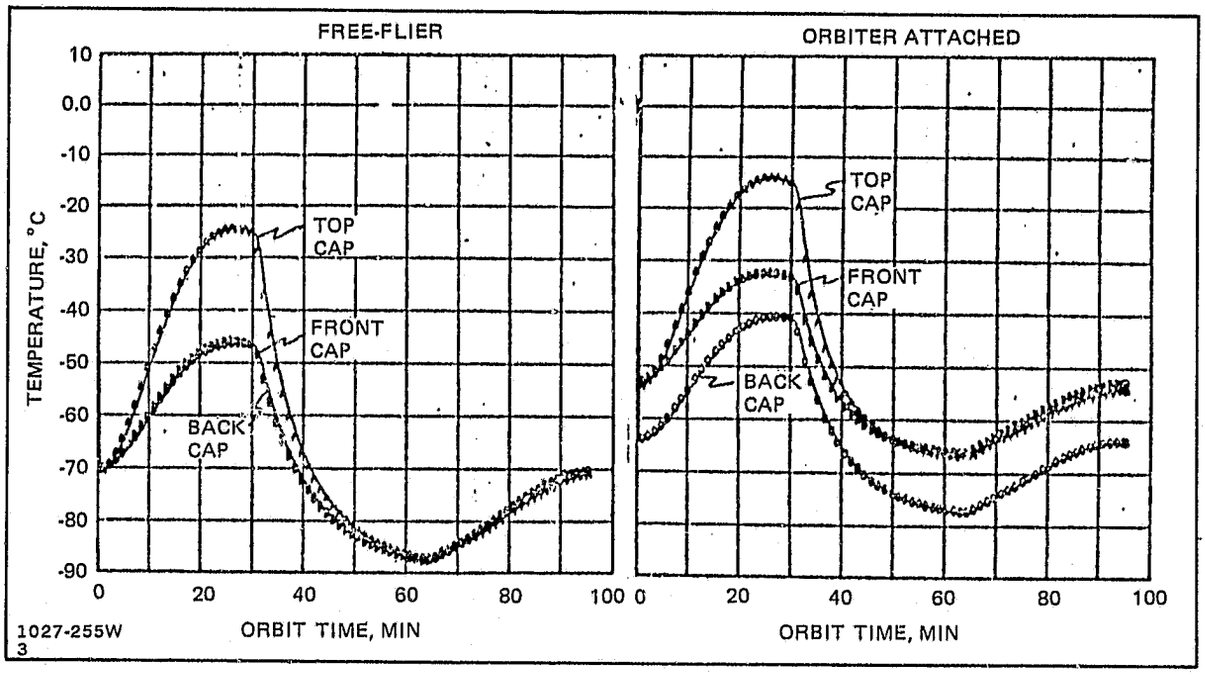

Fig. 5-17 Comparison of Free-Flier and Orbiter Attached Temperatures : LV Beam Caps

3

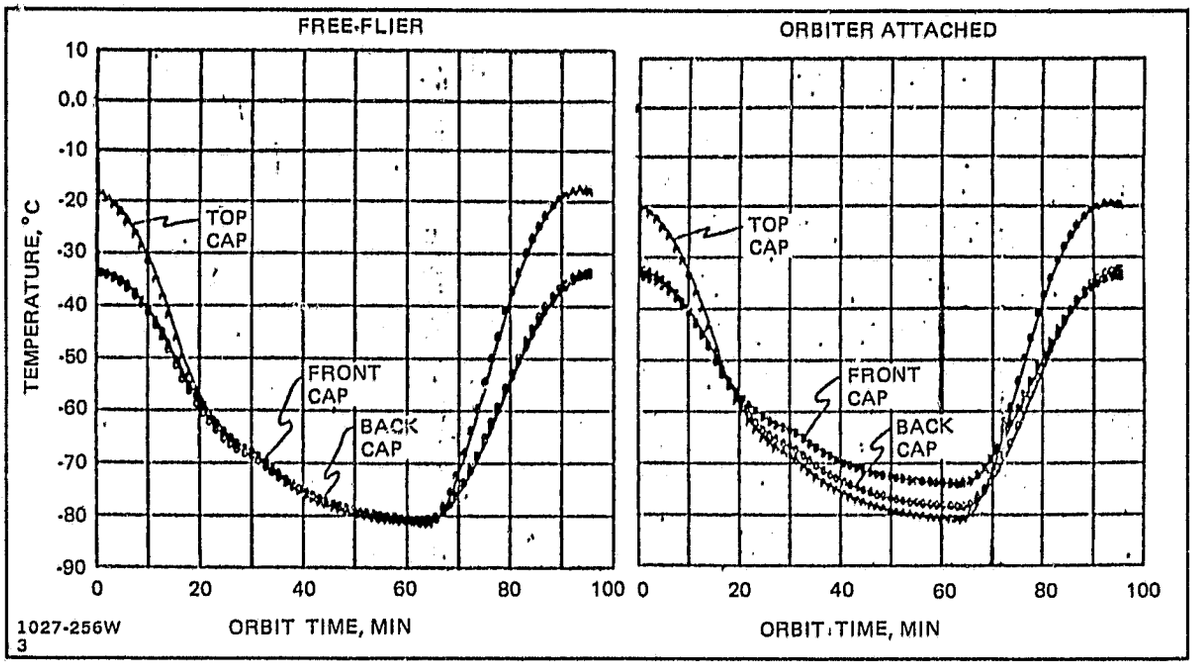

Fig. 5-18 Comparison of Free-Flier and Orbiter Attached Temperatures: AVV Beam Caps

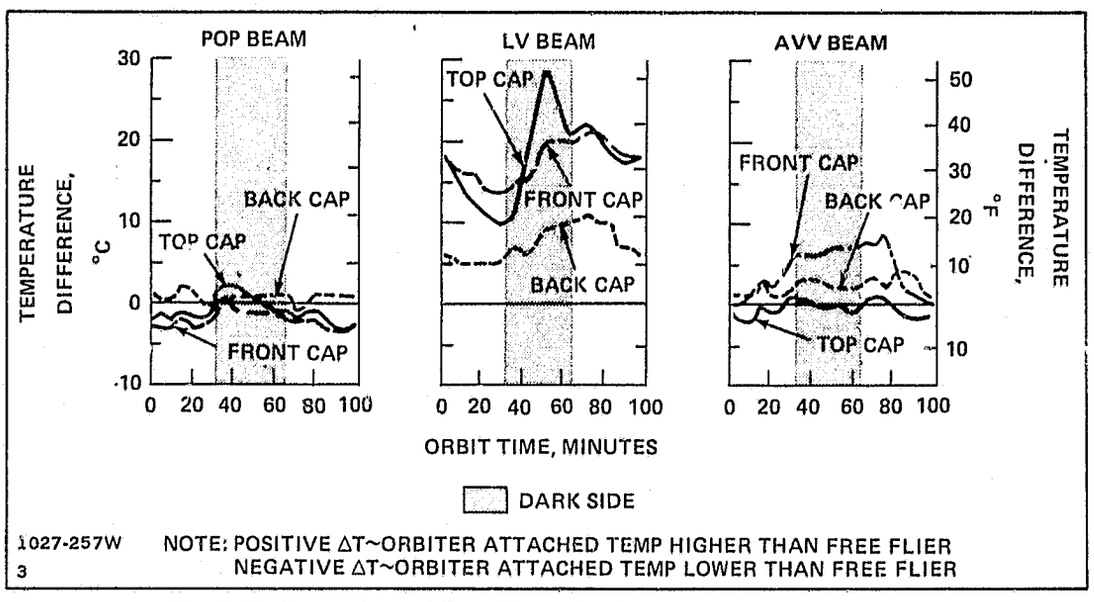

Fig. 5-19 Comparison of Free-Flier and Orbiter Attached Temperatures

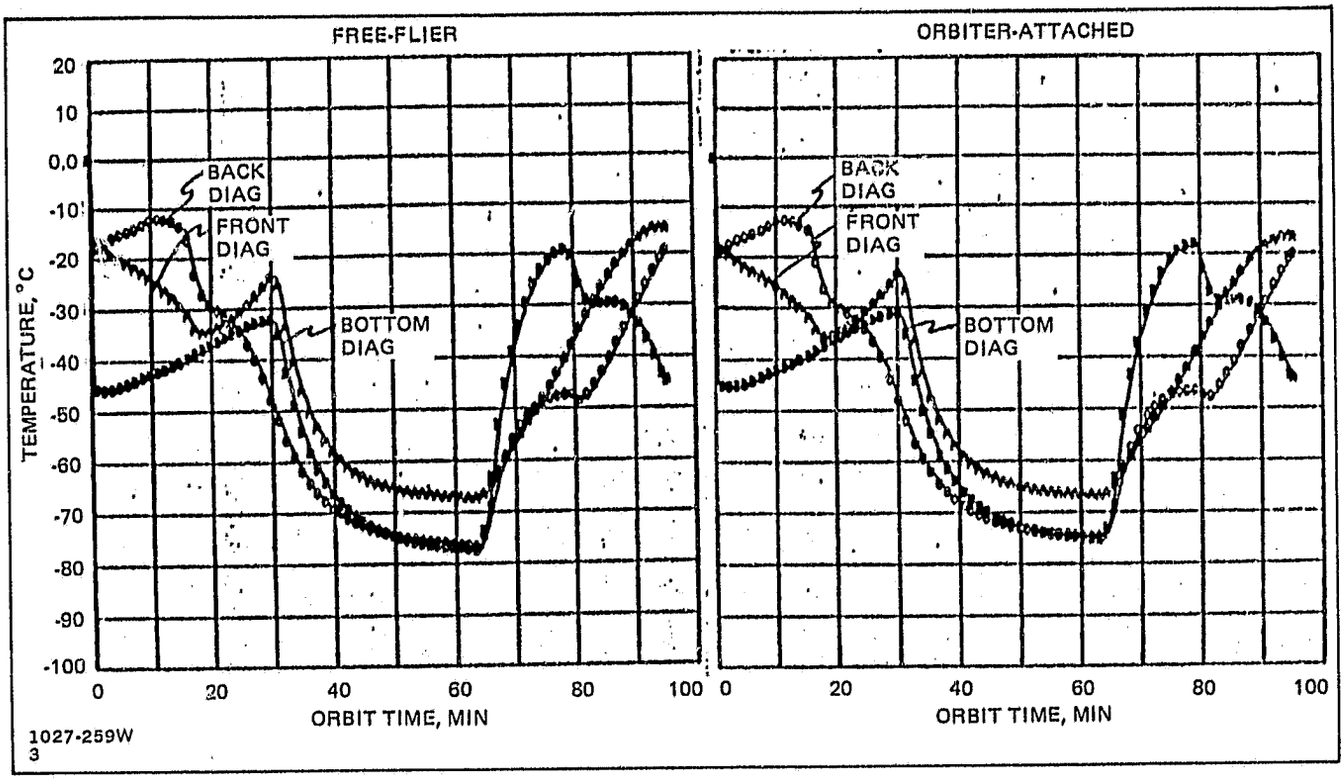

Fig. 5-20 Comparison of Free-Flier and Orbiter Attached Temperatures: POP Beam-Diagonals

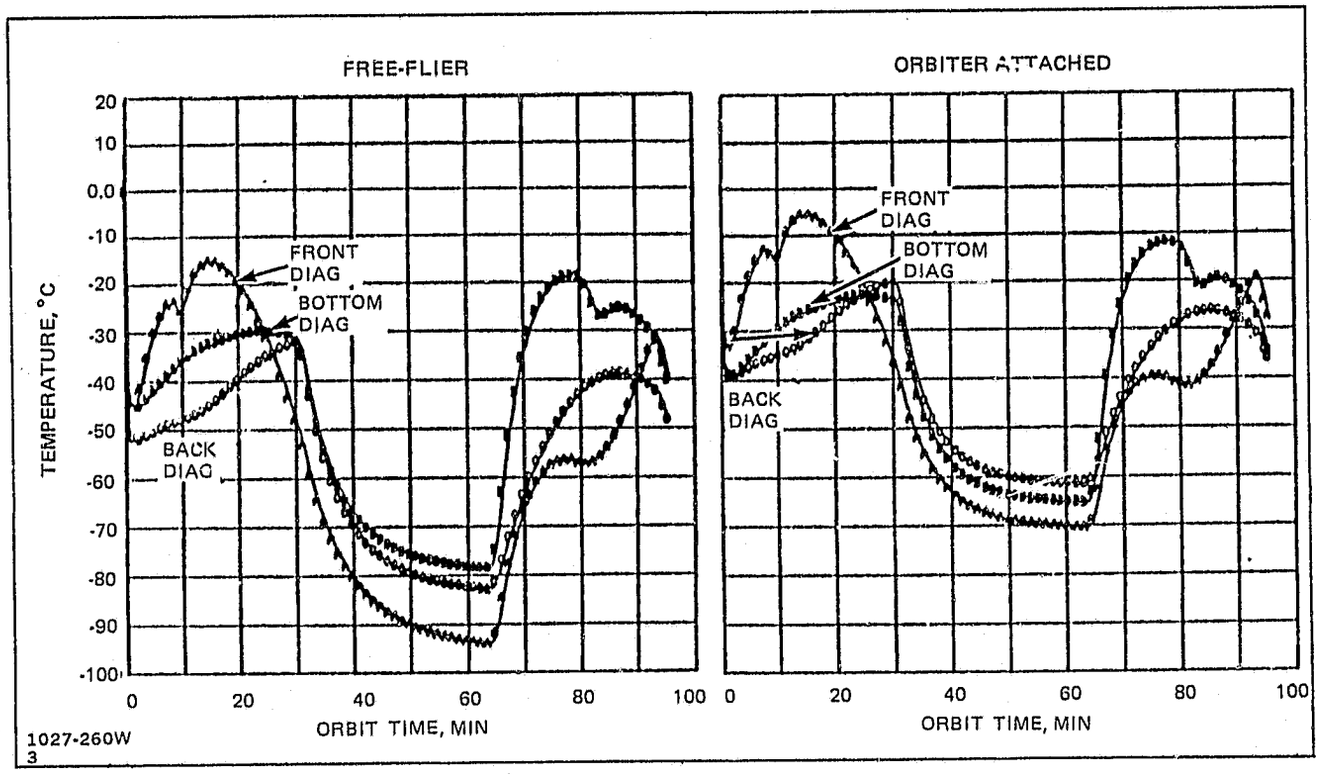

Fig. 5-21 Comparison of Free-Flier and Orbiter Attached Temperatures: LV Beam-Diagonals

3

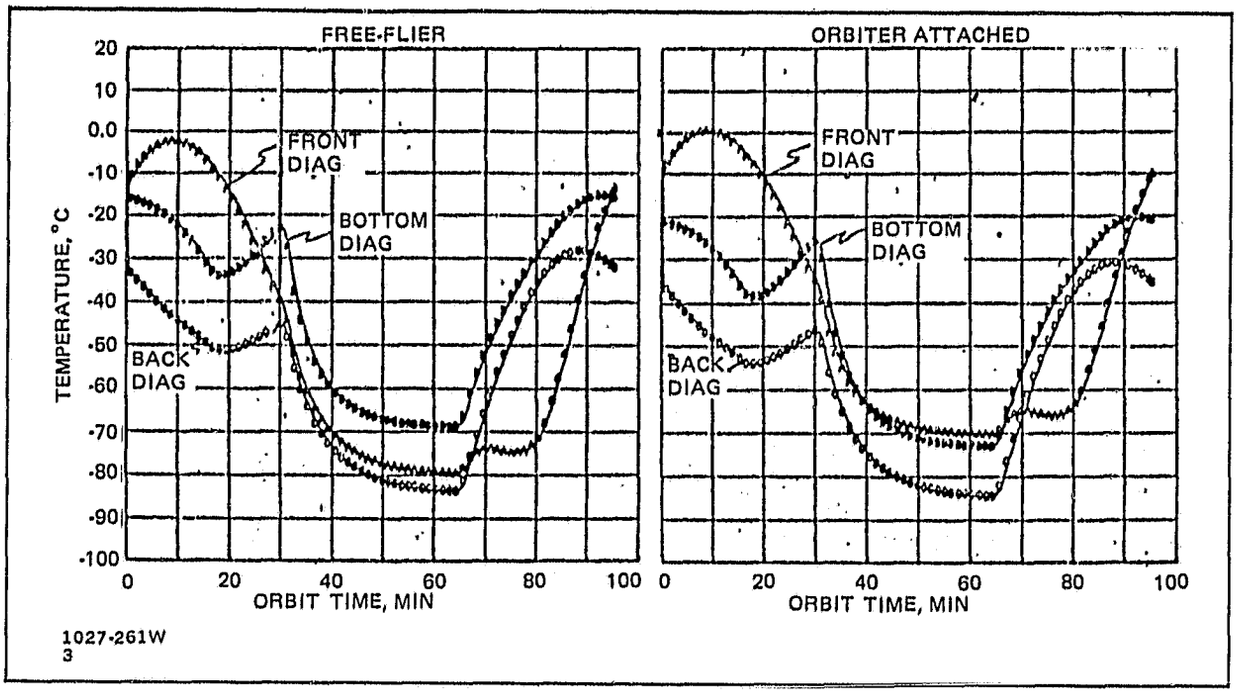

Fig. 5-22 Comparison of Free-Flier and Orbiter Attached Temperatures: AVV Beam-Diagonals

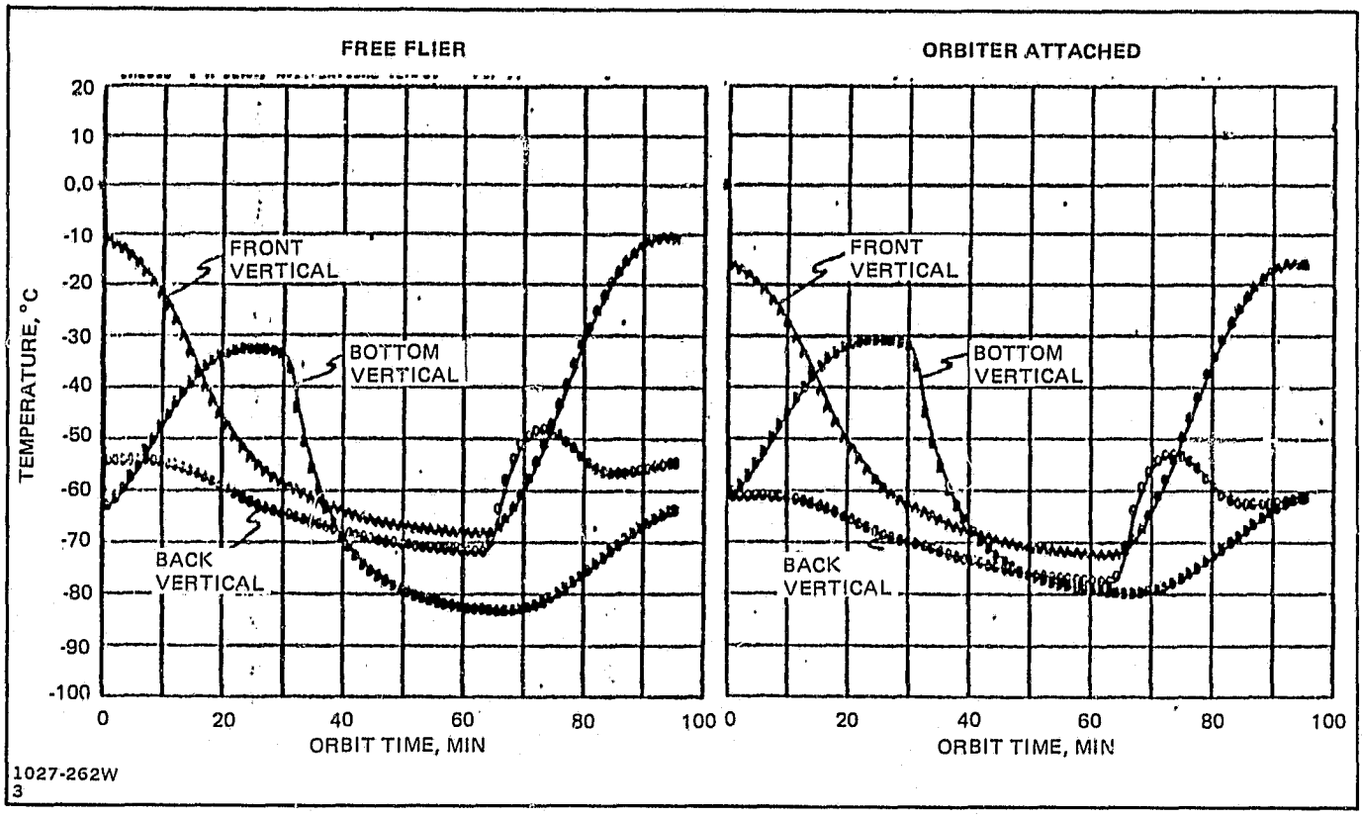

Fig. 5-23 Comparison of Free-Flier and Orbiter Attached Temperatures: POP Beam-Verticals

3

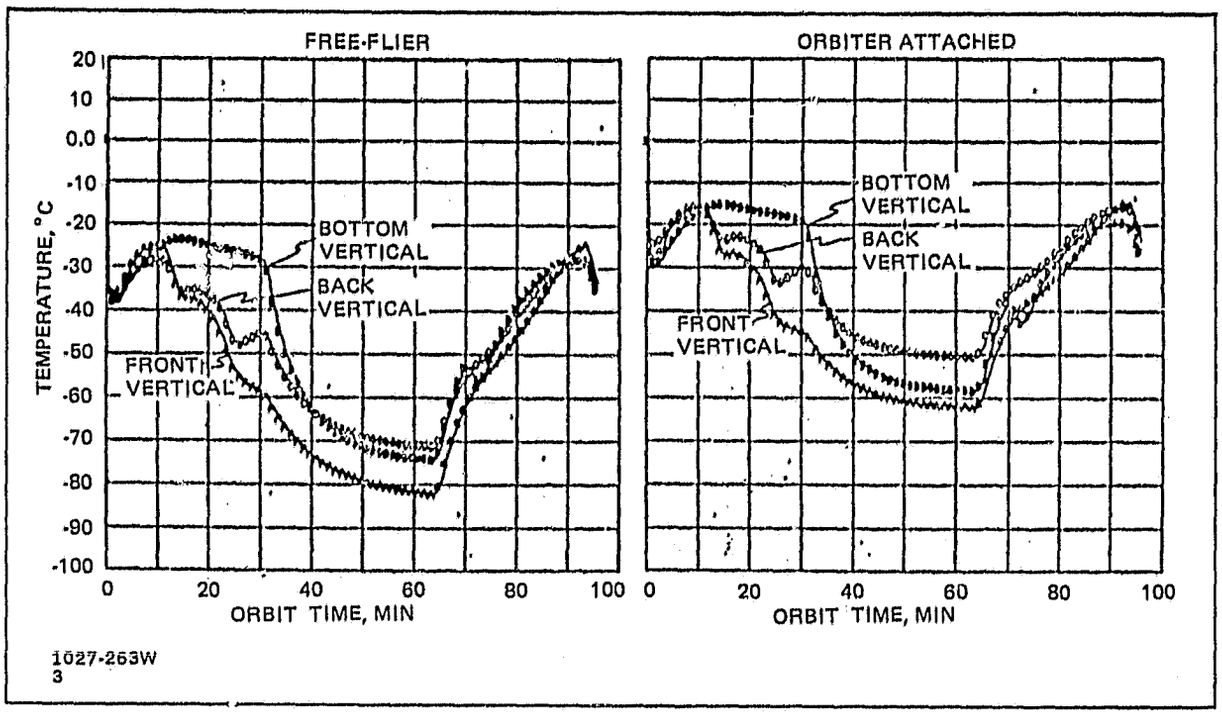

Fig. 5-24 Comparison of Free-Flier and Orbiter Attached Temperatures: LV Beam-Verticals

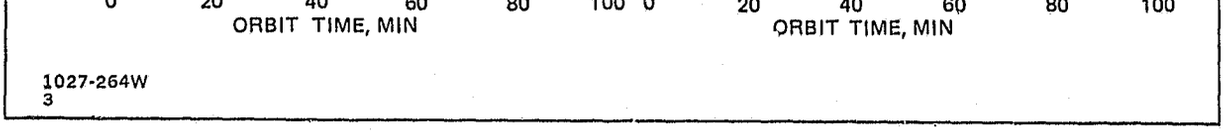

Fig. 5-25 Comparison of Free-Flier and Orbiter Attached Temperatures: AVV Beam-Verticals

3

6 - OBSERVATIONS AND RECOMMENDATIONS

6.1 OBSERVATIONS

Steady-state thermal analyses are inadequate for evaluating alternate thermal coatings or structural response of LSS in orbit. Transient thermal analyses reflecting blockage/shadowing of structural elements, during an orbit, are necessary. The transient analyses can readily be performed through adaptations of available computer programs which include considerations of solar blockage factors and can be conveniently handled through computer graphics. The 1-meter beam computer programs appear to be amenable to further simplification, but the extent of simplification possible without affecting the accuracy of the results remains to be determined.

Considerations of blockage/shadowing, and minimization of temperature gradients between structural elements of a 1-meter beam, favor the use of Alzak or white paint coatings. With these types of coatings, a 1-meter beam's structural response in orbit in terms of twist as a function of length, for example, appears to be similar to the manufacturing tolerances expected for comparable length beams.

Analyses of hybrid material combinations of 1-meter beam elements, involving the use of composite verticals and diagonals, indicate that distortions during an orbit are increased over those experienced by all-aluminum or all-composite beam structures. The use of mixed materials in primary LSS structures, therefore, should be carefully considered for their respective applications.

The linear motions and distortions of a beam are fundamental design considerations which must be reflected in joint designs, construction/assembly procedures, and operation of LSS. As shown in Fig. 6-1, the structure's response to the orbit environment in terms of distortion and displacement, coupled with manufacturing tolerances associated with fabrication of the basic structure, establish a condition which is "equivalent" to built-in pre-stresses within a structure. Above this base condition, the applied loads must be considered for each LSS application.

Our analyses indicate that the structural response of a single 1-meter beam "building block", in a worst case orientation, should adequately describe the limiting thermal design characteristics of an LSS composed of multiple building block elements.

However, the transient temperature characteristics of the "building block" structures, and their structural elements, are necessary to determine the distortion of an LSS in orbit. The blockage effects of payloads, subsystems, etc. mounted to an LSS also represent special cases requiring detailed analysis for each mission application.

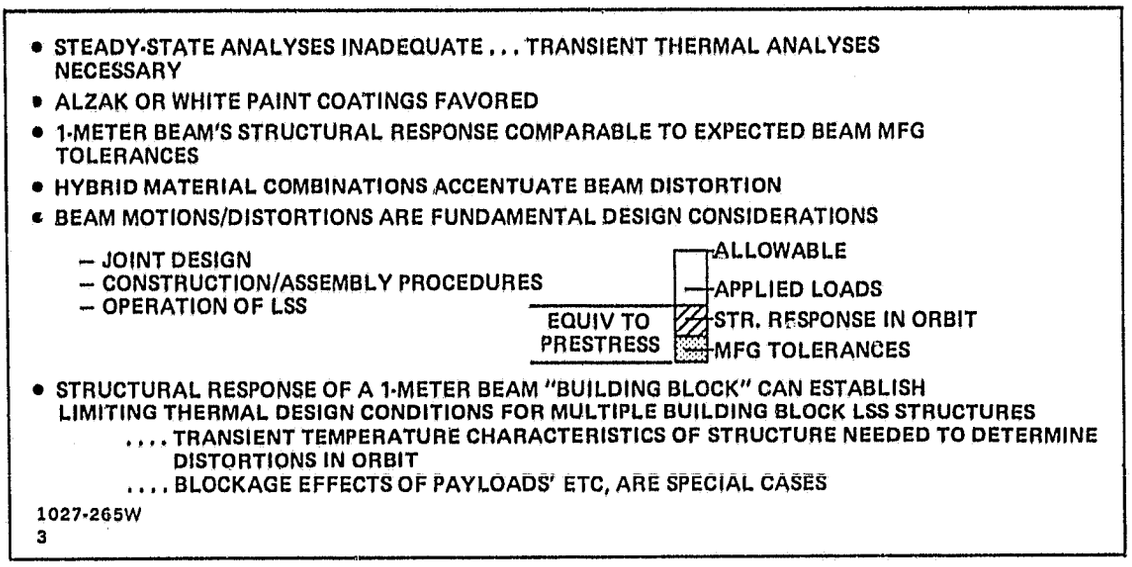

Fig. 6-1 Observations

6.2 RECOMMENDATIONS

Figure 6-2 summarizes the recommendations of the thermal analysis conducted during this study. The Z-93 white paint coating is presently recommended for 1-meter aluminum beam fabrication by the ABB. The handling problems associated with the use of this coating are expected to be considerably simpler than Alzak. It would be desirable, however, to investigate the applicability/suitability of Alzak coatings for ABB beam fabrication. Alzak has improved coating decay characteristics, as compared to white paint, and could be preferable for prolonged orbital LSS applications. Potential handling problems, both within the ABB and those associated with on-orbit construction, should be evaluated.

Further analysis of the structural response of the 1-meter beam is recommended. All possible orbit orientations should be evaluated to establish the worst case from a linear motion/distortion point of view. Other aspects that merit investigation are the effects of coatings degradation, modifying structural element configurations to minimize temperatures, gradients and distortions (e.g., perforating verticals), and the

3

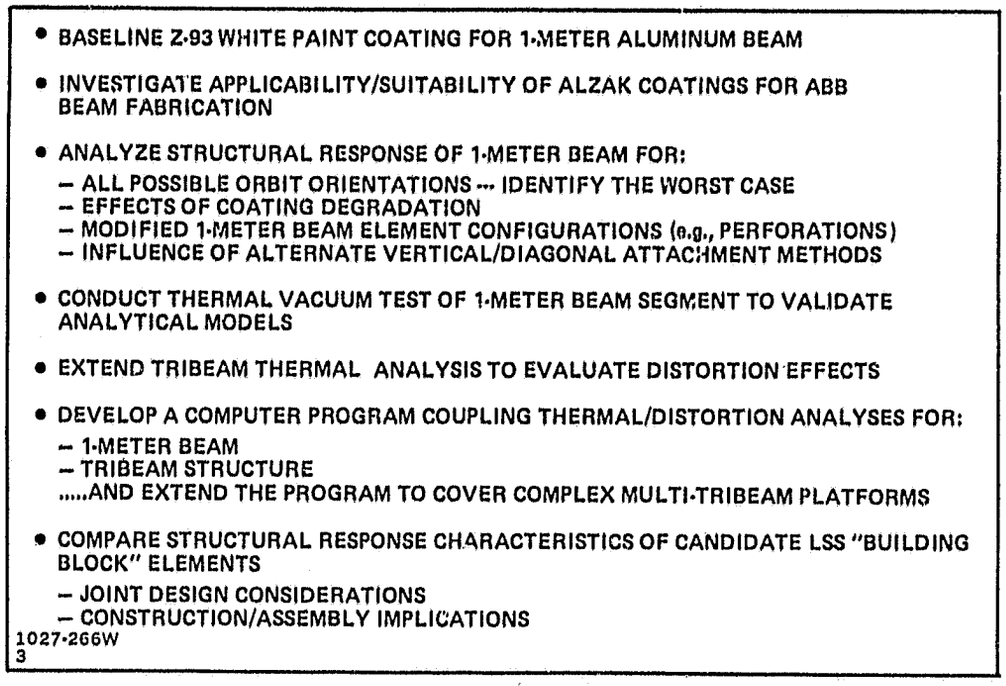

Fig. 6-2 Recommendations

effect of alternate vertical/diagonal attachment methods. To improve our understanding of the thermal and structural response of the 1-meter beam "building block", a thermal vacuum test of a beam segment is recommended. Through such a test, considerable confidence could be acquired as to the accuracy of our analytical thermal prediction models and the beam's response to orbit conditions.

The Tribeam thermal analysis, reported herein, should be applied to evaluate the structural distortion of the Tribeam to the orbit environment, for both Orbiter-attached and detached conditions. Further, a computer program should be developed, for both the 1-meter beam and Tribeam, which couples the outputs of the thermal analysis to the structural response analysis to directly output the linear motions and distortions of the structure. Subsequent efforts should then extend the program to more complex multi-Tribeam platform structures.

The transient thermal analyses and related structural response efforts, conducted during this study, underscore the importance of understanding the response of basic structural "building blocks" to the orbital environment. The awareness of a building

block's linear motion and distortion characteristics establishes fundamental design requirements which will affect the design of compatible joining techniques, construction and assembly approaches, and subsequent operational loadings on a large space structure. It is recommended, therefore, that other candidate building block structures, presently under consideration for LSS applications, be similarly analyzed for their structural response characteristics. These characteristics should subsequently be compared in terms of their implications on joint designs and construction/assembly operations, with the intent to potentially identify preferred (or standardized) building block approaches for future LSS.